CHALMERS

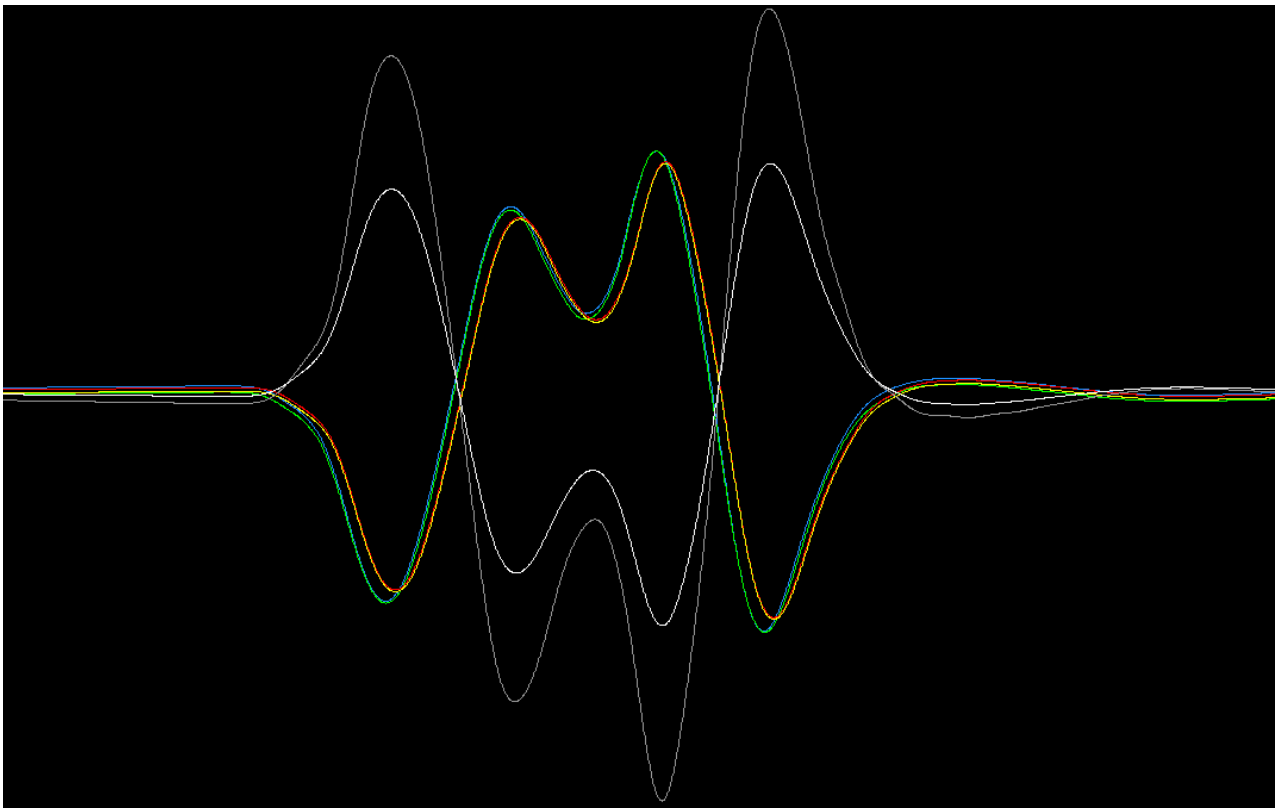

Suspension development for a prototype Urban Personal Vehicle

Master's thesis in Automotive Engineering

SERGEJ ABYZOV

Department of Applied Mechanics
Division of Vehicle Engineering and Autonomous Systems
Vehicle Dynamics Group
CHALMERS UNIVERSITY OF TECHNOLOGY
Göteborg, Sweden 2014
Master's thesis 2014:10

MASTER'S THESIS IN AUTOMOTIVE ENGINEERING

Suspension development for a prototype Urban Personal Vehicle

SERGEJ ABYZOV

Department of Applied Mechanics
Division of Vehicle Engineering and Autonomous Systems
Vehicle Dynamics Group
CHALMERS UNIVERSITY OF TECHNOLOGY

Göteborg, Sweden 2014

Suspension development
for a prototype Urban Personal Vehicle
SERGEJ ABYZOV

Master's thesis 2014:10
ISSN 1652-8557
Department of Applied Mechanics
Division of Vehicle Engineering and Autonomous Systems
Vehicle Dynamics Group
Chalmers University of Technology
SE-412 96 Göteborg
Sweden
Telephone: +46 (0)31-772 1000

Cover:
Double lane change manouvre at a speed of 50 [km/h],
with an anti-roll bar installed on the front axle.

Chalmers Reproservice
Göteborg, Sweden 2014

Suspension development
for a prototype Urban Personal Vehicle
Master's thesis in Automotive Engineering
SERGEJ ABYZOV
Department of Applied Mechanics
Division of Vehicle Engineering and Autonomous Systems
Vehicle Dynamics Group
Chalmers University of Technology

Abstract

This thesis describes the process of suspension development for a prototype Urban Personal Vehicle (PUNCH). The PUNCH is a crash safe prototype of an Urban Personal Vehicle developed at the Chalmers University of Technology, Gothenburg, Sweden.

The urban personal vehicle is designed for the dense urban areas of today. It's a small, car-like vehicle with space for one driver (and maybe one or two passengers) that is to be driven at city speeds (sub 50 [km/h]). It needs to be nimble and easy to drive.

The thesis starts by defining the requirements for this vehicle, limitations of project and the iterative process of suspension design. Thereafter the literature study is presented in the theory chapter. After that, the selection of design and parts is shown, design draft is made and analysed in a whole vehicle simulation computer programme. From the simulation results conclusions are made and recommendations for the physical fabrication and future work are given.

The finished concept is a double wishbone suspension font and rear. The suspension has a predictable character without any sudden changes. The suspension characteristics are as close as possible to the given targets, but for some limitation due to packaging issues presented by the already existing frame. The suspension front and rear share many components, so the final design requires less unique manufacturing (at a later phase/future work). Some components (as brake assembly, wheel hubs & bearings) are taken straight from a common road car (simple, cheap, off the shelf components). The ride is predicted to be comfortable without too much roll during cornering.

Keywords: Urban personal vehicle, suspension.

Acknowledgements

I'd like to start with thanking my mum for all patience and support.

The work was made much more interesting and gratifying by the valuable input and support of Edo Drenth at Modelon, guiding me in the use of IPG software, pointing out important areas to look at and Andrew Dawkes teaching and supervising in the art of vehicle construction.

I'm very grateful for all the help, knowledge and insights I've acquired from many of my collogues at Department of Applied Mechanics at Chalmers University of Technology. Many small and big questions have been answered and ironed out. I can't prise the working environment enough where the answer never been longer than a short walk away with always open doors.

Last but not least, I want to thank Professor Bengt Jacobson for supervising this project and
Associate Professor Sven B. Andersson for initiating the project.

Nomenclature

a_y - lateral acceleration $[m/s^2]$
A - acceleration $[m/s^2]$
ARB - anti-roll bar
c - spring rate [N/m]
c_{f_l} - spring rate front left [N/m]
c_{f_r} - spring rate front right [N/m]
c_s - spring rate [N/m] or [N/mm]
c_{s_f} - spring rate front [N/m]
c_{s_r} - spring rate rear [N/m]
c_t - tyre spring rate [N/m] or [N/mm]
c_{w_f} - wheel rate front [N/m]
c_{w_r} - wheel rate rear [N/m]
C_f - front cornering stiffness [N/rad]
$C_{f_{tot}}$ - total front rate (wheel rate and tyre rate) [N/m]
C_r - rear cornering stiffness [N/rad]
$C_{r_{tot}}$ - total rear rate (wheel rate and tyre rate) [N/m]
$C_{s_{tot}}$ - total vertical rate (wheel rate and tyre rate front and rear) [N/m]
CAD - computer aided design
COG - centre of gravity
d - damping constant [N*s/m]
d_{cr} - critical damping constant [N*s/m]
d_{cr_f} - critical damping constant front [N*s/m]
d_{cr_r} - critical damping constant rear [N*s/m]
d_f - damping constant front [N*s/m]
d_r - damping constant rear [N*s/m]
d_{trf} - damper travel front [m]
d_{trr} - damper travel rear [m]
DIN - Deutsches Institut für Normung
DLC - double lane change manoeuvre
δ_f - front wheel (one track model) turning angle [rad]
δ_i - inner wheel turning angle [rad]
δ_o - outer wheel turning angle [rad]
f_{r_f} - ride frequency front [Hz]
f_{r_r} - ride frequency rear [Hz]
F_f - vertical normal force (z-direction) front [N]
F_{fy} - lateral force (y-direction) front [N]
F_r - vertical normal force (z-direction) rear [N]
F_{ry} - lateral force (y-direction) rear [N]
F_{zr} - vertical force (z-direction) rear [N]
F_{zf} - vertical force (z-direction) front [N]
FL - front left
FR - front right
g_f - longitudinal distance WC front to IC_f [m]
g_r - longitudinal distance WC rear to IC_r [m]
GND - ground
h - height roll axis to centre of gravity
h_{COG} - centre of gravity height above ground [m]
h_f - height of IC_f[m]
h_{lift} - lifting height of front of frame [m]
h_PC - pitch centre height [m]
h_r - height of IC_r[m]
I_{xx} - moment of inertia about x-axis $[kg * m^2]$
I_{xy} - moment of inertia in the xy-direction $[kg * m^2]$
I_{yy} - moment of inertia about y-axis $[kg * m^2]$
I_{yz} - moment of inertia in the yz-direction $[kg * m^2]$
I_{zz} - moment of inertia about z-axis $[kg * m^2]$
IC_f - front instant centre of rotation (side view)
IC_r - rear instant centre of rotation (side view)
K_u - understeer coefficient
l or L - wheel base [m]
l_f - distance COG - front axle
l_r - distance COG - rear axle
m - mass [kg]
m_s - sprung mass [kg]
M + S - mud and snow (winter tyres)
MR_{f_0} - motion ratio of front wheel about curb level
MR_{r_0} - motion ratio of rear wheel about curb level
μ - friction coefficient
μ_{road} - friction coefficient road-tyre
ω - angular frequency [rad/s]
PC - pitch centre
ϕ - roll angle [deg]
p_x - roll gradient [rad/g]
PUNCH - Plug-i n Chalmers
R - distance vehicle COG to common point of rotation [m]
R_e - equivalent rolling radius of tyre [m]
R_r - distance centre of vehicle to common point of rotation [m]
R_e - wheel radius [m]
RC - roll centre vertical position (height)
RL - rear left
RMS - root mean square
RR - rear right
S - length [in]
v_x - vehicle longitudinal speed [m/s]
v_y - vehicle lateral speed [m/s]
w - track width [m]
W - weight [lb]
WC - wheel centre
WUSIWYG-UI - what you see is what you get user interface
x - displacement/compression of spring [m]
ζ - damping ratio

Contents

Chapter 1
Introduction

This chapter will give an introduction to the thesis. Starting with a background to the subject, followed by the objective of the thesis. Thereafter the deliverables will be presented to further clarify the goals and finally will the delimitations be declared.

1.1 Background

As a partial solution for reducing the effects of climate change and urban congestion new sorts of vehicles for personal transport are needed. One vehicle type for this are smaller vehicles for 1-3 persons, here called Urban Personal Vehicle, UPV. These vehicles should however not only be energy efficient, low polluting but also safe. This is exactly what the PUNCH project is aiming to do, producing a showcase for sustainable but yet safe, personal transport. In order for this vehicle to be desired for everyday life it has to be able to withstand the elements and bring the driver to his or hers destination comfortably. To provide ride comfort and adequate handling characteristics a suspension system is to be developed.

1.2 Purpose and goal

The aim of the thesis is to develop a front and rear suspension for a prototype of a urban personal vehicle. This is needed for further development and work on the urban personal vehicle project PUNCH at Chalmers University of Technology. The PUNCH project is aimed to be used as a test bed for different technologies and a platform for design an development projects for students within the scope of their education. As for this thesis, the thesis the main set objective is to develop an easily adjustable suspension that satisfies the users's needs for comfort and performance (more on requirements in Chapter 3). In order to do so an analysis of different solutions has to be made, as well as setting requirements that wasn't present at the thesis start.

1.3 Deliverables

The main deliverables of the thesis is:

- Complete the requirement list initiated by previous works in the project.
- A conceptual design (fulfilling the requirements of Chapter 3) of a suspension geometry front and rear.
- Verification of the suspension design by dynamic simulation of complete vehicle.
- Full CAD of suspension assembly.
- Verification of the strength of the suspension link members by stress analysis/finite element analysis.

1.4 Delimitations

Some subsystems and processes of the suspension development had to be left out due to time constraint. The following steps are outside the thesis:

- Manufacturing/acquisition of parts.
- Acquisition of some auxiliary parts (as e.g. rims and tyres).
- Assembly of suspension on the vehicle frame.
- Full scale track testing of vehicle prototype for evaluation.

1.5 Limitations

The existing frame is built for a roll-stiff vehicle, as opposed to a cambering vehicle. This, and 4 wheels on 2 axles are, taken as pre-requisites and thus limiting the design of suspension. The thesis main aim is to provide a functioning suspension for the vehicle. This will however also involve in incorporating a braking system into the design. If possible the project will also deliver some recommendation or even a functioning design for steering system, but this is not the main goal. The thesis won't look into the detailed elastokinematic characteristics of the designed suspension due to time constraint other than ensuring that the elastokinematic elements in the full vehicle simulation are of a common and reasonable type.

1.5.1 Frame

The existing frame (developed in the past [1] & [2], represented in Figure 1.1) embodies geometrical limitations. As it is 870 [mm] wide at the possible position of the axles dictates the minimum track width. If taking the wished track width of sub 1,5 [m] into account and still making the vehicle be able to perform i.e. the wanted turning circle (set to 6 [m] in Chapter 3). The frame in conjunction also dictates the wheel base possible to have for the car, as the wheels need to be mounted to the frame (wheel base can't exceed the frame length too much) and the wheels should not rub against the frame at turning (critical as frames middle section is wider than the front and rear portion). The frame was set not to be modified in any way, but adding reinforcements and mounts for the suspension.

1.5.2 Old target values

In previous works done for the PUNCH project the suspension target values seen in Table 1.1 and 1.2. These are to be used as a indication on what the suspension is awaited to perform. They were set up in cooperation with Adj.Prof. Gunnar Olsson [3]. To that a recommended target value of track width $< 1,5$ [m] was set.

Table 1.1: Static target values from previous works [1] & [2] set for front and rear axles

Static values	Unit	Permitted max. value	Permitted min. value
Static toe angle	deg	0,5	0,75
Static camber angle	deg	-0,5	-0,75
Static castor angle	deg	3	2
Castor trail (at hub)	mm	0	0
Kingpin angle	deg	12	10
Kingpin offset (wheel centre)	mm	50	40
Kingpin offset (ground)	mm	0	-10
Mechanical trail (castor trail)	mm	20	14
Roll centre height front	mm	60	20
Roll centre height rear	mm	100	30
Anti dive	%	20	0
Anti lift	%	70	20-10
Longitudinal compliance	mm	3-4	0
Target insulation freq.	Hz	1,2	1

Table 1.2: Derivative target values from previous works [1] & [2] set for front and rear axles

Static values	Unit	Permitted max. value	Permitted min. value
Toe angle change	deg/mm travel	-0,004	-0,0015
Camber angle change	deg/mm travel	-0,0082	-0,0122
Wheel base change	mm/mm travel	0,008	0
Bump steer	toe in	toe in	0 toe in

Figure 1.1: *Rear view of the frame*

1.5.3 OEM parts

As the thesis doesn't have any intention to design or invent new types of commercially widely available parts like tyres, rims, brakes, steering racks, springs and dampers they are to be acquired to make the construction of the prototype vehicle possible. These parts will inevitably dictate limitations as their weight, shape and function are not easily altered within the thesis scope.

1.5.4 Software

The software used to achieve the results (simulation and computation) is limited to the at Chalmers during thesis time available software. For kinematic analysis Lotus SHARK, IPG Kinematics and Matlab is to be used. For whole vehicle simulations IPG CarMaker. Catia V5 is used to make the CAD models needed and Catia V5 and/or Ansys is used to perform the FEA analysis. As there some problems with the software combination was experienced an evaluation was made as well as a Matlab script for IPG Kinematics post processing. This as the built in functions were found to require too much manual work. The evaluation and Matlab script is shown in Appendix F.

1.6 Report structure

In the thesis the results of work are presented and theoretical terms needed to understand the text are explained. It describes the requirements, process, brief theory of different solutions and ends by making full vehicle driving simulations drawing conclusions.

Chapter 2

Method - An iterative design process

This chapter will give a proposed sequence for efficient and correct development of suspension systems similar to this case. The case in this development was governed by the limitation of an already existing frame that couldn't be altered because it had been tested for crash safety in the existing shape and no resources were available to redo this work if modifications should have been wanted.

This step by step guide is written as I have in this work been faced quite often with the problem of an iterative process with many possible starting points and no clear idea where to start, as the work process just seems to go round and round.

1. Make an estimate of all known vehicle components COG, coordinates and inertias. This is needed to be able to estimate the overall COG coordinates and inertia for design of suspension. This is either done by real life measurements, or by modelling in a CAD-software.

2. Set the desired static value spectrum of wheel base, track width, turning circle, static angles, anti lift/dive etc. (as stated in Section 3.1).

3. Set the desired angle changes due to roll, bump/rebound.

4. The turning circle needs to be checked to the ratio of wheelbase to turning radius.

5. The articulation of wheel needs to be checked to track width and whatever limitations the existing body/frame imposes, i.e. ensure that the wheel can turn the desired angle.

6. Selection of suspension type that complies to set target values in points 1 to 5.

7. The suspension geometry is to be designed at this point, complying with the set data in steps 1-4 above.

8. Now create (virtual) CAD models according/complying with the geometry (step 7).

9. Test the designed suspension against the set requirements (in some simulation software).

10. Now perform an iteration of point 1 to 9. Repeat this until the needed changes in coordinates of total COG is neglectable (i.e. you have at this point found the COG for which you designed your suspension geometry)

The process is visualized by the flow chart on next page.

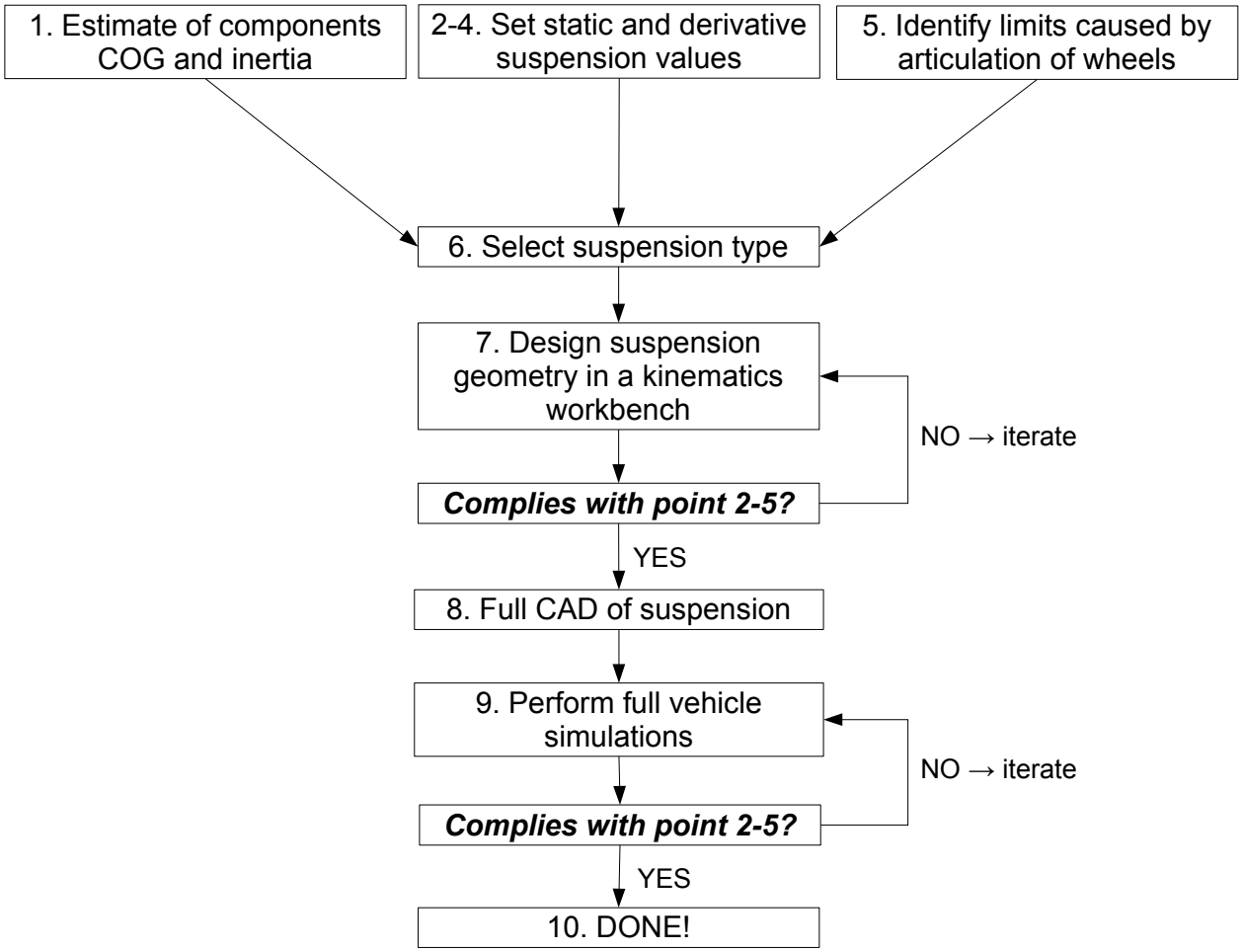

Figure 2.1: *Flowchart or suspension design process*

Chapter 3
Requirements

This chapter covers the set requirements on the suspension performance and design. The requirements were set by results of literature study, prescribed and assumed values. As the vehicle didn't have a concrete requirement list this step needed to dictate the direction of the development work.

3.1 General requirements

The general requirements for this vehicle describes and dictates the non-measurable (as in without a number value) performance and features of the suspension.

- The suspension should be wheel-individually adjustable, so that various modifications and testing can be done with this vehicle as a test bed (prescribed feature from Chalmers).
- The vehicles suspension should perform well in it's main driving environment (cities), at speeds not exceeding 50 [km/h] (assumed requirement).
- The vehicle should feel and be safe, not rolling too much during cornering or drive (prescribed from Chalmers).
- The vehicle should be comfortable, as in soft, not back braking "sporty" hard (prescribed from Chalmers).
- The manoeuvrability should fulfilling the drivers needs to easily and with a safe feeling get through city traffic (prescribed from Chalmers).
- The vehicle should be capable of carrying a driver equivalent to a 2 [m] tall, 100 [kg] heavy person.

Although the vehicle should mainly be driven at speeds of maximum 50 [km/h] the suspension should still be able to handle at least 90 [km/h] for general knowledge of how this vehicle type can handle higher speeds (prescribed from Chalmers).

3.2 Requirements on complete vehicle dynamics

The following are the requirements on the complete vehicle, which are tested in simulation Chapters 7 and 8.

- Static ground clearance of 160 [mm] (assumed by study of various cars and city obstacles).
- Track width maximum 1,5 [m] (set by earlier work [1] & [2]).
- Turning circle target 6m, allowable 7,5 [m] (set after study of competitor vehicles and road lane widths).
- All parts should be dimensioned for the loads that can occur at higher speeds (90km/h) (prescribed in Section 3.1).
- Soft/comfortable ride (RMS value of sub/around 1) (EU Directive 2002/44/EC).
- Target eigenfrequency 1-1,2 [Hz] ([2] & [4]).
- Roll limited to 7 [deg/g] ([4]).
- Rim/tyre size as narrow as possible due to the low weight of the vehicle (assumed as most car tyres will easily carry the load that this type of sub 500 [kg] vehicle might generate).
- The vehicle should be understeered (as it is safer for the average driver).
- The vehicle should not roll over (untripped) during a double lane change manoeuvre (DLC) at neither 50 [km/h] or 90 [km/h] (prescribed from Chalmers).

3.3 Requirements on vehicle suspension

As the vehicle should run at lower speeds lateral performance is not central. The suspensions main task is to insulate the driver/vehicle body from bumps when going in a longitudinal direction, e.g. one wheel bump and two wheel bump scenarios.

- Wheel travel ± 100 [mm].
- Camber should according to Gunnar Olsson [3] be -0.5 [deg] at static case and "maximum" -4 [deg] at full bump. For rebound opposite values are to be achieved.
- The steering is to be designed as close to the ideal Ackerman of 100 [%] as possible at endpoints and sub 100 [%] elsewhere.
- The suspension parts shall be able to withstand forces corresponding to vertical acceleration of 16g, to ensure no instant failures in case of driving into a very hard bump or pothole.
- The suspension components that are not bought off the shelf need to be manufacturable with manual machines in the workshop of Chalmers.
- The number of individual components should be kept to a minimum to reduce cost and time for fabrication.

To the target values above, the old kinematic targets in Table 1.1 & 1.2 are added. These target values are used as a reference and the result might deviate somewhat from them.

The target values (in Section 3.2 and 3.3) are then evaluated with simulations in LSA SHARK and IPG CarMaker/Kinematics (see Chapter 8 and Appendix F.1.1).

The target values set as input for the development and simulation are used as a guiding staring point for the iterative development process, as no historical data on similar type of vehicle is found available.

Chapter 4
Theory

This chapter will give a brief overview of the theoretical part behind the thesis work. This is done mainly by describing the components of the suspension and their function and influence on the vehicles characteristics.

4.1 Tyres

Tyres are one of the main limiting factors of any suspension. They are the only parts of a car, or any other vehicle with wheels that has contact with the surface the vehicle is being driven on, and thus transferring the longitudinal and lateral forces from/to the vehicle as well as through their deformation isolating the vehicle partially from the road harshness. From this it is to be seen that the tyre is not only responsible for a vehicles handling, but also for the comfort of the driver. The handling of the vehicle influences on the vehicles manoeuvrability/controllability and thereby on the safety of the vehicle. The rolling resistance of a tyre must also be considered as it influences the energy consumption of a vehicle, and thereby the environment and economy. In this section the most common tyre types, tyre characteristics/physical behaviour will be explained. This section is based on parts of [5] & [6]. A key factor in the later selection of tyre is it's rolling resistance and grip as that both influences the vehicles handling and range. According to Wong [6] the main contributor to rolling resistance (about 90-95%) is made up of the internal losses due to the tyres hysteresis. Hysteresis is a phenomenon that occur on on any material that is deformed, but is significantly high for e.g. rubbers. In short part of the force that is absorbed by the rubber is not released as in a spring (when it springs from compressed to uncompressed state) but is instead converted to heat. Hysteresis is frequency/speed dependent as it acts with a certain delay after the unloading/changed loading of a part. The data used [6] is though for a higher speed range, but as the tyre is deflected and deformed at any speed. Wong also states that about 2-10% of the rolling resistance of a tyre is from friction against the surface and the rest of the rolling resistance is from aerodynamic effects. Furthermore there is an indication that the rolling resistance is influenced by the tyre diameter, especially on softer & less even surfaces. The rolling resistance decreases overall with increasing tyre diameter.

4.1.1 Tyre types

There are three main tyre types: bias-ply, bias-ply belted and radial-ply belted. The plies and belts are usually made up of (usually) nylon or steel cords. The function of the plies and belt is to add support and stiffness to the less stiff rubber. Bias-ply tyres (cross ply or diagonal tyres) are uncommon in road vehicle application nowadays. They consist of plies arranged in a criss-cross pattern with an angle of about 80 [deg] versus each other, or about 40 [deg] to the centre line of the tyre (crown angle). This method results in a vertically rougher stiff tire with strong side walls and a fairly low weight. Due to this stiff arrangement the tyre has a higher rolling resistance. This type of construction is in modern times mainly found on some motorbike tyres, as they require low weight and stiff side walls.

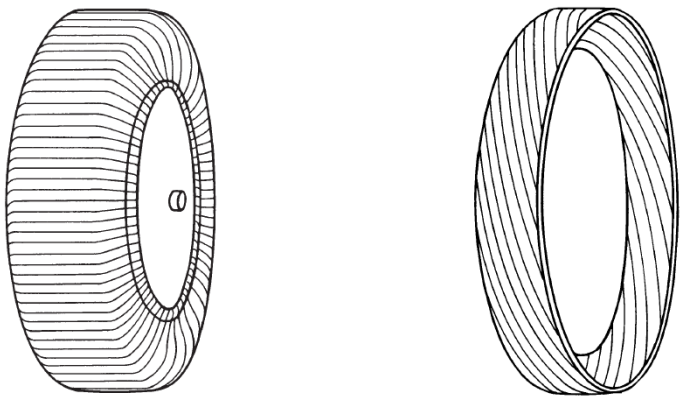

Figure 4.1: *Example of a radial tyre belt (left) and diagonal belt (right). [7]*

Nowadays mainly one commercially available tyre type for road cars exists. It's the radial-ply tyre (also referred to as radial tyre, radial belt tyre and sometimes radial steel belted tyre, steel radial tyre etc.). Its main characteristic is the orientation of the plies. They are oriented in the radial direction, and give the tyre it's softer side walls (which is good for easy deformation and thereby lower rolling resistance and higher comfort). This tyre must however be reinforced with belts which run circumferentially between the plies and the thread. The belts are also made up of cords, arranged usually with a crown angle of 20 [deg]. This results in a marginally heavier tyre but with much less rolling resistance than the bias-ply and better vertical springing comfort. The traction of the radial-ply tyre is in most cases superior the traction of the bias-ply. Furthermore it exists a bias-ply-belted tyre, which is has the characteristics somewhere in between the bias-ply and the radial-ply. Examples on tyre belts for radial and diagonal can be seen in Figure 4.1. Tyres are classified by the weight they can support and the forces (introduced by the vehicle travel speed) they can withstand. The load rating is standardized by ETRTO [8] and is usually in the range of 60-110 [laod units] for passenger vehicle type of tyre. That corresponds to a maximum load of 250 - 1060 [kg/tyre]. The speed rating is quoted in a unit range system (for the most common tyres) of Q to V, which corresponds to a maximum speed of 160-240 [km/h]. The tyres vary in tread width (width of the tyre contact patch cross section), inner diameter and profile height. Generally the higher the tyre the softer it can be without the risk of damaging the rim and also makes it possible for the tyre to deform sideways more easy. This then can account for a softer ride over a lower profile tyre. The larger the tyre, the easier it generally rolls [6]. As one of the main contributors to mechanical rolling resistance is the hysteresis in the tyre due to deformation, thinner sidewalls and treads are preferable.

4.2 Suspension

A vehicles suspension connects the main body and the wheel (rim with tyre). As the name indicates the vehicle body is suspended by the suspension. The suspension usually consists of some sort of fixture that holds the wheel in fixed (with some minor deflections) in x- & y-plane and permits the wheel to travel in the z-direction. This fixture includes in most cases a spring and damper combination. The spring taking up the weight of the vehicle, permitting the wheel to move parallel (or almost parallel to) the z-plane and returning the wheel/body to it's original position/height. The damper thereby absorbs the acceleration of the movement and prevents the system from oscillating. For comfort the longitudinal compliance (hence how good the wheel can move in the x-direction at impact) is important, as the wheel then at impact can travel backwards and up instead of just up, or up and forwards and by doing that reducing the instantaneous force peak sent into the body/frame later transferred to the driver. In this section the most common suspension types will be explained. This section is based mainly on parts of [5], [9] and [7]. Suspension types can be categorized into three groups, non-independent, semi-dependent and independent. A non-independent suspension is of a type where one wheels motion directly upsets/influences an other wheels motion, angles etc. A semi-dependent is in between the non-independent and independent type with movements somewhat less interfering with the opposite side, but still interfering somewhat. An independent suspension is by definition the contrary to the non-independent one. The angles and motion of the wheels can though be upset by forces that are transferred through the body or introduced due to e.g. body roll.

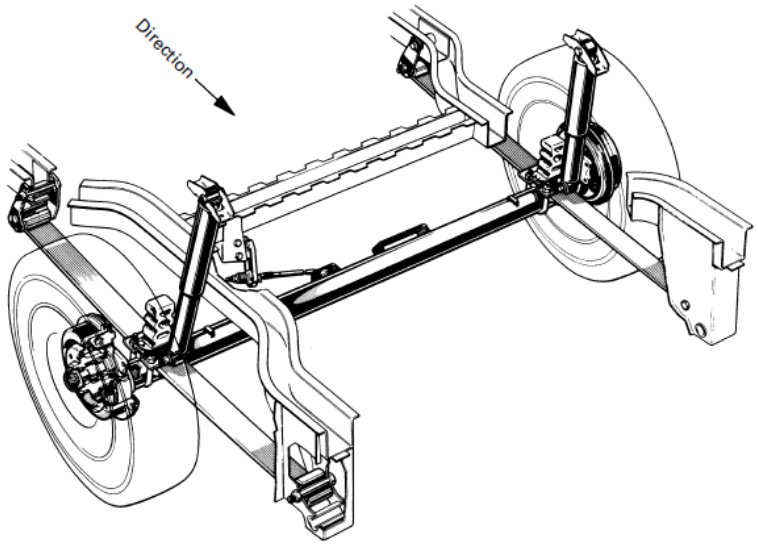

Figure 4.2: *Example of a solid or "dead" axle as on the Ford Escort Express (rear, non-driven). [7]*

4.2.1 Non-independent suspension

A non-independent suspension is when the movement of a wheel on one side of the vehicle directly interferes/alters the angles of the wheel on the opposite side, as they are interconnected with a (ideally) fully rigid axle which don't permit independent movement. There are mainly 2 different types of non-dependent suspension for cars: the beam axle (divided in the driven "live axle" and the non driven "dead axle") and the De Dion axle (driven). The later one allowing a lower unsprung mass than the ordinary non-dependent beam axle. Apart from the unsprung mass they are fairly similar in the overall function. An example of the dead axle can be seen in Figure 4.2. When going over a 2-wheel bump the whole axle is translated vertically without angle changes. As the wheels are connected via a stiff member there is no track width alternation. Over a one wheel bump however the wheel angles are altered as one side is directly connected to the other. During cornering it there are no camber changes, but on other hand one can instead get wheel lift. The main advantage of this suspension type is simplicity and rigidity. The disadvantages are a lack of any greater kinematic and elastokinematic tunability, high unsprung mass, bad longitudinal compliance and that the wheel angles have a interconnected dependent behaviour. This type of suspension is nowadays usually found in off-road vehicles, commercial vehicles and vehicles where rigidity and durability is a key issue over comfort. The axle is kept in position with either links or as in some case with a leaf spring.

4.2.2 Semi-dependent suspension

The most common semi-dependent suspension is the twist beam (Figure 4.3). It's a light torsional beam that interconnects a "trailing arm" on each side of the vehicle. This type of suspension is somewhere between the rigid axle and the trailing arm. It is cheap, fairly light and compact (simplifying packaging). The performance is not as good as most of the independent suspension types. It is to be found as a rear axle on may cars (mainly low power non sports cars, where price is more important than performance).

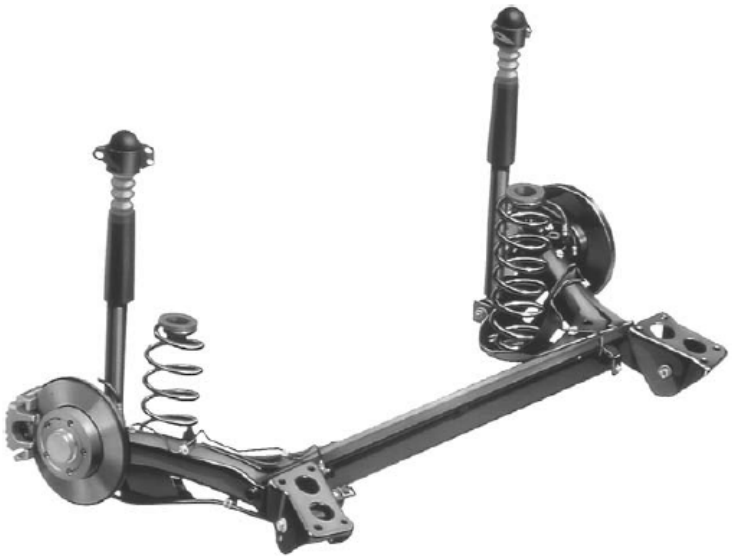

Figure 4.3: *Example of a twist beam axle of the VW Golf Mk 4 (rear, non-driven). [7]*

4.2.3 Independent suspensions

These types of suspensions allow the individual wheel to move without interfering with any other wheel. This allows to be able to control angle changes directly at each specific wheel due to bumps, drop, roll etc. These systems are overall much more complex than the non-independent and semi-dependent ones, but usually allow however much greater possibilities for tuning and also result in a lower unsprung mass. It is hard to generally quantify a "better" or "worse" type, as they are tunable and therefore a simpler type can have as good performance (if not better) as a less good executed complex solution. The independent types of suspension have generally more degrees of freedom over the non-independent and therefore can poses (if designed correctly) a better longitudinal compliance than suspensions with fewer degrees of freedom (i.e. non-independent and semi-dependent). The independent suspensions are most common as a suspension solution for most of today's cars (especially as front suspension), and have been implemented since the 1920's. There are quite some variety of different types, and the most common/relevant will be explained briefly.

4.2.3.1 Sliding pillar

Maybe most known from early Morgan cars this suspension has been to be seen in various cars (mainly made by Morgan) since end of 19th century and mainly in the first half of the 20th century (Figure 4.4). Though Morgan is still using them. The suspension functions by the movement of the hub/upright/pillar assembly up and down through some guiding pillar in an otherwise rigid axle or arms. This type of suspension allows not too much travel, requires fairly many specially made parts, has not too good longitudinal compliance and the track width changes during vertical movement of the wheel. The unsprung mass is slightly lower than for the semi-independent and non-independent suspension types, but that is about the biggest benefit of it. It is generally only used for front suspension on cars, but can also be found in the rear of a few motorcycles (the called a plunger suspension).

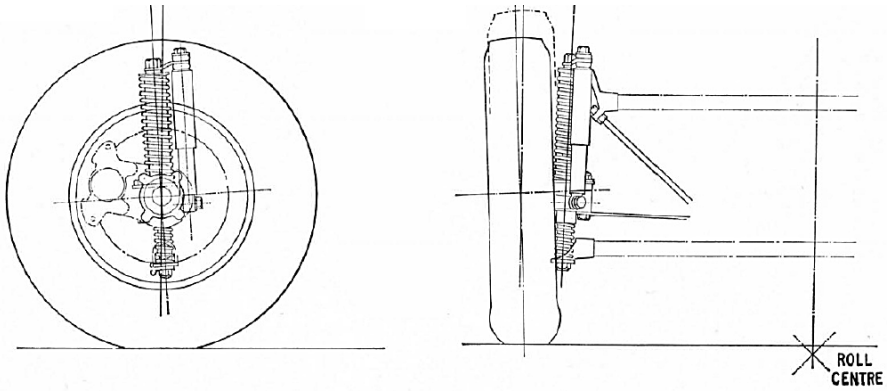

Figure 4.4: *Example of a Morgan sliding pillar suspension (front, non-driven). [9]*

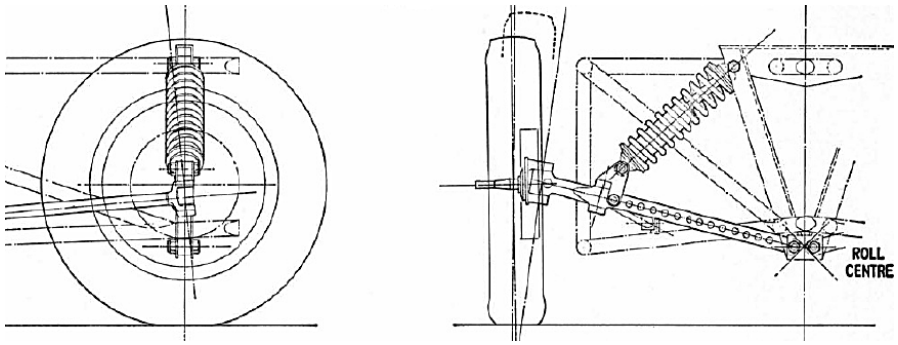

Figure 4.5: *Example of a swing axle from a Lotus Mk 8 (front, non-driven). [9]*

4.2.3.2 Swing axle

The swing axle suspension (Figure 4.5) consists of a lower arm (in vehicles y-direction) mounted fairly central (or just made up of the driven axle coming out of the rigidly mounted differential). It is assisted in x-direction by either linkage, leaf spring or the arm itself if mounted in 2 points. The main benefits is that the wheels can travel independently, the unsprung mass is lower than for beam axle. The drawbacks are greater camber change at travel compared to other e.g. the double wishbone suspension, as the wheel is mounted with a fixed angle to the drive shaft/arm holding it. It is the predecessor of the double wishbone suspension. It has been among others used on original Volkswagens and a few British cars in the 1950's and 1960's. There it showed a tendency for jacking during cornering. It can easily be fairly unstable and therefore less safe than other, as simple or cheap solutions. The setup itself is about as heavy or light as the double wishbone or the McPherson. It has previously (before the introduction of double wishbone and McPherson) been mostly found as suspension on driven axle (but it also existed non-driven applications).

4.2.3.3 Double wishbone

The double wishbone suspension (Figure 4.6) consists of two arms (often of a triangular wishbone-like shape, this suspension is also called "double A-arm") that holds the upright. It allows the upright to partially retain the camber angle on bump/drop/roll. The double wishbone is more complex than the McPherson strut, usually also less compact and hence more bulky and expensive. It is usually found on sports cars. It has been the predominant suspension type of choice of may sports car manufacturers and racing teams since its introduction in the 1930's. In order to minimize the alteration of the camber angle and track width the arms have to be fairly long, which in most cases can seem impractical due to packaging restraints. It generally doesn't have as good longitudinal compliance as the multi-link type, but on the other hand is far less complex on average.

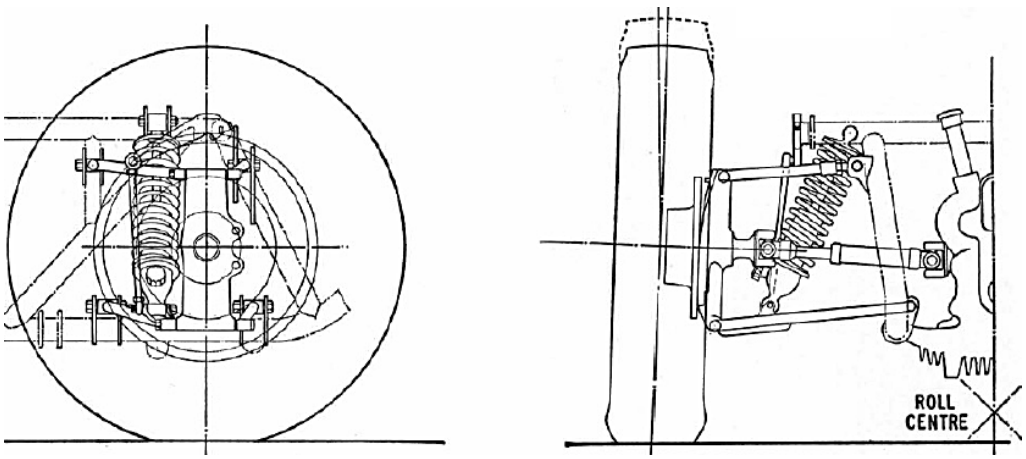

Figure 4.6: *Example of a double wishbone suspension, Lotus Nineteen (rear, driven). [9]*

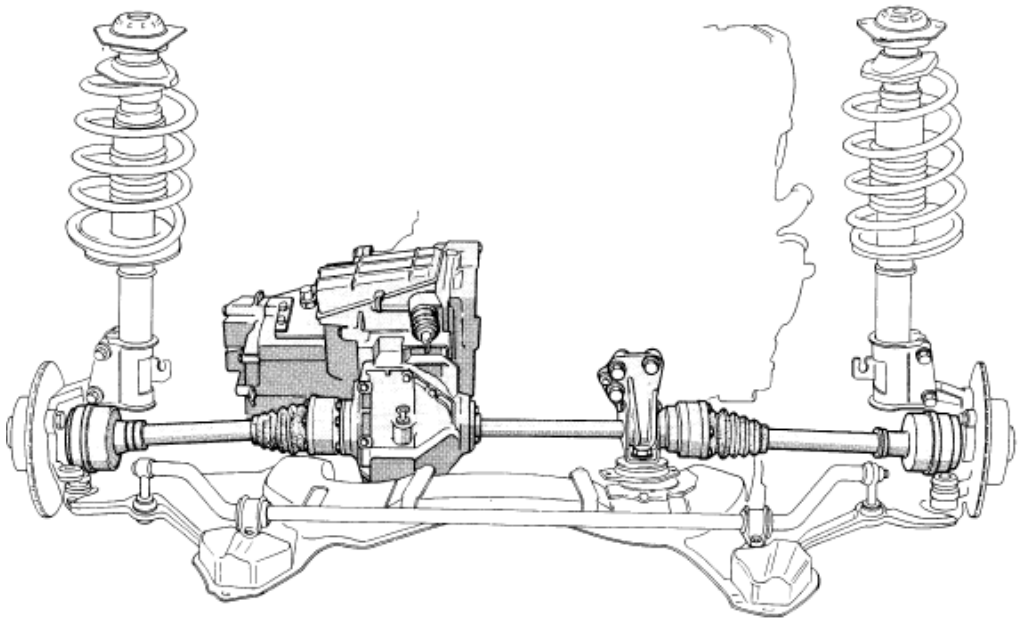

Figure 4.7: *Example of a McPherson strut as on the Lancia Thema (front, driven). [7]*

4.2.3.4 MacPherson strut

The MacPherson (Figure 4.7) strut is a suspension that consists of a lower arm, a control arm and an upright which is usually blended with the lower mounting of the damper and spring assembly. It is rougher simple and compact, allowing usage of shorter lower arm without generating too much camber angle change at bump. It is usually utilized as front suspension on most modern cars. Some models even has it for rear suspension. Its main advantages are cost effectiveness and the compact arrangement, while the disadvantages are that is generally not as adjustable as a double wishbone or multi-link. With tuning of the elastokinematics (selection of correct bushings) this type of suspension can posses a favourable longitudinal compliance characteristic, not far from a good multi-link suspension. It's main strength is performance close to the double wishbone and multi-link but generally a cheaper design.

4.2.3.5 Chapman strut

The function and structure of the Chapman strut is a variety of the McPherson strut (used only on non-steered, driven axles), with the difference that the drive shaft can be used as a control arm. This results in slightly lower unsprung mass compared to the standard McPherson.

4.2.3.6 Trailing arm

A trailing arm (Figure 4.8) is an arm, connected usually in the front of the wheels position (x-direction). The arm can swivel about the front connection point(-s). This type of suspension is compact and simple. Depending how it is constructed it can be more or less prone to influence the camber angle and track width during bump and cornering. It is usually used as rear suspension. It has been however used as front suspension on the Citroën 2CV (then referred to as a leading arm).

Figure 4.8: *Example of a trailing arm suspension as on the Mercedes-Benz A class Mk1 (rear, non-driven). The lateral round beam is a part of the rear subframe. [7]*

4.2.3.7 Multi-link

A multi-link suspension (Figure 4.9) has multiple links (more than the double wishbone) and is the most independently tunable system of them all (each parameter can be set without upsetting other parameters if designed correctly). It has more degrees of freedom than the other suspension types (number depends on design) and can therefore have good compliance (both mechanic and/or elastokinematic) resluting in good road holding and ride comfort. It is however the more complex and expensive. It is usually utilized where handling performance is the key issue rougher than cost, but can in some cases also be utilized for packaging reasons. It has been most common in the rear of cars, but some cars utilize it in the front as well. The unsprung weight is generally on pair if not slightly higher compared to the double wishbone suspension.

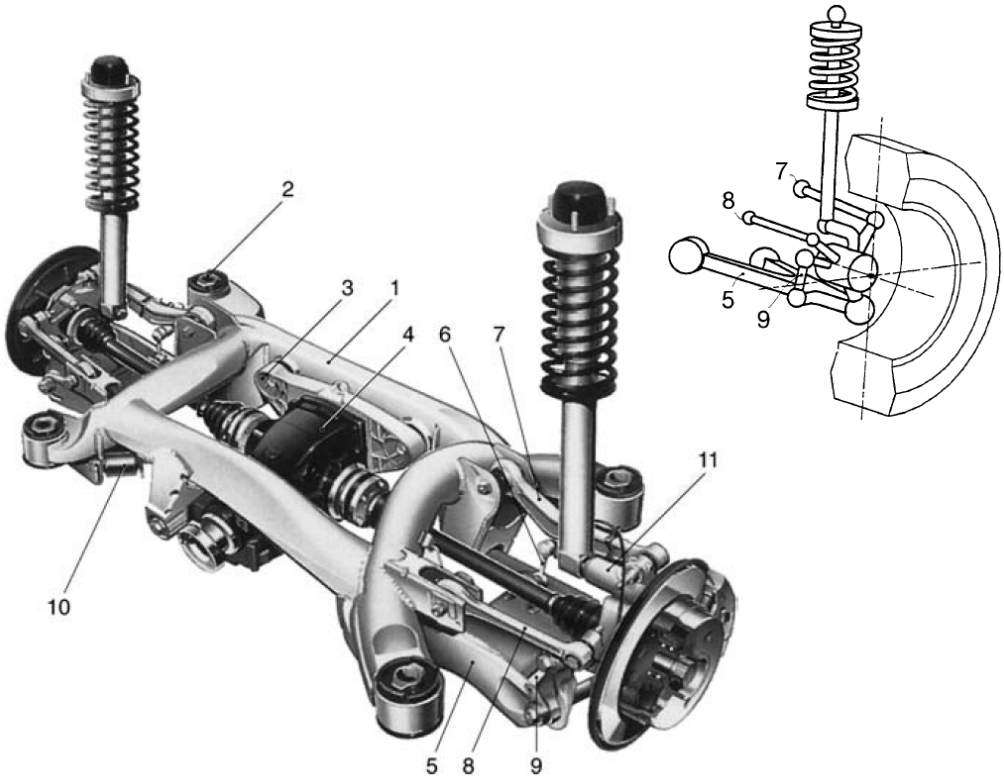

Figure 4.9: *Example of a multi link rear suspension as on the BMW 5-series E39 (rear, driven). [7]*

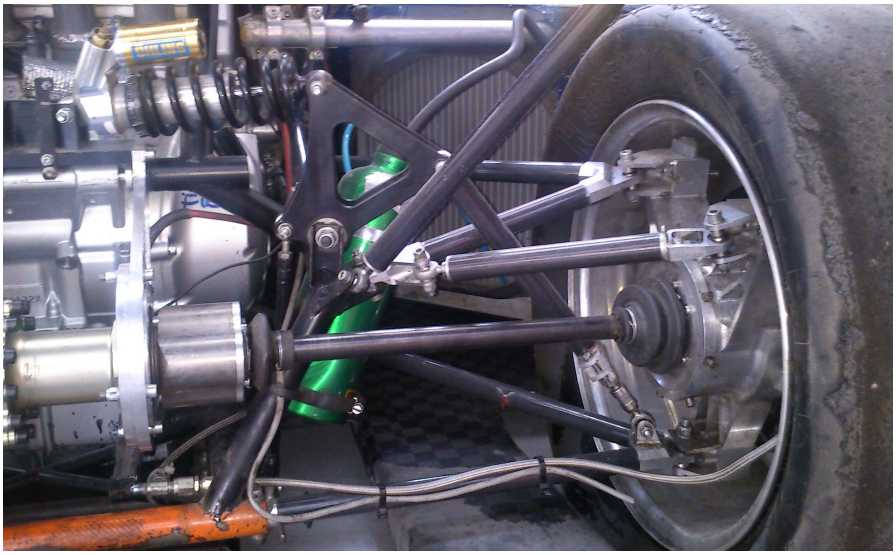

Figure 4.10: *Example of push rod on double wishbone arrangement as on Chalmers Formula Student car 2012 (rear, driven).*

4.3 Pull and push rod

The connection of damper, spring or damper and spring assembly in a suspension system can in a few cases be done via pull or push rods. If the rod is stressed by compression during bump it is referred to as push rod, if it is tensed it is referred to as pull rod. The utilization of either or can enhance various characteristics of the vehicle and it's suspension. The use is most common on vehicles with double wishbone and multi-link type suspension but can also be used on swing axle suspension. By using either or, the damper, spring or damper and spring assembly can be placed in a more favourable way (for vehicle COG optimization) aid packaging restraints or reduce the effect of installation ratios (also called motion ratios) by introducing leaver effects over the pivot link. By using pull or push rods one can also reduce aerodynamic drag (as often seen on F1 cars). The downside is a generally higher unsprung weight over direct mounted damper and spring (e.g. direct body to lower wishbone on double wishbone suspension). An example of a push rod arrangement can be seen in Figure 4.10.

4.4 Springs

Springs are the key component that keeps the vehicle level by carrying the sprung vehicle weight and lets the wheels still deflect vertically versus the vehicle body. Here are the most common types described and briefly explained.

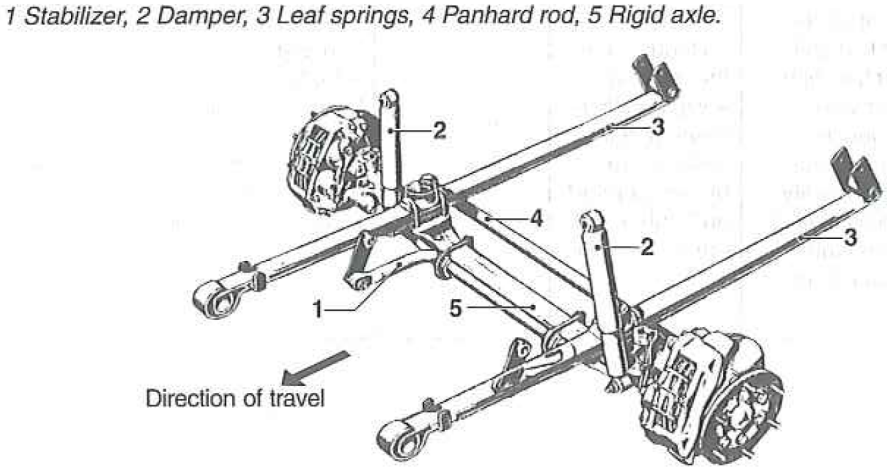

Figure 4.11: *Example of leaf spring arrangement, non-driven axle. [10]*

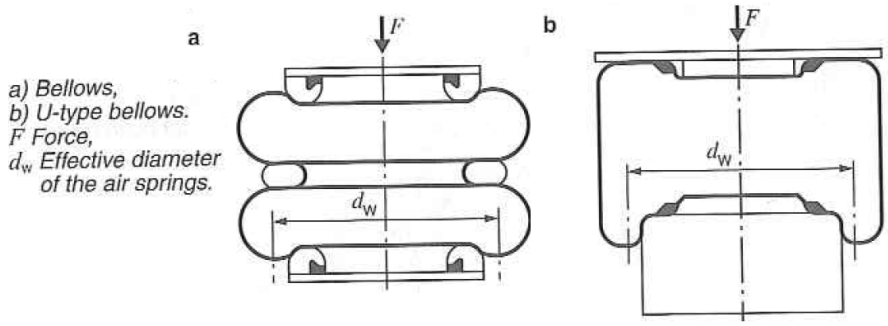

Figure 4.12: *Example of pneumatic (gas) spring. [10]*

4.4.1 Leaf spring

The leaf spring (as illustrated by Figure 4.11) is a elastic component made up of flat rods (usually steel, but composite ones also exist). The leaf spring has been used for centuries and is in modern time mainly used on heavy and utilitarian vehicles. It can often be built very durable. Usually the suspensions utilizing it lack good comfort both due to their compatibility as e.g. the live/dead axle as described in Section 4.2.1.

4.4.2 Pneumatic / hydropneumatic spring

Air springs (pneumatic) and combined air and hydraulic springs (hydropneumatic) has been in use in various applications from small components on cars to springs for truck suspension. The spring functions by compression of a fluid (usually air). The spring rate can be easily altered by variation of compressed fluid in the system and thereby adapt ride and ride height. The downside is a complex and costly system. An example can be seen in Figure 4.12.

4.4.3 Torsion spring

Torsion springs consist of a bar that reacts elastically due to a turning (twisting) momentum that is excreted on it (Figure 4.13). This type of spring is usually very durable and cheap, but can be a limitation to the design due to limit of elastic range of the material before it deforms. Higher deviations need longer bars to twist and can therefore end up too long. Maybe the most common use is the suspension of the old VW Beetle and old Porche 911's.

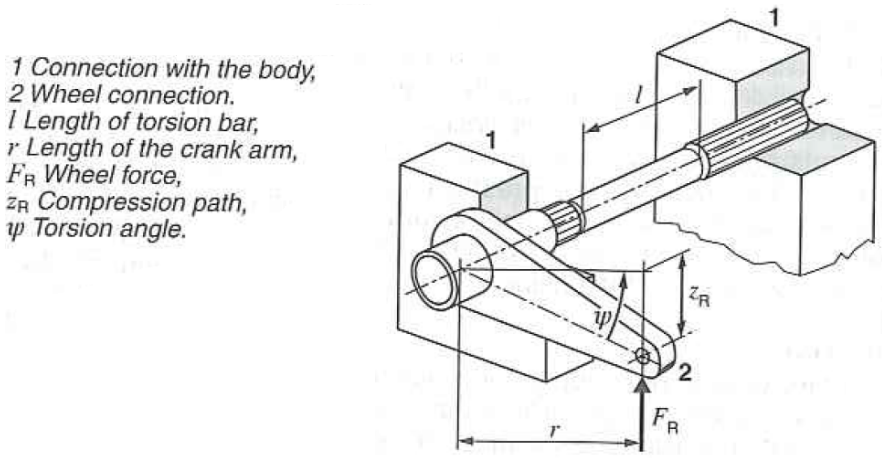

Figure 4.13: *Example of torsion spring. [10]*

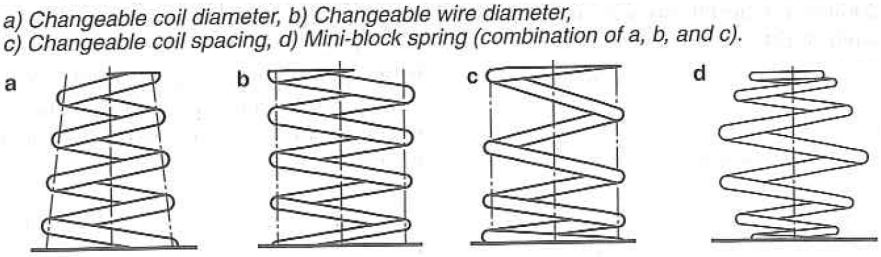

Figure 4.14: *Example of coil springs with non linear characteristics. [10]*

4.4.4 Coil spring

The coil spring is today the most common type of spring. It consists of a coil (usually in steel) that can be compressed in the direction of the coils. This type of spring can allow a compact and still light and fairly robust design. It can easily be altered to give the wanted spring rate (by altering the wire or coil diameter). In some applications it can have a non linear spring rate depending on geometrical deviation from the perfect uniform coil (Figure 4.14). It can be mounted either separate or in a coil over damper arrangement to save space (Figure 4.10).

4.5 Anti-roll bar

The anti-roll bar (also known as stabilizer bar/spring) consist usually of a torsion spring interconnecting the right and left side of a suspension (front or rear), thereby hindering the body to roll by contra-acting on the opposide side of wheel movement. I.e. at roll, one side (the side that the body rolls towards, usually the outer side during cornering) has compression in the suspension due to the roll movement. The body then at the same time also wants to lift on the opposite side. The anti-roll bar contra-acts this movement by creating a lifting force on the inner wheel (upwards force) and thereby exerting a aligning torque about the roll axis.
An example of anti-roll bar can be seen in Figure 4.7, where it's the bar connecting the two wishbones.

4.6 Shock absorbers

Shock absorbers (also referred to as dampers) are a part of almost any the conventional suspension system to prevent oscillations. They dissipate the force that otherwise could make the suspension and vehicle to oscillate due to road unevenness. To do this the mechanical work done by the piston movement is transformed into heat and then dissipated into the dampers surroundings. They are classified into single and twin tube type (Figure 4.15). The single tube dissipate this heat better than the twin tube and is generally lighter, but tends to be longer for the same stroke length (less compact). The twin tube damper has generally a softer response. The twin tube damper is the more common type in the average road car. The damper characteristics can be altered by altering the valves on the pistons, in the twin tube case changing the channel characteristic between the outer and inner tube, but also by changing the gas volume / compensating chamber pressure. Both type of dampers can be equipped with different stages by incorporation channels inside the tube where the piston acts, so that for some part of the stroke some fractions of the fluid can e.g. escape through a bypass and thereby make the damping characteristic somewhat softer in that region.

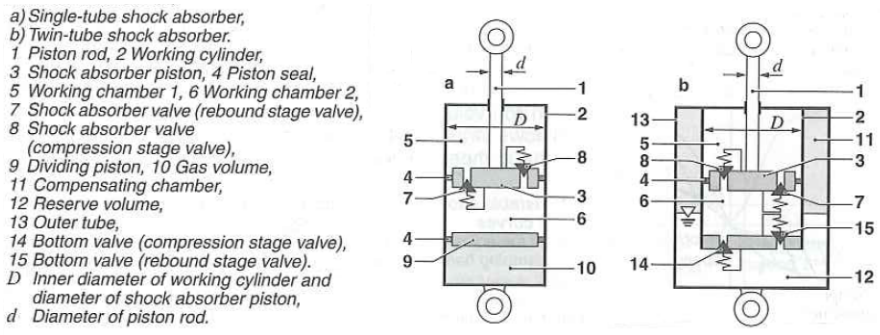

Figure 4.15: *Example of single- and twin-tube shock absorbers. [10]*

4.7 Tyre slip

The slip is the amount/fraction of the speed of wheel or vehicle versus the speed (directional) of the tyre tread. Generally in both longitudinal and lateral direction the maximum grip is achieved for some low slip (that is greater than 0). This as if slip is equal 0, the tyre tread doesn't deform and the contact patch isn't increased.

4.7.1 Longitudinal slip

The longitudinal slip describes the relationship between the wheel's (and vehicles) longitudinal speed and the speed that is achieved by rotation of the tyre, i.e. the treads peripheral speed versus the ground.
Due to deflection during rolling the speed of the tread and the speed of the wheel are not totally equal.
The longitudinal slip is defined in different ways depending if it's a breaking or accelerating manoeuvre (Equations 4.1 and 4.2).

$$s_{x_{driven}} = \frac{R_e * \omega - v_x}{R_e * \omega} \ [\%] \tag{4.1}$$

$$s_{x_{brake}} = \frac{R_e * \omega - v_x}{v_x} \ [\%] \tag{4.2}$$

4.7.2 Lateral slip

The lateral slip is defined as a fraction between the lateral velocity and the transportation speed of the tyre surface elements through the contact patch (Equation 4.3).
The lateral velocity is due to the cornering of a vehicle.

$$s_y = \frac{v_y}{|R_e * \omega + v_x|/2} \ [\%] \tag{4.3}$$

The slip angle α is defined as in Equation 4.4.

$$\alpha = \arctan(\frac{v_y}{v_x}) \ [rad] \tag{4.4}$$

The slip angle can tell one about how well (or bad) the tyres track versus the direction they are thought to go. If one has little slip angle the tyres travel in the same direction that they are pointed, while for big slip angles the tyres are less prone to do so. As mentioned earlier, for low slip angles the lateral grip actually increase, but then decreases fast.

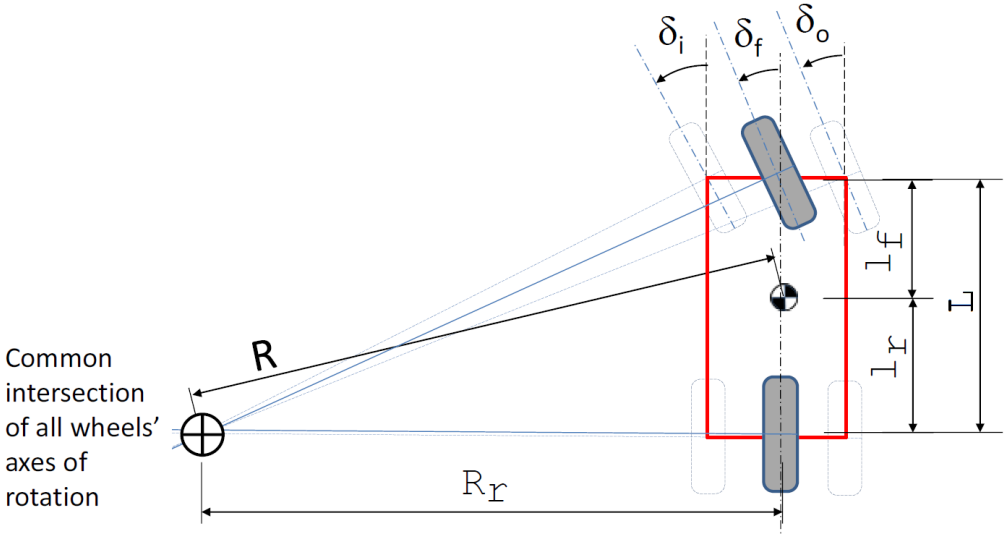

Figure 4.16: *One track model. [5]*

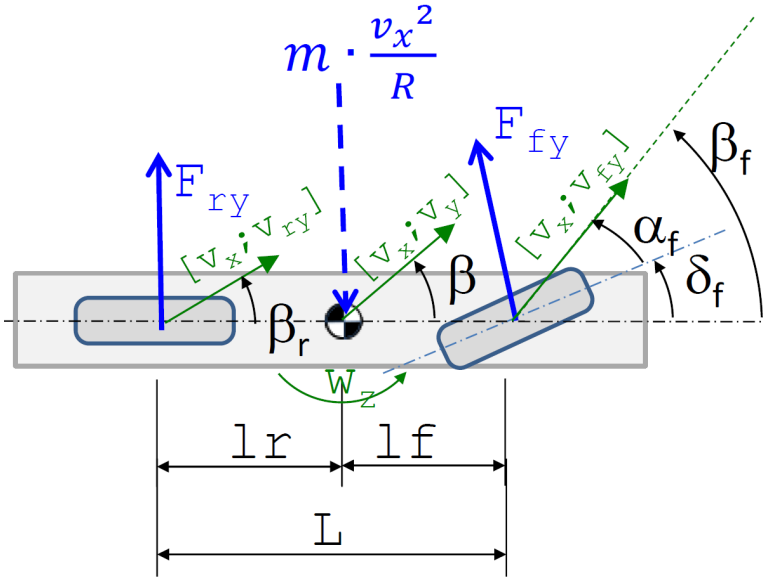

Figure 4.17: *One track model with slip. [5]*

4.8 Basic steering - one track model

The one track model is an approximation of the vehicles two sides as seen in Figure 4.16. This model is used for various computations when an approximation is judged to be sufficient to reduce computation.
Assuming big radii R_f can be approximated to $R \approx R_r$. This then leads to an expression for the theoretically needed steering angle δ_f in Equation 4.5.

$$\delta_f = \frac{L}{R} \tag{4.5}$$

4.9 Oversteer and understeer

From Equation 4.9 it can be seen that the needed steer input, for a certain turning radius R and wheelbase L is affected by the slip angles front and rear. Over-, neutral- and understeer is expressions telling if the vehicle yaw/turning behaviour is greater, smaller or linear to the steer input angle. The characteristics can be either deduced from comparison of the slip angles, or by computation of the understeer coefficient K_u (which involves the slip angles). The Equations 4.6 - 4.11 are cited from [5] using the case pictured in Figure 4.17.

$$Force\ equilibrium: \quad m * \frac{v_x^2}{R} = F_{fy} + F_{ry} \tag{4.6}$$

$$Moment\ equilibrium: \quad F_{fy} * l_f - F_{ry} * l_r = 0 \tag{4.7}$$

$$Constitution: \quad F_{fy} - C_f * \alpha_f; \quad F_{ry} = -C_r * \alpha_r \tag{4.8}$$

$$Compatibility: \quad \delta_f + \alpha_f - \alpha_r = \frac{L}{R} \tag{4.9}$$

$$Steer\ angle: \quad \delta_f = \frac{L}{R} + K_u * \frac{m * v_x^2}{R} \tag{4.10}$$

$$Understeer\ coefficient: \quad K_u = \frac{C_r * l_r - C_f * l_f}{C_f * C_r * L} \tag{4.11}$$

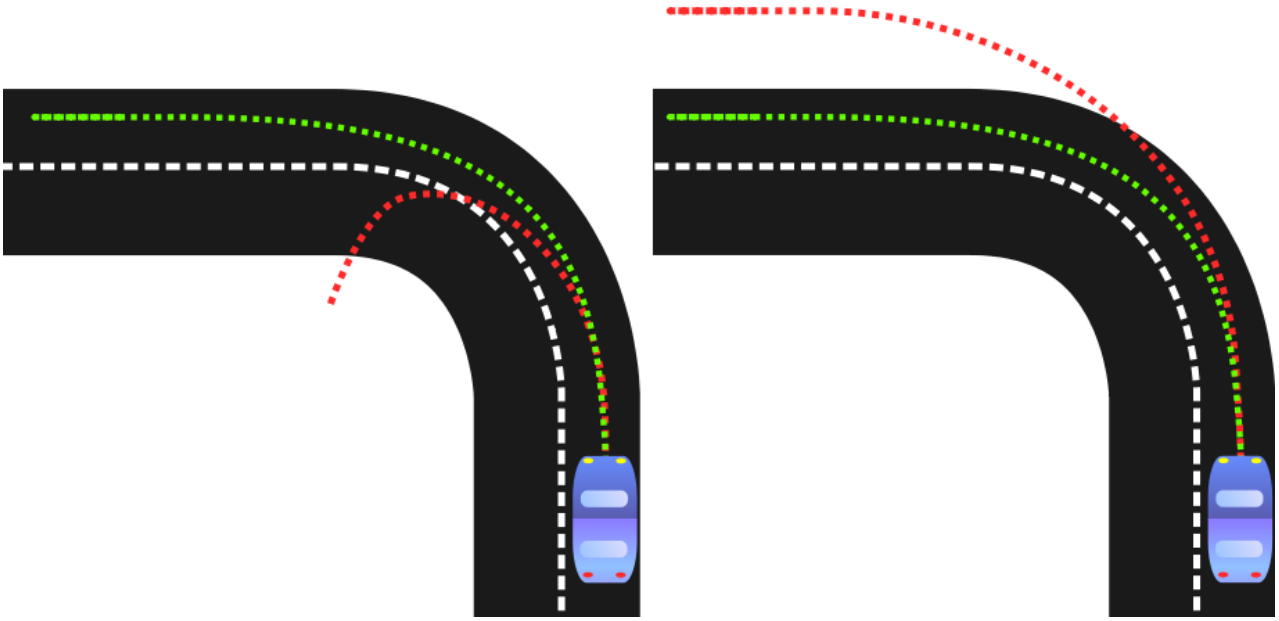

Figure 4.18: *Green - desired vehicle path, neutralsteer. Red left path, oversteered. Red right path, understeered. [11]*

4.9.1 Neutral steer

In Equation 4.9 if the front slip angle (α_f) is equal to rear slip angle (α_r) the needed steer input as δ_f i.e. the same as for the case without side slip. This behaviour is called neutral steer, as the vehicle yaw/turning is linear to the steer input. It is theoretically the wanted behaviour, but is hard to achieve in real life and as it is on the edge between over- and understeer it can be hard to control. The understeer coefficient $K_u = 0$ for neutralsteer case. The type of path this behaviour gives is represented by the green line in Figure 4.18.

4.9.2 Oversteer

If the rear slip angle (in Equation 4.9) is greater than the front slip angle the needed input is smaller than δ_f which means that the vehicle tends to turn more than what the driver intends by a given steering input (oversteered, as in left of Figure 4.18). Oversteer can be described of an over-amplification of the yaw gain versus for a given steering input making the vehicle turn more about its z-axis than intended enabling the vehicle easily spin out. The understeer coefficient is $K_u < 0$ for oversteered vehicles.
Oversteer is regarded as an unstable reaction of the vehicle (although it can be exploited by an experienced driver to make the vehicle corner faster) and therefore is generally refrained from as handling characteristic for the average vehicle which instead is preferred to be understeered.

4.9.3 Understeer

If the front slip angle (in Equation 4.9) is greater than the rear slip angle the needed input is greater than δ_f which means that the vehicle tends to turn less than what the driver intends by a given steering input (understeered, as in right of Figure 4.18). Understeer can be described as an under-amplification of the yaw gain for a given steering input making the vehicle turn less about its z-axis than intended and thereby slide forwards. The understeer coefficient is $K_u > 0$ for understeered vehicles. Understeer is regarded as the default wanted response of a vehicle, as it is easier to handle for a less experienced driver and therefore can be seen as more predictive without quick surprising behaviour (minimizing the risk of spinning out).

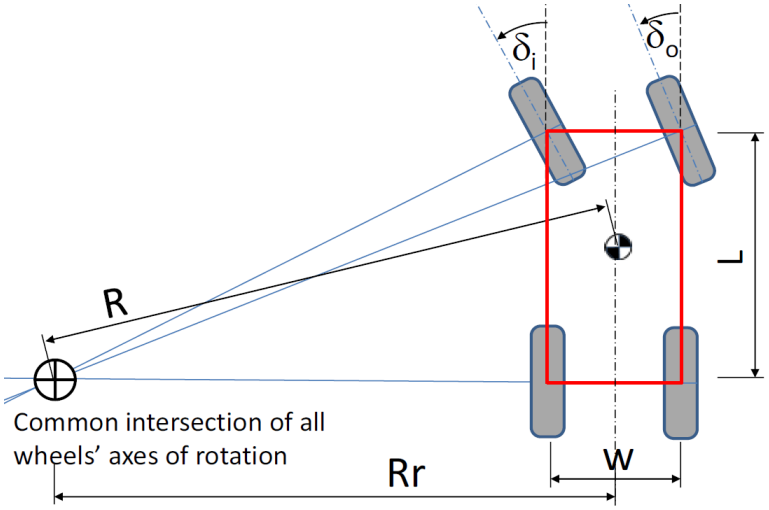

Figure 4.19: *Ackermann steering geometry, front steering axle. [5]*

4.10 Ackermann steering

The Ackermann steering geometry is designed in such way that the inner front wheel (assumed that the vehicle is steered over the front axle) turns more than the outer wheel when cornering (as illustrated in Figure 4.19). This results in a common rotational point for both the front wheels and the rear axle. This results in it's turn that the scrub of the tyres (non rolling lateral/partly lateral sliding motion) is reduced to 0. The result is a vehicle with good manoeuvrability (and less heavy steering feel). However it is less practical for high speed stability, where the parallel steering arrangement is preferred (both front wheels steer the same amount).
As noted previously, assuming big radii R_f can be approximated to $R \approx R_r$.

4.11 Wheel alignment characteristics

To describe the suspension characteristics one also needs to understand the fundamental wheel alignment angles of a suspension system. These are shown in Figure 4.20 as for a double wishbone suspension, but the same is applicable to all suspensions.

4.11.1 Camber angle

The camber angle is the angle that the wheel has versus the xz-plane. This inclination is defined as positive if the wheel is tilted outwards versus the zx-plane (and negative if wheel is tilted inwards). The angle shown in Figure 4.20-a is positive. The camber angle can influence both the rolling resistance (varying amount of hysteresis depending on angle) and lateral characteristics of the vehicle (by camber thrust). It also influences the straight line stability of the vehicle if it is driven over a bump. Generally one prefers slight negative camber change at bump, as it then (if the wheels are operated at camber close to 0 °) the camber thrust is created or enlarged forcing the vehicle towards it's centre line and aiding straight line stability.

4.11.2 Kingpin angle and axis

The kingpin axis is the axis that passes through the upright's (sometimes referred to as steering knuckle) two swivel points (Figure 4.20). In case of a multi-link arrangement this angle is computed on the virtual swivel points created by the rotating (about an axis slightly angled versus the z-axis) movement of the upright. This axis angle versus the xz-plane is defined as the kingpin angle. This angle is positive if the axis leans inwards (to the vehicle centre plane) at the top. The kingpin angle can also influence the steering depending on its size. The bigger the angle the more the tyres needs to be deformed or vehicle front lifted as the wheels are pivoted by the kingpin axis.

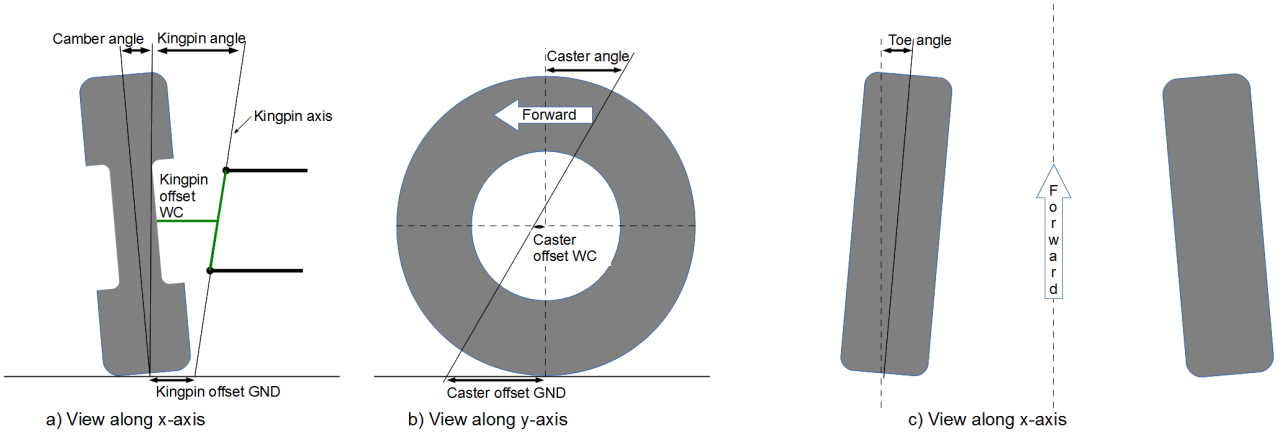

Figure 4.20: *Wheel alignment angles*

4.11.3 Scrub - kingpin axis offset at ground

The point that the kingpin axis intersects at ground level gives arise to the kingpin offset (versus the wheel centre line). This distance is also referred to as scrub radius in some contexts. It describes the leaver that the forces from the tyre contact at ground will exert it's momentum with about the kingpin axis. It is defined as positive if it is closer to the vehicle centre plane (xz-plane) than the wheel centre plane and negative for the contrary. If the scrub radius is positive the wheels tends to be pushed towards toe out during braking manoeuvre and toe in for negative scrub.

4.11.4 Castor angle

The castor angle is the angle is the angle that the kingpin axis creates when the vehicle and wheel is viewed from the side (in the xz-plane). This angle is positive when the kingpin axis top point is tilted towards the rear of the vehicle (Figure 4.20-b). The distance between the wheels vertical axis and the point that the kingpin axis intersects the ground is the caster offset at ground level, also referred to as wheel trail or castor trail. The caster angle influences the straight forward stability and steering force (force needed to articulate/turn the wheels). The greater the caster angle (<45 °) the higher the longitudinal stability, but also the greater the steering force.

4.11.5 Toe angle

The toe angle is the angle created by the offset of the wheel longitudinal plane and the vehicles longitudinal plane (Figure 4.20-c). It is defined positive when the front of the wheel is pointing towards the vehicle centre plane (toe in) and negative when pointing outwards (toe out). For straight line stability toe is an important angle. Generally the toe should be designed in such way that the wheels are turned forwards by the driving torque (driven wheels) or rolling resistance (non driven wheels), eliminating play and pensioning the elastokinematic suspension elements (bushings and alike). The turning direction is dependent on the scrub radius and it's direction (positive/negative) and length. During this thesis this elastokinematic motion will be disregarded as it is outside the thesis scope.

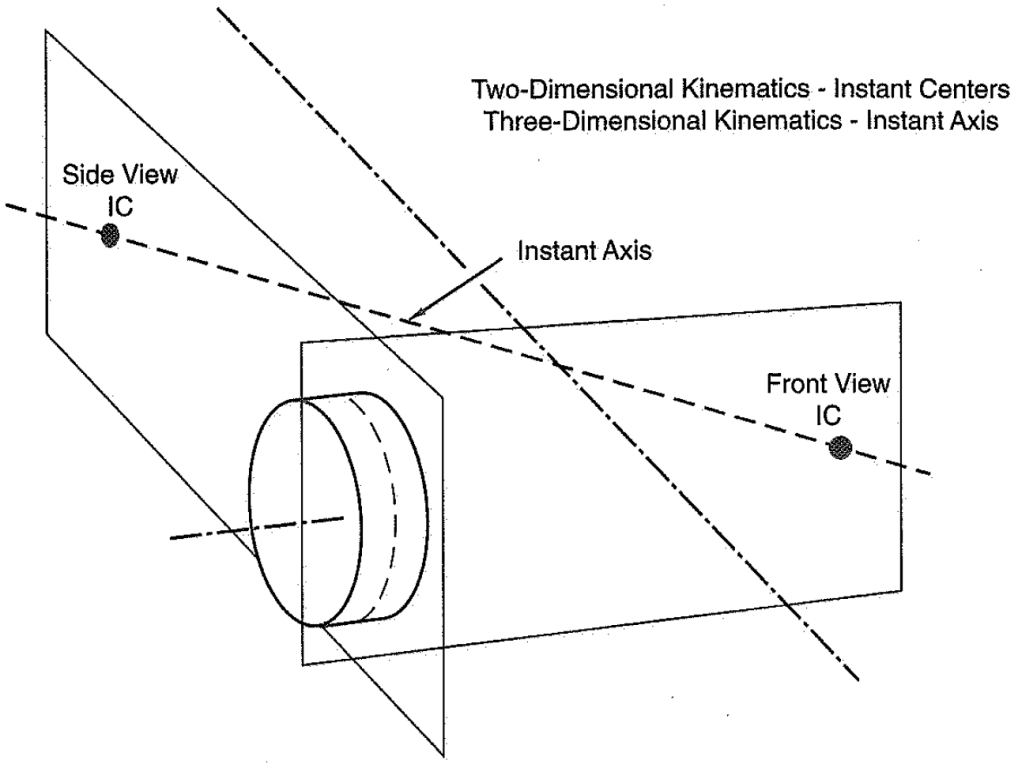

Figure 4.21: *Instant centres of rotation and the instant axis of rotation [4]*

4.12 Movements

A few factors, that occur due to suspension and body movement relevant for this thesis body roll, anti dive and anti squat are explained for better understanding of the text. The explanation given covers a simplified 2D-case movement of mainly the suspension versus the vehicle body, though in real life the movement is of course in 3D. The instant centres of rotation shown in Figure 4.21. In the 2D case the movement only along the xz-plane or yz-plane is studied separately approximating the movement in the 3D as e.g. the wheel moves about the instant axis and not about the instant centres separately.

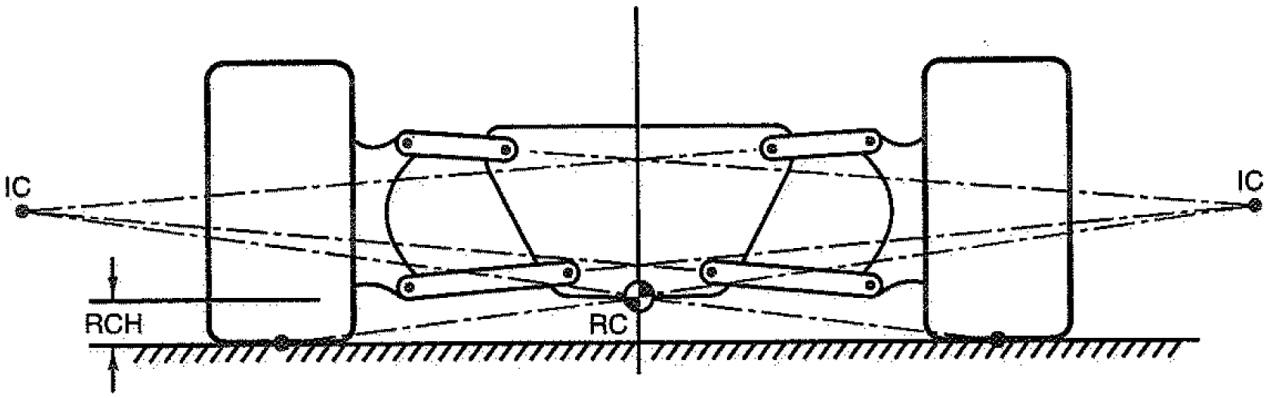

Figure 4.22: *Roll centre of a double wishbone suspension [4]*

4.12.1 Body roll

Body roll is the movement the vehicle body performs about the vehicles roll axis due to lateral acceleration. It describes the vehicle bodys sideways tilting movement about the roll axis. The roll axis is a virtual axis interconnecting the front and rear roll centre (RC). The movement is usually measured with a roll angle defined as the angle between the z-axis and the xz-plane through the centreline of vehicle and a roll rate or gradient that defines degrees roll per lateral acceleration [deg/g].

4.12.2 Anti dive

Anti dive is a measure of the suspension linkage geometry restrictive influence on the vehicles tendency to pitch downwards the front by compressing the front suspension during braking manoeuvre. It can be approximated as in Equation 4.12 (illustrated in Figure 4.23). Ordinary passenger cars usually have anti dive value in a range of 5 to 25 [%].

$$Anti\ dive\ [\%] = \frac{e_f}{g_f} * 100 \tag{4.12}$$

4.12.3 Anti squat

Anti dive is a measure of the suspension linkage geometry restrictive influence on the vehicles tendency to pitch downwards in the rear by compressing the rear suspension during acceleration manoeuvre. It can be approximated as in Equation 4.13. Ordinary passenger cars (if rear wheel driven) usually have anti squat value in a range of 10 to 70 [%].

$$Anti\ squat\ [\%] = \frac{e_r}{g_r} * 100 \tag{4.13}$$

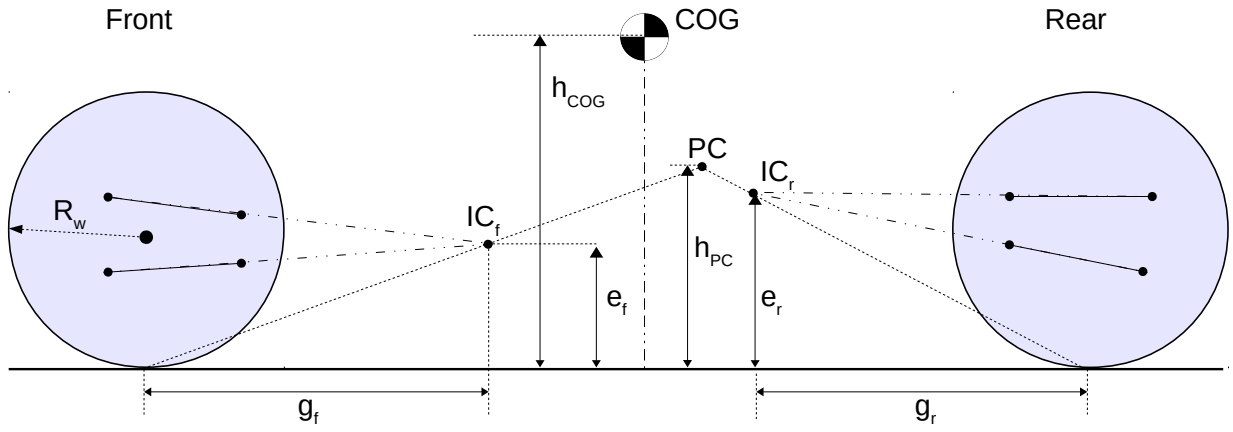

Figure 4.23: *Anti dive and anti squat*

Chapter 5
Selection of tyre and suspension

In this chapter the selection of tyre and suspension type, size is explained.

5.1 Selection of tyre

The selection of tyre is much more limited than the selection of suspension type. A new tyre type/model can't be created specially for this project. The result is that the tyres to use must be available market. The tyre is a main component of the unsprung mass. The ratio of unsprung to sprung mass is ideally kept to minimum. This because the inertia of the unsprung mass should be much lower than the one of sprung mass so that the unsprung mass easier can move without transferring the movement to the sprung mass and thereby insulating the sprung mass from the road. Due to this, the aim is as light tyre as possible. As most of the road tyres are built in fairly the same way, with the same components this results in a recommendation for the smallest (and therefore lightest) tyre (i.e. the same size of the average tyre weigh approximately the same as any other competing tyre). This however contradicts the wish for a big radius tyre as tyres with bigger radii have lower rolling resistance and easier glide over uneven parts of the road surface. Adding to that it is also not to be forgot that this vehicle should be able to be driven in wintertime, which requires M+S tyres. M+S tyres are not available in the smallest/narrowest dimensions.

5.1.1 Tyre rolling resistance rating

The rolling resistance (COMMISSION REGULATION (EU) No 228/2011) declared for the narrower tyres however is not as good as the for e.g. 195 width, which is common with the hybrid, eco, high mpg etc. cars. Rating might though not be accurate this case here as the load is much lower than for what the regulation prescribes (60-90% of the tyre's load capacity, i.e. at least 200 [kg/tyre] in PUNCH case, which is no where close to the target weight). Running narrower tyres with a high profile however results in a smaller cross section being deformed at road contact, i.e. lower hysteresis losses and softer/higher side walls which results in better insulation from the road and therefore comfort. A narrow tyre has also the advantage over the wider one that it is less sensitive to camber change due to wheel travel. For simplicity reasons it is strongly favoured to utilize same width tyre front and rear to keep the number of components low.

5.1.2 Selected tyre dimension

A reasonable, available (exists as both summer and winter tyre) compromise to size is a 135 wide tyre on a 15 inch rim. The rim width should be 4 inch wide according to ETRTO [8]. Using the 15x4J rim also allows using of 145 wide tyres in case of the 135 wide tyres not being available. As the available 135 wide tyres typically have a load rating of 70 (335kg) the load rating can be neglected, as the awaited loads of the vehicle are much lower. The speed rating is also neglected due to the vehicles low top speed versus the typical rating of (T=190km/h) for this size of tyre. Hence PUNCH is to run 135/70 R15 tyres on 15x4J rims (for vertical ride comfort in wheel hop mode and better road adhesion due to lower inertia of the wheel).

5.1.3 Selected rim

After making the conclusion on tyre size above the market was surveyed for suitable rims and tyres. It turned out that narrow rims are very uncommon, with just 3-5 models from car OEM's available that used suitable sizes. It is among others Citroën C0, Peugeot iOn, Mitsubishi i-MiEV and the Smart ForTwo (front wheels). As most of the cars using 15x4J rims as standard are not the long and big series models making acquiring parts a potential problem. Fortunately the first generation of Ford Focus utilized this size as its spare wheel. Although the Ford Focus spare wheel runs a 125/80R15 tyre, the rim can house a wider tyre (Section 5.1.2) if needed and parts as brakes, drive shafts, etc. are easily and widely available on the market.

5.2 Selection of suspension

The selection of suspension type is performed with weighted Pugh matrix, also known as a decision matrix. Therein one of the suspension types is set as reference and the rest are evaluated compared to the reference. The weights are selected/set to the more/less important features. The solution with the most points is the technically best solution.

Table 5.1: Weighted Pugh matrix

Weight	Characteristic	Beam axle	De Dion	Twist beam	Sliding pillar	Swing axle	Double wishbone	MacPherson	Chapman	Trailing arm	Multi-link
4	Unsprung mass	0	1	2	2	2	4	3	4	2	4
6	Packaging freedom	0	1	2	3	2	4	5	5	2	4
7	Development time	0	-1	-2	-2	-2	-3	-3	-4	-2	-3
5	Ease of manufacturing	0	-1	-1	-2	-2	-3	-3	-4	-2	-3
8	Adjustability	0	0	1	2	2	4	3	3	2	5
3	Camber change bump	0	0	-1	0	-1	0	-1	-1	-1	-1
2	Camber change roll	0	0	1	-1	-1	-1	-1	-1	-1	-1
1	Track change bump	0	0	-1	-1	-2	-1	-1	-1	-1	-1
		0	-2	7	15	5	33	24	16	6	38

From the Pugh matrix in Table 5.1 it is to be seen that this evaluation criteria (which are interpretations of the requirements in Chapter 3) gives a clear choice of the multi-link suspension type. In this evaluation multi-link it is interpreted as described in Section 4.2.3.7 (note: the Figure 4.9 represents a rear axle assembly). In a front assembly the links 7 or 8 in the picture might be moveable or have an extra link for steering.). To lower the complexity of the suspension (keeping it cost effective) the slightly simpler solution of double wishbone is chosen.

5.3 Selected solution

The selected solution consists of the subsystems and parts shown below (all Ford Focus parts are from the 1998-2005 model). If not stated, the same type of component is intended for all four wheels.

- Double wishbone suspension
- 135/70R15 tyre on 15x4J rim (or the Ford Focus 125/80R15 tyre as it is supplied with the rim)
- Ford Focus front wheel hubs
- Ford Focus front wheel bearing units
- Ford Focus front wheel hubs
- Ford Focus rear brake discs
- Ford Focus rear brake callipers
- Ford Focus rear clipper holder
- Some rack and pinion type steering that can be made to fit the hard points and characteristics (Subsection 7.2.3)
- TrakSPAX DA120/190 damper (for packaging reasons, easy to source and are built to specification on order) with corresponding valves to achieve a damping coefficient of: d_f=216 [N*s/m] (with preferred adjusting range 130-300 [N*s/m]) in the front and d_r=300 [N*s/m] (with preferred adjusting range 180-420 [N*s/m]) in the rear, as computed in Subsubsection 6.1.2.2 with one fourth of the damping coefficnet for bump and three fourths in rebound.
- Springs with spring rate (front) c_{sf}= 2018,5 [N/m] and (rear) c_{sr}= 3893 [N/m] mounted directly over damper, as computed in Subsubsection 6.1.1.7
- ARB with rate 4400 [N/m] and a motion ratio of 0,79 at the front axle (from full vehicle simulation in Subsection 8.2.2).

Chapter 6
Full vehicle simulation input data

This chapter covers the computation of the needed input data for the full vehicle simulations. The needed input data consists of data for springs, dampers, COG of parts, inertia of parts and mass of parts.

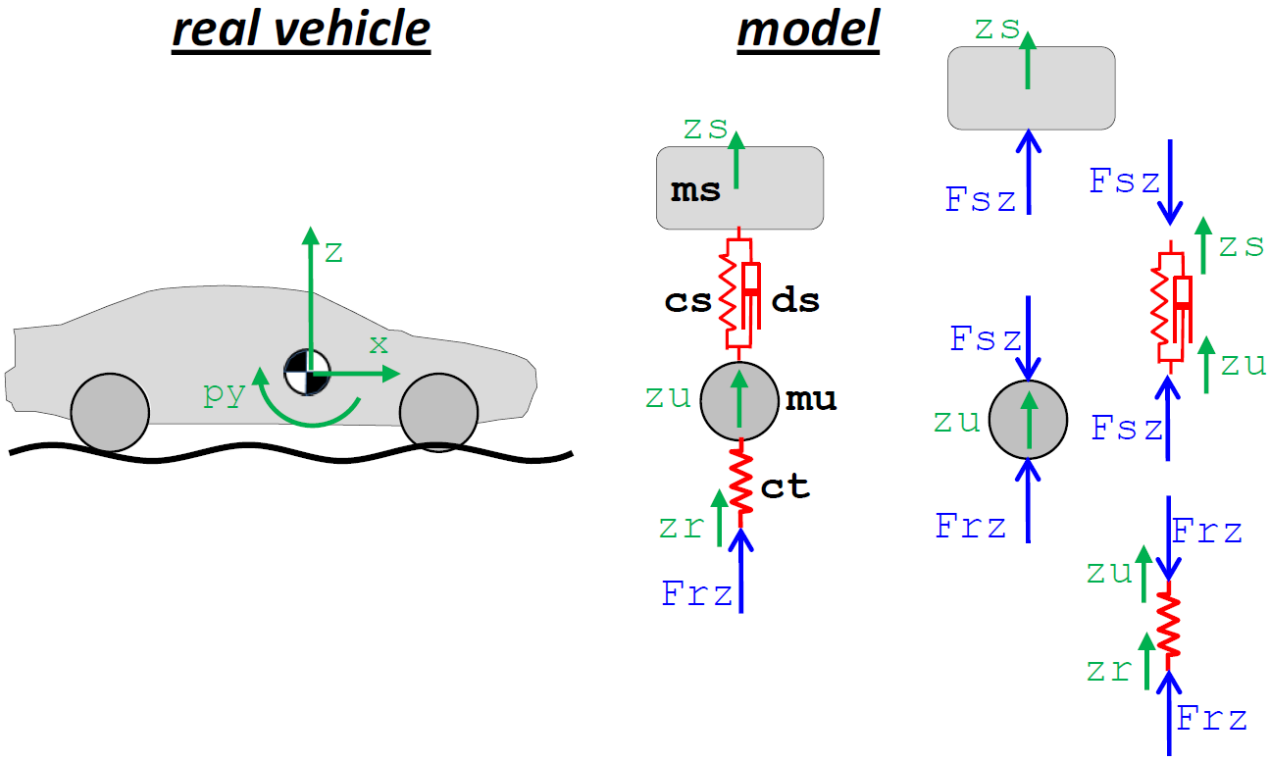

Figure 6.1: *1D model with two dynamic degrees of freedom [5]*

6.1 Spring and damper dimensioning

This section covers the calculations of the suspension characteristics, as spring rate, damper rate, roll rate/-gradient. Springs let the suspension move versus the body (in contrary to rigidly mounted wheels) whereby insulating the vehicle body and the driver from the road unevenness. The dampers in an automotive suspension refrains the spring from oscillate freely and makes the ride less shaky for the driver, as they usually are tuned to dampen out the oscillation induced by a bump within one to two periods of spring movement (assuming the movement of the spring to be described by e.g. a sinusoidal function). To ensure that the vehicle keeps the right ride height at curb level and that driver isn't exposed to road harshness correct spring rates and damping coefficient is crucial. The MATLAB code for the calculations performed in this section can also be seen in Appendix C.1.

6.1.1 Spring rate

The spring rate describes the amount of force it takes to compress a spring a certain distance. The usual SI-unit to describe this is [N/m], however in motor sport (as the damper used is of motor sport type) spring rates are often given in [N/mm] or [lbs/in] depending on manufacturer. The ride height is dependent on the spring rate, as the force needed to keep the vehicle body at the curb ride height should be exerted by the spring due to it's compression by the wheel travel from full rebound to curb height level.

6.1.1.1 Spring travel and damper travel

From the values in Appendix B, Figures B.3 and B.4, it is possible to read the damper travel for a the complete wheel travel presented in Table 6.1.

Table 6.1: Damper travel front and rear from full rebound to curb level [m]

d_{dtrf}=0,135 [m]	d_{dtrr}=0,138 [m]

6.1.1.2 Motion ratio

The motion ratio describes the ratio of movement of the suspension versus the movement of the wheel. The motion ratios front and rear MR_{f_0/r_0} at curb level can be read from Figures B.3 and B.4, Appendix B. As it is to be seen, the motion ratio is roughly 0,68 around curb level. This means that for an arbitrary vertical movement of 1 [length unit] of the wheel the spring and damper assembly moves 0,68 [length unit] close to curb level. The motion ratio however changes depending on the length of suspension travel. For longer travel during bump it increases and for longer rebound it decreases. This influences the damping in the way that the damping gets more effective for bigger bumps (harder damping) and less damping for rebound (wheel travels faster down to reach the ground).

6.1.1.3 Hooke's law - theoretical spring rate

The damper travel is equal to the compression of the spring from full rebound to curb level. This creates a force, according to the Hooke's law [12]:

$$F = c * x \tag{6.1}$$

In Equation 6.1 c=spring rate [N/m] and x=the displacement [m]. The displacement is equal to the damper/spring travel as in Table 6.1. The vertical component of force F keeps the vehicle body suspended at right ride height at curb level.

6.1.1.4 Normal loads

The unsprung mass is estimated to 40 [kg], which is equivalent to a normal force of ≈ 392[N].
From the model set up in IPG CarMaker the values for normal force subtracted the unsprung mass is extracted:

Table 6.2: Normal force (z-dir.) that the spring needs to support front and rear [N]/quarter

F_f=227 [N]	F_r=377 [N]

F_f and F_r are the quater-car normal force from the road on the front and rear wheels minus the unsprung mass (i.e. the weight that the springs need to support).

6.1.1.5 Ride frequencies

The ride frequencies (undamped frequency of the body during motion) are chosen to be typical values for passenger cars according to Equation 6.2 and 6.3 according to [4] and [13].

$$Front : f_{r_f} = 1[Hz] \tag{6.2}$$

$$Rear : f_{r_r} = 1,1[Hz] \tag{6.3}$$

f_{r_r} is selected to be 10% larger than f_{r_f} which is wanted according to [13].
The eigenfrequency for a harmonic undamped motion of the spring is given by [12] Equation 6.4.

$$\omega = \sqrt{\frac{c}{m}}\ [rad/s] \Leftrightarrow f = \frac{1}{2\pi}\sqrt{\frac{c}{m}}\ [Hz] \tag{6.4}$$

Where c [N/m] is the spring rate (wheel rate in this case) and m [kg] the mass in the mass spring system (unsprung mass in our case). Solving for c, with $\omega = f * 2 * \pi$ gives the wheel rate.

6.1.1.6 Wheel rate

The wheel rate (c_w) describes the "virtual spring stiffness" that the wheel "sees" vertically. For the evaluation in this case the motion ratio about the curb level point is used. The wheel rates can be seen in Equations 6.5 and 6.6.

$$c_{w_f} = (2 * \pi * f_{r_f})^2 * m_s f\ [N/m] \tag{6.5}$$

$$c_{w_r} = (2 * \pi * f_{r_r})^2 * m_s r\ [N/m] \tag{6.6}$$

6.1.1.7 Spring rate

The spring rate (c_s) describes the spring stiffness needed for holding the vehicle at a given curb height and for wanted eigenfrequency and wheel rate. It is defined as the wheel rate divided by the motion ratio (MR) squared. The computation of the spring rates are performed with Equations 6.7 and 6.8.

$$c_{s_f} = \frac{c_{w_f}}{MR_{f0}^2} = 2018,5[N/m] \tag{6.7}$$

$$c_{s_r} = \frac{c_{w_r}}{MR_{r0}^2} = 3893[N/m] \tag{6.8}$$

This are the wanted spring rates for the vehicle (i.e. the spring rates to be acquired). The free length should correspond to the dampers specifications and the compressed length (as computed in Subsubsection 6.1.2.4). The spring rates could however need to be tuned (resulting in slightly higher spring rates) once the vehicle is built, as the weight distribution estimation needs to be confirmed by full scale model.

6.1.1.8 Spring preload

The spring preload is the difference between the free length of spring and it's installed length. In this case it is needed to perform a minor preload on the springs so that they support the vehicle at the wanted curb height and not rattle if suspension is in it's fully extended mode (full rebound). The calculations for this are to be followed in Appendix C.1. In short the front spring should be (pre-)compressed $\approx$ 28 [mm] and the rear $\approx$ 13 [mm] during installation.

6.1.2 Damping

The damping in the spring and mass system reduces oscillations of the system. The damping force is proportional to the damper pistons speed. To express the damping force at a certain point a factor that is referred to as the damping coefficient is used. This coefficient is usually quoted in [Ns/m]. This damping coefficient value is not always linear, partially because the valving of the damper can give it different characteristics for various speeds, but also due to the motion ratio phenomenon that is described in Subsubsection 6.1.1.2. It is common to have a relation of 1:3 bump to rebound, e.g. if the bump value is 1000 [Ns/m] then the rebound is 3000 [Ns/m]. This so that the bump force at bump is deflected by movement of the wheel rougher than enlarging the shock wave travelling through the suspension linkage to the vehicle body. To compute the needed damping a few factors need to be computed.

6.1.2.1 Damping ratio

The damping ratio is the fraction of the damping coefficient divided by the critical damping coefficient ($\zeta = \frac{d}{d_{cr}}$). It describes the time it takes for the system to approaches it's final output value for a given input signal. The lower the ζ the faster is the response, but the bigger overshoot error occurs. For higher values of ζ the system response is slower, but with considerably lower overshoot error. In the case fo a spring damper system the overshoot error can be interpreted as under damping of the system and thereby reduction of comfort while a too slow response is a result of over damping and will give a harsh and unresponsive ride. According to [13] typical values are 0,25 for ride comfort maximizing road cars. Both this and the chosen value in Equation 6.9 can be tested on the finished vehicle if the damper is built adjustable and if the adjustment is of a favourable range. The chosen value (Equation 6.9) is a typical damping ratio for the average road car.

$$\zeta = 0,5 \ (chosen) \tag{6.9}$$

6.1.2.2 Damping coefficient

The damping critical coefficient (Equation 6.10 and 6.11) and the damping coefficient (Equation 6.12 and 6.13) is computed for the chosen data of ζ, c_w and m_s for front and rear according to [13].

$$d_{cr_f} = 2 * \sqrt{c_{wf} * m_{sf}}/MR_f \ [N * s/m] \tag{6.10}$$

$$d_{cr_r} = 2 * \sqrt{c_{wr} * m_{sr}}/MR_r \ [N * s/m] \tag{6.11}$$

$$d_f = d_{cr_f} * \zeta \approx 216 \ [N * s/m] \ for \ \zeta = 0.5 \tag{6.12}$$

$$d_r = d_{cr_r} * \zeta \approx 300 \ [N * s/m] \ for \ \zeta = 0.5 \tag{6.13}$$

This means that the bump coefficient should be 1/4 of the calculated damping coefficients and the rebound 3/4.

6.1.2.3 Damper length - first iteration

In order to know the needed damper length both the damper travel and the spring rates needs to be known. IPG CarMaker "model parameter check" computes the weight distribution on front and rear axis. The total weight (without body) is estimated to $\approx$ 292 [kg] and the weight distribution is 40/60 front to rear. This results in a normal force of $\approx$ 569[N] in the front and $\approx$ 864[N] at the rear.
The model check and IPG Kinematics gives a spring travel (equivalent to damper stroke) result of $\approx$ 140-150 [mm] for the $\pm$ 130 [mm] travel.
This would then require using the DA120/180 SPAX damper unit [14] which has an open length of 457 [mm] and closed length of 305 [mm].

The front lower wishbone has an approximate length of 272 [mm] (y-direction) between the centreline connecting the bushings at the car side and the outer ball joint connecting to the upright. The articulation of 130 $\pm$ [mm] results in an angle of $\pm$ 0,4983 [rad] ($\pm$ 28,55 °). As the distance of the damper mounts at the body (with coordinates in [mm]) [2440, 460, 470] and at the lower wishbone [2480, 650, 470] is = 358 [mm] and shows thereby that the damper can't be mounted at the desired place as it would bottom out for stroke of $\pm$ 75 [mm].

This then requires an alteration of the coordinates for damper so that the minimum length is 380+ [mm] in static position (as the damper closed length is minimum 305 [mm] and is then achieved at full bump). The rear shows roughly the same characteristic and problem.

A solution could be done by reducing the needed stroke of the damper/spring assembly.
This could be achieved by either moving the damper mount point lower at the body end or inwards at the lower wishbone end. As the lower wishbone can be approximated as a tube/beam one don't want to load in close to the centre of the span as it then is subjected to bending rougher than axial loads (that it can withstand better). So the only solution in the case of making the damper stroke shorter would be to move the inner

mounting point downwards. However this would reduce the damper ratio and thereby reducing ride comfort and handling levels.

Another solution would to mount the damper shifted slightly downwards versus the horizontal plane of lower wishbone. This would not reduce the damper ratio but still enable to extend the damper closed length.

At this stage it was decided to do an iteration of the design as now multiple points/characteristics (bump-toe angle characteristic and damper mounts) needed to be altered for a more optimal function.

6.1.2.4 Second iteration damper length alteration

The second iteration resulted in an altered positioning of the damper mount points front and rear. An other damper was selected DA120/190 as it's closed/open lengths are close to the DA120/180 one but permits longer stroke if needed in future. It however results in somewhat larger unsprung mass.

6.1.3 Anti-roll bars

To ensure that the vehicle doesn't lean more than wanted during a manoeuvre one uses various methods to limit the rolling motion. One of those methods is by using an anti-roll bar (ARB). The main reason for using ARB's over stiffness varying (active) springs and other solutions is that ARB is a simple and cheap method of limiting the roll. ARB's also influence a vehicles tendencies to over-/under-steer during manoeuvres. Generally a higher front roll stiffness results in a more under-steering vehicle, which in the case of a small city vehicle is to be regarded as a wanted safety feature/characteristic.

6.1.3.1 Roll gradient

The roll gradient describes the roll the vehicle will perform for a certain lateral acceleration. The unit used for calculations is [deg/g], i.e. degrees of roll per 1g lateral acceleration. In the case of PUNCH it is desired for it to behave close to an average family sedan. According to [4] a typical roll rate for a "Semi-Soft-Contemporary-middle-market sedan" is 7 [deg/g]. The roll general expression for the gradient is described by [13] Equation 6.14 where A is acceleration and ϕ the desired roll angle.

$$\frac{\phi}{A} = 7\ [deg/g]\ (chosen\ value) \tag{6.14}$$

6.1.3.2 Evaluation of roll

Most of the literature (as [13], [4] etc.) computes the desired roll rate as a function of front and rear stiffness together. To that the h-term (distance COG to roll axis) and W (weight of the vehicle) is computed for the whole vehicle at once. A mixed approach of [13], [4] and [5] will mainly be used in this thesis (with H=distance to roll axis - COG at the x-position of COG $H \approx 450$ [mm]), as analysing a new approach is outside it's scope. However this approach should be used with a bit of precaution, as the relative "COG" or more correct the weight distribution axis will not be even or at the same height of the vehicle and so won't the roll axis. This should ultimately mean that the front and rear of a car should be addressed individually, or with a formula taking the different heights of the weight distribution into account (an integral of the regional COG height along the x-axis) and which should reasonably result in that the desired roll rate will then differ front to rear.

First the total vertical spring stiffnesses are calculated (Equation 6.15 and 6.16). They consist of the front and rear wheel rate combined with the tyre rate (also in Appendix C.1).

$$C_{f_{tot}} = \frac{1}{(1/c_{w_f}) + (1/c_t)} \tag{6.15}$$

$$C_{r_{tot}} = \frac{1}{(1/c_{w_r}) + (1/c_t)} \tag{6.16}$$

Coupling the front and rear spring rates gives a combined virtual spring contra acting the roll movement (Equation 6.17).

$$C_{s_{tot}} = C_{f_{tot}} + C_{r_{tot}} \tag{6.17}$$

The lateral weight transfer is then computed with Equation 6.18.

$$F_{yw} = a_y * (m_s f + m_s r) \tag{6.18}$$

This can then be plugged into the expression for vehicle inclination due to roll (Equation 6.19).

$$p_x = \frac{a_y * m * h * 2 * (c_{f_l} + c_{f_r})}{(c_{f_l} + c_{f_r})^2 * w^2} \tag{6.19}$$

According to the Equation 6.19 p_x - the roll gradient should correspond to $\approx$ 4,5 [deg/g]. This would then mean that no ARB is needed for the vehicle as the vehicle then rolls much less than the initial wanted value (Subsubsection 6.1.3.1).
An other approach can be used by including the extra load due to movement of COG on the outer springs that than would give even more roll.

$$p_x = \frac{a_y * m * h * 2 * (c_{f_l} + c_{f_r})}{(c_{f_l} + c_{f_r})^2 * w^2 - m * g * h * 2 * (c_{f_l} + c_{f_r})} \tag{6.20}$$

The Equation 6.20 gives an approximately 10 % higher value than Equation 6.19. This is though far from the value of 13,5 [deg/g] that the simulations (Section 8.2) in IPG CarMaker results. The value from the simulations are also far greater than the wanted roll gradient (Subsubsection 6.1.3.1).

6.2 Computation of centre of gravity and moment of inertia - frame

This section covers the computation & measurement of the centre of gravity (COG) of the frame. It is to be noted that coordinate system used is according to the DIN-70000, i.e. x-axis positive in the direction of vehicle (forwards), y-axis positive right to left (top view) and z-axis positive upwards. Origin is situated at the rear most point of vehicle at ground level, along the centreline.

6.2.1 x-coordinate

The placement of COG in the x-direction is deduced from weighting the frame and then taking the moment equilibrium about a point. Computing the moment equilibrium about front wheel contact point:

$$F_{\mathrm{zr}} - mg * l_{\mathrm{r}} = 0 \Rightarrow l_{\mathrm{r}} = \frac{F_{\mathrm{zr}}}{mg}; l_{\mathrm{f}} = l - l_{\mathrm{r}} \tag{6.21}$$

This equilibrium 6.21 can be deduced from the free body diagram 6.2 with $\alpha = 0$.
The coordinate value is the same as $\mathrm{l_r}$ in Appendix A.1 because there $\mathrm{l_{r/f}}$ is computed in a slightly modified way, to the end of frame rougher than to the wheels as there aren't any on the frame prior the suspension development.

6.2.2 y-coordinate

The placement of COG in the y-direction is deduced from symmetry. As the frame is symmetric about the xz-plane at the centreline of the frame, the COG is then placed on the centreline of frame i.e at y=0.

6.2.3 z-coordinate

In order to estimate the COG in the z-direction two measurement of multiple angles of the frame was made. Those measurements were conducted by raising the front of the frame, and keeping the rear at the one level standing on a scale. For each height the measured weight was noted down in Table 6.3 and then put into MATLAB for computation of the actual height of COG. The equations for this are given in Equation 6.22 and 6.23. The deviation seen in Table 6.3 must be due to the fact that the scale wasn't standing on a roller

platform and thereby the z-component couldn't be measured accurately enough.
After the computation of height of COG in Appendix A.1 an average value is computed and 160 [mm] of ground clearance is added to this value (giving the overall value of 445.2 [mm]).

$$h = \frac{\Delta l_{\mathrm{r}}}{h_{\mathrm{lift}}} * l \tag{6.22}$$

$$\Delta l_{\mathrm{r}} = F_{\mathrm{rz}} * g * \frac{l}{m} - l_{\mathrm{f}} \tag{6.23}$$

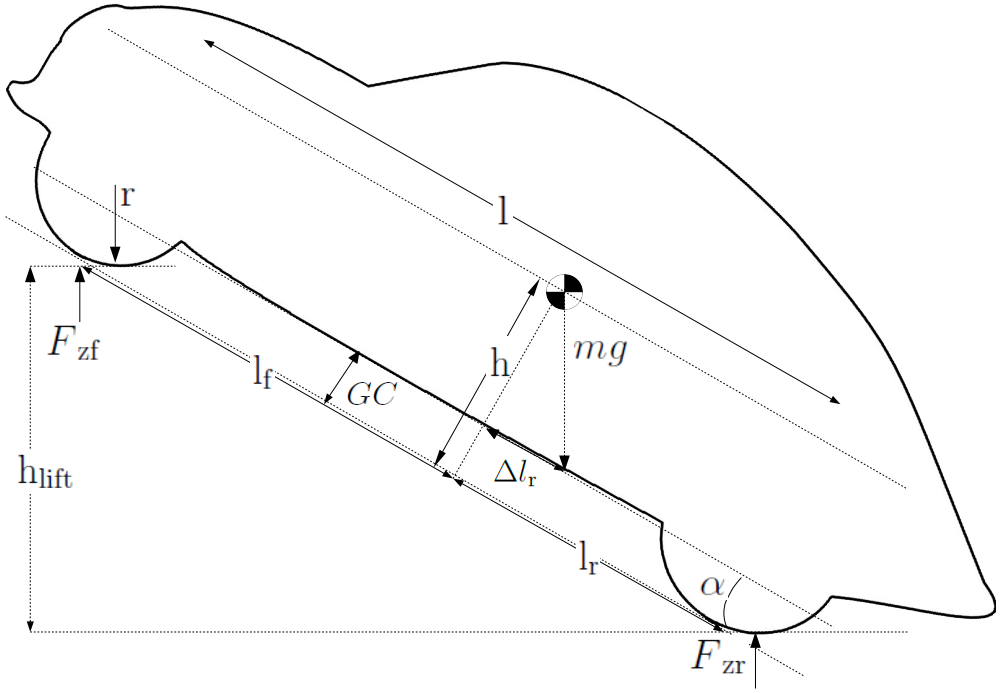

Figure 6.2: *General figure for computation of vehicles COG height*

Table 6.3: h_{lift} - Lift of frame [mm]

Lift of frame h_{lift} [mm]	1st test - F_{rz}*g [kg]	2nd test - F_{rz}*g [kg]
0	23,39	26,6
100	26,64	26,77
200	26,91	26,9
300	27,06	26,97
400	27,14	27,07
500	27,3	27,29
600	27,62	26,65
700	27,81	27,71
800	28,1	27,77
900	28,29	28,27
1000	28,49	29,34
1100	28,57	28,4
1200	28,5	28,97

6.2.4 Computed COG coordinates of frame

From what is learned in Subsections 6.2.1, 6.2.2 and 6.2.3 it is computed that the coordinates of COG lies at (according to the DIN-70000, Table 6.4).

Table 6.4: Computed COG coordinates [mm]

X	Y	Z
1292.2	0	445.2

Note is that (as shown in Appendix A.1) the result of COG-coordinate in the z-direction is found out to deviate by 7.25% from the initial computed value due to a little type error in the initial calculations. This results in a lower COG than initially computed and therefore the graphs and results in LSA SHARK are not fully correct. The main effect this error however will have on the results is that the anti dive and anti squat values will go up slightly, the body roll decrease but the angle changes of the wheels should stay intact. This is though not the final verdict, as will be seen in Section 6.2.5.

Table 6.5: CATIA V5 computed COG coordinates [mm]

X	Y	Z
1356	0	524

6.2.5 COG coordinates according to CATIA V5

To verify/check the COG computed from measurements (which were used in the SHARK analysis), a complete model of the frame was created in CATIA and the mass, COG and inertia measured. This gave a deviating result of different COG (mainly along the z-axis) than the computed one. The difference in values (Table 6.4 versus 6.5) might have been caused by not good enough measurement methods. A main contributor/error might have been due to that the scale wasn't placed on rollers during measurement, and therefore the measured weight wasn't the strict vertical component but rougher the z-component of a weight which also due to the fixed placing of the scale had a x-component. The results from CATIA are declared in Table 6.5. The z-coordinate computed by CATIA was tested by placing a metal pipe under the frame (on its side) which confirmed its correctness as the frame balanced well on that point.

6.2.6 COG conclusions - selected value

The coordinates of Table 6.5 was chosen for utilization in IPG CarMaker simulation, as they proved to be the most correct. This then also gave the inertias of the frame, which then didn't need to be computed by assumptions of the shapes (by summing up the individual inertias and COG positions correlations of the individual pipes).

6.2.7 Inertia of frame

The inertia of frame was computed in CATIA as mentioned in Subsection 6.2.5, results as in Table 6.6.

Table 6.6: Inertia of frame [kg*m^2]

$$
\begin{array}{lcc}
I_{xx} & = & 13{,}989 \\
I_{yy} & = & 39{,}868 \\
I_{zz} & = & 39{,}103 \\
I_{xy} & \approx & 0 \\
I_{xz} & = & 2{,}409 \\
I_{yz} & \approx & 0
\end{array}
$$

6.3 Computation of centre of gravity and moment of inertia - the human body

This section covers the computation & measurement of the centre of gravity (COG) of the human body and it's moment of inertia. It is to be noted that coordinate system used is according to the DIN-70000, i.e. x-axis positive in the direction of vehicle (forwards starting at rearmost point of the spine in sitting position), y-axis positive right to left (top view) and z-axis positive upwards with origin at the lowermost point at the posterior of the pelvic region. The load that the human body exhibits on the car during driving is important to include into any simulation and computation of the vehicle as in this case the human body is awaited to contribute to as much as 25-35 % of the total vehicle mass.

6.3.1 COG of human body

The centre of gravity of the human body is strongly dependent by the posture the body is in. This could be measured for each individual case of different weights, but is time consuming and in this case fairly irrelevant as the rough estimate is needed to enable first iterative simulation. Data for this is instead taken from the "Anthropometric specifications for large sized male dummy" [15] which is regarded to be a good approximation. From Figure 6.3 using the above stated axis system it can be deduced that COG lies approximately at the cooridnates shown in Table 6.7. These coordinates are then put into the IPG CarMaker (Chapter 8) to describe the point load that the human body represents.

Table 6.7: COG of human body [mm]

x	=	350
y	=	0
z	=	300

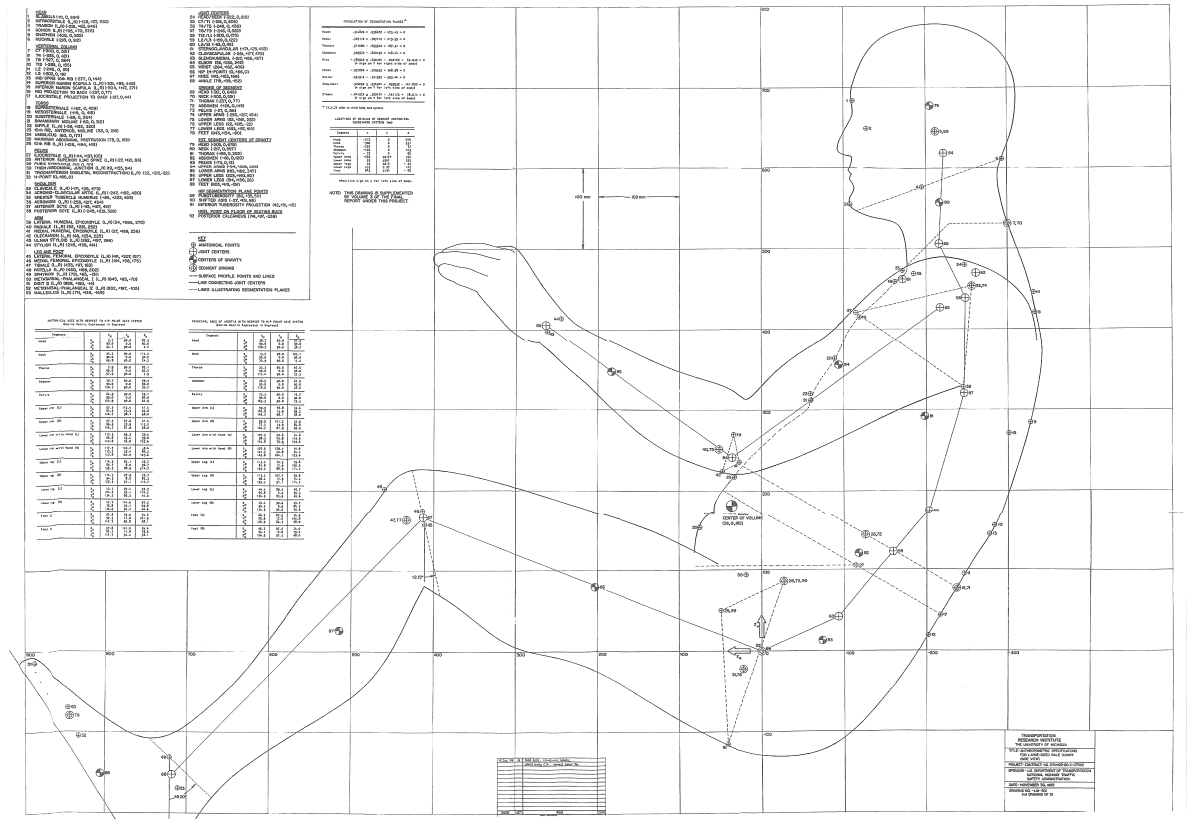

Figure 6.3: *Anthropometric specifications for large sized male dummy (side view) [15]*

6.3.2 Inertia of human body

As the driver is contributing a big amount of the total weight of the car, his inertia and COG is to be counted with (to get realistic results from the simulation done in IPG CarMaker F.2). As the human body is complex, non linear and with an uneven density the only way to estimate this inertia in a good manner is to conduct a series of measurements. This was thankfully done by the Federal Science Laboratory/North American Aviation Inc. back in 1962 [16]. Although these measurements were made for use in the aerospace industry, and they don't cover the exact position as in a car, the sitting position with arms to the front as described is regarded as close to the position that this thesis needs. As no better data was found on the subject and no resources were available to conduct own experiments to gather better data, the data found was chosen to be used in the simulation. The inertia of human body in sitting position is given by the equations in Table 6.8.

Table 6.8: Inertia of human body [lb*in*sec^2]

I_{xx}	=	-91,6+1,43*S+0,322*W
I_{yy}	=	-135+2,26*S+0,268*W
I_{zz}	=	-52,8+0,76*S+0,201*W

With S in [in] and W in [lbs] in Table 6.8. In this case the car is supposed to be designed for a person of a statue of 2 [m] and weight of 100 [kg]. This results in values of S = 78,75 [in] and W = 220,5 [lbs].
As CarMaker computes with inertia in [kg*m^2] a conversion needs to be made: 0,738*lb*in*sec^2 = kg*m^2. Inserted in the values of Table 6.8 yields values of Table 6.9.

Table 6.9: Inertia of human body [kg*m^2]

I_{xx}	=	67,8866
I_{yy}	=	75,3030
I_{zz}	=	37,9003

The computed values seems to be fairly in line with the in the experiment measured values (shown in [16]). The computed values are a little bit bigger than the in [16] shown test data, but it is most probable that the subjects of the study wasn't of as big posture (as prescribed in Section 3.1) and therefore the recorded test values for inertia are slightly lower.

6.4 Computation of centre of gravity and moment of inertia - various point loads

This section covers the computation & measurement of the centre of gravity (COG) and moment of inertia of the human body. It is to be noted that coordinate system used is according to the DIN-70000, i.e. x-axis positive in the direction of vehicle (from part's rearmost point), y-axis positive right to left (top view) and z-axis positive upwards with origin at the lowermost point of the part. The load that the various parts exhibit on the vehicle are of high interest, especially if the loads are of the higher value, e.g batteries and differential. The point loads of ICE, EM and other components is not taken into account as the packaging isn't finalized.

6.4.1 COG and moment of inertia battery pack

The centre of gravity of the battery pack is situated at the centre of it's mass. The battery packs are of cuboid shape with sides of 280x255x185 [mm]. Assuming that the battery is placed along the centre line of the car, with the first battery just under the seat and the second in front of the rear one. The 280[mm] edge placed in the y-direction (b), the 255 [mm] edge parallel to the x-axis (a) and 185 [mm] edge parallel to the z-axis (c) the COG lies approximately at coordinates stated in Table 6.10. The mass (m) of one battery pack is 18,32 [kg]. The moment of inertia can be found in formula tables [12] B31 and results in inertia shown in Table 6.11. The coordinates (Table 6.11) are then put into the IPG CarMaker to describe the point load that the battery pack represents.

Table 6.10: COG of one battery pack [mm]

x	=	127,5
y	=	0
z	=	92,5

Table 6.11: Inertia of battery pack [kg*m^2]

$$I_{xx} = \frac{1}{12}m(b^2+c^2) = 0{,}1748$$

$$I_{yy} = \frac{1}{12}m(a^2+c^2) = 0{,}1540$$

$$I_{zz} = \frac{1}{12}m(a^2+b^2) = 0{,}2225$$

6.4.2 COG and moment of inertia differential

The centre of gravity of the differential is situated at the centre of it's mass. The differential (Quaife QDF7Z5R) is approximated to a cylindrical shape with r = 53,5 [mm] and h = 90[mm]. The differential is placed in the vehicles centre line with it's centre at the same height as the wheels at level position which gives a COG position (Table 6.12) relative its rearmost and lowest point/edge. The mass (m) of the differential is 5,6 [kg]. The moment of inertia (Table 6.13) can be found in formula tables [12] B31. These coordinates are then put into the IPG CarMaker to describe the point load that the differential represents.

Table 6.12: COG of differential [mm]

x	=	53,5
y	=	0
z	=	53,5

Table 6.13: Inertia of differential [kg*m^2]

$$I_{xx} = \frac{1}{12}m(3{*}r^2+h^2) = 0{,}0078$$

$$I_{yy} = \frac{1}{2}m{*}r^2 = 0{,}0080$$

$$I_{zz} = \frac{1}{12}m(3{*}r^2+h^2) = 0{,}0078$$

Chapter 7
Suspension characteristics

The performance of a suspension system is governed partly by the angle changes due to suspension travel and vehicle roll and partly by the deformation of bushings (elastokinematics). The first step is to make sure that the angle changes due to wheel travel and vehicle roll is controlled and limited within values that gives the vehicle predictable characteristics.

7.1 Ranking of wheel angle importance

1. The most important angle to control is the toe-angle. This is the angle that the two wheel on same axle has versus each other and the x-axis of the vehicle. This angle is the main contributor to the lateral forces needed to turn a vehicle about the z-axis and is therefore important to control during bump and roll so that no (or acceptably low) steering input is performed by the wheel movement or vehicle roll, i.e. the vehicle should handle predictable and not steer/veer off if the driver doesn't give it an input by turning the steering wheel.

2. The angle of second highest importance is the camber angle, as it contributes to the vehicles lateral characteristics (camber thrust during cornering).

3. Third most important are the castor and kingpin angles, as these mainly contribute to the feedback feel in the steering wheel. They also contribute to some self centring effects as the vehicle is (for positive castor and kingpin) virtually lifted up in the front by the turning of the wheels.

7.2 Angle alterations due to wheel travel & steer

The initial analyse was performed in Lotus Engineering Software SHARK. In shark the movements were modelled and analysed. The hard points were tuned to fit the set requirements 3. After the simulation in Lotus SHARK the hardpoints (Chapter B) were exported to IPG CarMaker, mainly IPG Kinematics where they were fine tuned to fit the simulation results (Chapter 8) to the vehicle requirements (Chapter 3). The reason to do the kinematic analysis prior to the full vehicle simulation is that if one does not do it one cannot predict the masses, inertias of parts by doing a rough CAD model as the hardpoints then are not known. On top of that, if the kinematic movement of the wheels doesn't correspond to the wanted values (Chapter 3) or doesn't even have the same trends one has a suspension with an unwanted characteristic, that can e.g. make the vehicle unstable during disturbance of a bump or steering.

7.2.1 Wheel movement characteristics - kinematic simulation

The simulations were performed in IPG Kinematics and then interpreted with the aid of a MATLAB-script (Appendix F.1.1). This script semi-automate the plotting of comprehensive graphs from the output data file. It was then used to plot the wheel angle change due to parallel bump (Figure 7.1) and the characteristics due to steering rack movement (Figure 7.2). The simulations were performed in an iterative process and the hard point positions were modified to fulfil the set target values (Chapter 3) as close as possible given the restrictions and limits set (Section 1.4, 1.5 and the frame geometry). All simulations are performed for payload weight, as one has to take the mass of driver into consideration. Loads from luggage are overseen as this vehicle is not intended to carry any larger quantities of load but a little bag of groceries.

7.2.2 Angle and geometry change during bump

During parallel bump motion of the wheels for the whole wheel travel of 260 [mm] (130 [mm] in bump and rebound respectively including some 40-60 [mm] for bump stop. This value deviates from the set target of ± 100 [mm] but on the other hand takes distance for bump stops and a safety margin against lock-up at endpoints into consideration.) the wheel angles are altered. The motion can be followed in Figure 7.1. As the contact force is greater at bump then at rebound the bump characteristics are regarded as more important over the rebound characteristics. Any change should be linear or at least smooth to be regarded and interpreted as predictable and there for acceptable as a design. If the change of any variable isn't linear or smooth, the driver might during certain manoeuvres trigger an unstable behaviour and be surprised and overwhelmed with an unexpected vehicle response which can lead him or her to loose control of the vehicle.

7.2.2.1 Toe angle change

Looking at the toe curve (top row, second from left Figure 7.1) it can be seen that the toe characteristic are fairly linear. The graph tells us that the toe is increasing for bump wheel movement, i.e. when wheel runs over a bump it is turned slightly inwards during the vertical motion and pushes the vehicle therefore towards its centreline. The toe angle change is on average (for the whole bump stroke) 0,0038 [deg/mm travel] for the front and 0,0007 [deg/mm travel] the rear wheels. Comparing this with the toe angle change values of Table 1.2 it is to be noted that they don't deviate heavily from the old set target value, but for the sign. A guess to explain the sign difference is that the values of the target are extracted from a big heavy front wheel driven car rougher than a small rear wheel driven car. If the absolute value of the target and achieved value is compared it can be seen that the rate of change is within the absolute value of the set target limits. Given also that the vehicle will be travelling at fairly low speeds and that the suspension movement of 100 [mm] is not awaited to be the operating point, but rougher a suspension movement of approximately ± 50 [mm] the results can be interpreted that the toe angle change is almost neglectable, as the total toe angle change of 0,1 respectively 0,02 [deg] can be seen as very small and within any adjustment tolerance.

7.2.2.2 Camber angle change

The camber curve (top row, second from right Figure 7.1) it can be seen that the camber characteristic are fairly linear. The graph tells us that the camber is decreasing for bump wheel movement, i.e. when wheel runs over a bump its upper half is tilted slightly inwards (toward vehicle centre plane) during the vertical motion and pushes the vehicle therefore towards its centreline (due to created camber thrust). The camber angle change is approximately -0,05 (front) and -0,062 (rear) [deg/mm travel] for both the front and the rear wheels (during bump). Comparing this with the camber angle change values of Table 1.2 it is to be noted that this deviates somewhat from the old set target value. The camber angle target set cannot however be met due to geometrical restrictions. As the vehicle is only allowed to have a track width of 1,5 [m] and the frame is 0,87 [m] wide at the parts where the wheels are to be applied, the wishbones end up being fairly short. This is not good for the camber angle change (and change rate) but is geometrically unavoidable. The maximum camber angle of -4 [deg] is not exceeded, but only at a wheel travel of 70-80 mm and above. This will probably only occur at impact if the vehicle lifts of the ground, in which case the camber angle is not the main concern or problem. As the vehicle will be travelling on thin, high profile tyres, while the vehicle that the target values were set for used a wider, lower profile tyre. As the camber angle not only exerts the camber thrust but also can lead to (if too big) to loss of grip and uneven wear of tyre it is generally wanted to be controlled hard. In the case of PUNCH the high profile, thin tyre will be less stiff sideways over a lower profile tyre, letting it easier to deform and adapt to a less optimal camber angle. Therefore this less favourable result can be regarded as ok (but it still needs to be evaluated in full vehicle test).

7.2.2.3 Track change

The track width curve (top row, rightmost Figure 7.1) it can be seen that the track change characteristic are fairly linear. The graph tells us that the track width is decreasing for bump wheel movement, i.e. when wheel runs over a bump it is also moving slightly inwards (toward vehicle centre plane) during the vertical motion. This can lead to increased tyre wear and unnecessary lateral loads in the suspension linkage. However it can also be seen hat the track width change is almost 0 [mm/mm travel] for a suspension movement of approximately ± 30 [mm]. There isn't any targets set for this deviation, but it is ideally kept to as little as

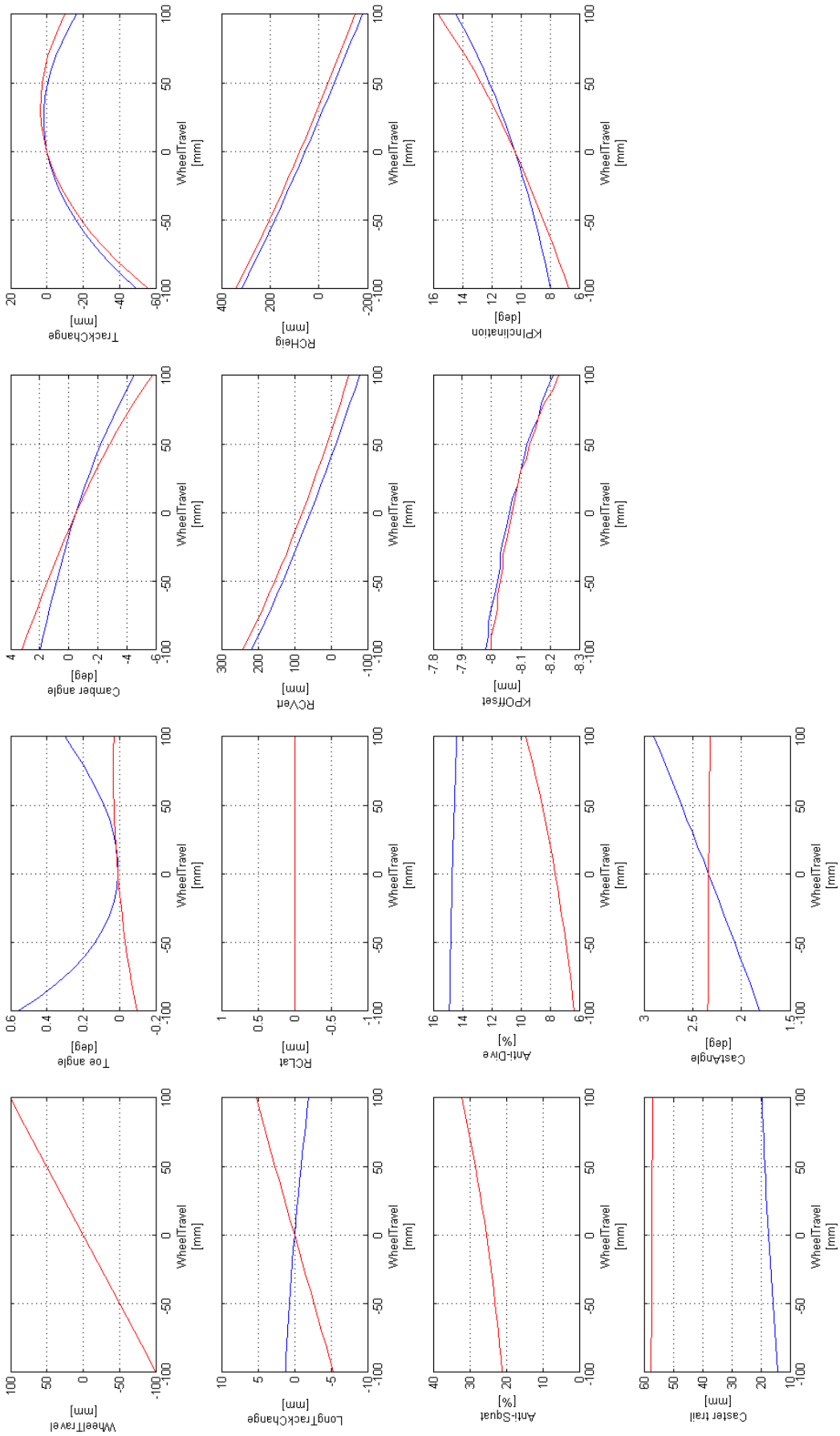

Figure 7.1: *Wheel angle changes due to parallel bump and rebound movement of wheels. Blue lines represent the front wheels and red lines represent the rear wheels. Front and rear are simulated separately and shown overlaid for comparison.*

possible. This can't be done as the wishbones used need to be short, in contrary to the theoretically ideal long ones to minimize track change during wheel travel. This could also be solved if it was decided to use some trailing arm type of suspension arrangement instead of the double wishbone or by simply limiting the wheel travel.

7.2.2.4 Wheel base change

The wheel base change curve (second row, leftmost Figure 7.1) indicates a linear characteristic. The graph tells us that the wheel base is decreasing for bump wheel movement in the front and does the contrary in the rear (also referred to as longitudinal compliance). When front wheel runs over a bump it is also moving slightly forwards (contrary the direction of vehicle movement) during the vertical motion. The opposite happens for the rear wheel. This behaviour is favourable as the wheels will absorb some of the bump force moving rearwards and a lower shock wave will be transmitted to the vehicle body/frame. The change is within reason close to the limits set by the initial targets in Table 1.1 (but for front wheels, as they travel forward, if not considering the possible kinematic compliance). The sum of change is slightly higher than the set targets, but that could however enhance the vehicles vibration and shock isolating properties resulting in a less harsh ride. This change also allowed the incorporation of anti dive and anti squat functionality/geometry (Subsubsection 7.2.2.7 & 7.2.2.8) in the front.

7.2.2.5 Roll centre lateral

The roll centre lateral curve (second row, second from left Figure 7.1) shows an unexpected, transient behaviour. This is thought to be a computational error from the software (as it is extremely transient and local) and is therefore neglected. It can also be observed that the roll centre is along the vehicles centre line.

7.2.2.6 Roll centre height

The roll centre height curves (second row, first and second from right Figure 7.1) shows that the roll centres for front and rear axle (at curb height) corresponds to the set targets and doesn't change in a non linear way. Why these two curves deviate slightly from each other is unclear, as they should according to Modelon AB show the same result.

7.2.2.7 Anti squat

The anti squat curve (third row, rightmost Figure 7.1) shows that the anti squat corresponds to the set targets. It can also be seen that the anti squat is rising for suspension movement, which will be felt as a progressive damping of the squat movement (the more squat the less reaction the vehicle will give to more torque at driven wheels).

7.2.2.8 Anti dive

The anti dive curve (third row, second from right Figure 7.1) shows that the anti dive corresponds to the set targets.

7.2.2.9 Other parameters

The other parameters (kingpin offset at ground and wheel centre, kingpin angle, caster trail and caster angle) do also meet their target values. They deviate very little and are therefore not thought to give any greater contribution to the handing.

7.2.3 Steering effects

The Figure 7.2 shows how the wheel angles are influenced by the motion of the steering rack. The most interesting values to note are that the Ackerman goes from approximately 0 [%] (at no lock) to almost 60 [%] at full lock. This means that the wheels move parallel for small angle alterations (typically big radius turns at higher speed) and the inner wheel gets a greater angle (hence reducing scrub) at sharper turns (that are usually made at low speeds) and by that also reducing the force needed to operate and keep the vehicle turning. It is

also to be noted that the turn diameter is estimated by IPG Kinematics to 7,26 [m] which corresponds well to the set targets in Chapter 3 & Section 3.2.

7.3 Ride quality, RMS

According to the European Union directive 2002/44/EC [17], a driver shall not be exposed to a RMS value higher than 1,15 $[m/s^2]$ per an 8 [h] period. This is computed in Appendix D.3. The result is a RMS value of 0,53 $[m/s^2]$ which is less than the threshold value, hence the driver should in theory be able to drive the vehicle for at least 8 hours at given speeds without experiencing any higher discomfort (given that the vehicle is not driven on very rough terrain). That said in Appendix D.4 when computed it can be seen that the magnitudes of the transfer functions (suspension travel, ride comfort) grow strongly for higher frequencies. Interpreting this leads to the conclusion that the vehicles ride comfort is reduced with the speed of travel.

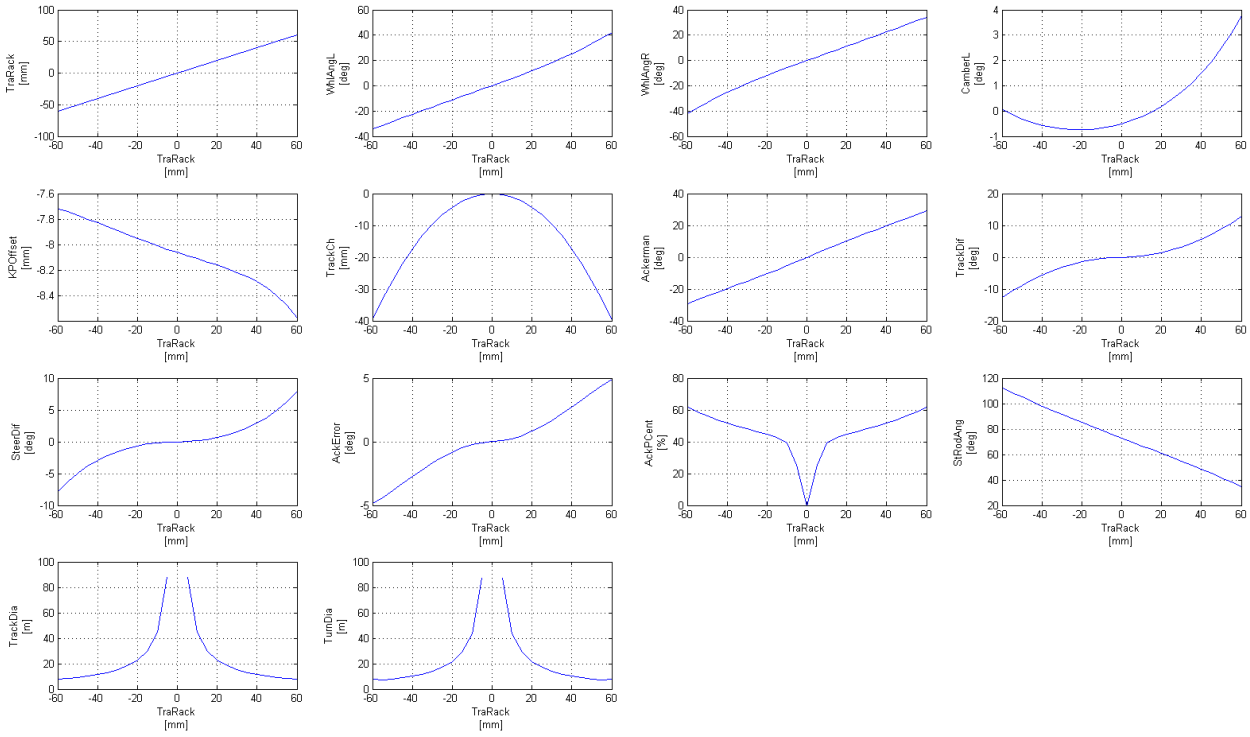

Figure 7.2: *Wheel angle changes (front) due to steering movement of the front wheels.*

Chapter 8
Complete vehicle simulations

This chapter covers the complete vehicle simulations done. It also covers the potential input data that was needed for the simulations. The simulations were done in IPG CarMaker with the suspension kinematic files created in IPG Kinematics with the coordinates from LSA SHARK analysis. It is to be noted that because there wasn't any tyre models in the wanted/selected dimensions available for the simulations, the simulations were performed with the nearest tyre dimension (165/70R13) and then for a set of larger dimensions (195/65R15 and 225/60R15) to visualize any handling trend.

8.1 Suspension values

Following suspension values have been put into IPG CarMaker for simulation setup.

8.1.1 Springs, dampers anti-roll bars

The values for springs, dampers and anti-roll bars (ARB) are computed and chosen in Appendix C and are therefore not described here in detail. The computations in Chapter 6 gave the result of front spring rate of $c_{s_f} = 2018,5[N/m]$ and the rear spring rate of $c_{s_r} = 3893[N/m]$. The damper coefficient was computed to: $D_f = 216[N/m * s^2]$ and $D_r = 300[N/m * s^2]$. The damping coefficient is distributed as 1/4 for bump and 3/4 for rebound (1:3-distribution, which is common practice e.g. as described in [4], [13]).

8.1.2 Suspension hardpoints

The suspension hardpoints were created with Catia V5, LSA Shark and IPG Kinematics. First by getting the rough kinematics right in LSA SHARK, then importing them to IPG Kinematics, tuning them with use of the plotting script (Appendix F.1.1), drawn in Catia V5 and then iterated back into IPG Kinematics with a final test in IPG CarMaker. They final hardpoints are shown in Appendix B. They were then imported into IPG CarMaker to do the complete vehicle simulations (Section 8.2 and 8.3).

8.2 Steady state 42 [m] circle manoeuvre

In order to evaluate the roll and under-/over-steer characteristics a series of tests were conducted for a steady state 42 [m] radii circle track with no banking angle turning left. This is awaited to show some roll gradient and side slip characteristics that are to be evaluated (Chapter 4).

8.2.1 Steady state no ARB

The first run was a steady state turning manoeuvre at a speed of approximately 50 [km/h] (Figure 8.1).
In Figure 8.1 the following two phenomena are to be seen:

- The roll angle for the lateral acceleration is too high (approx 12,6 [deg/g] instead of 7 [deg/g] 6.14).
- The rear right tyre has a slightly higher side slip versus the left tear tyre. This is interpreted as a slight tendency to oversteer.

The problem of too big roll angle can be corrected by enhancing the vehicles total roll stiffness (resistance to roll) by adding one anti-roll bar (ARB) in the front, rear or both.

To compute the needed ARB rate calculations were made (Subsubsection 6.1.3.2 and Appendix C.1) according to formulas in [5]. The formula used indicated that the awaited roll should have been much less than the roll experienced in the simulation. This might be the result of the formulas being over simplified, with too few degrees of freedom and not taking the real weight distribution into account fully.

An iteration was performed and it was to be found that a front ARB (of 4400 [N/m] rate) had a wanted impact on the system (limiting roll and keeping design simple).

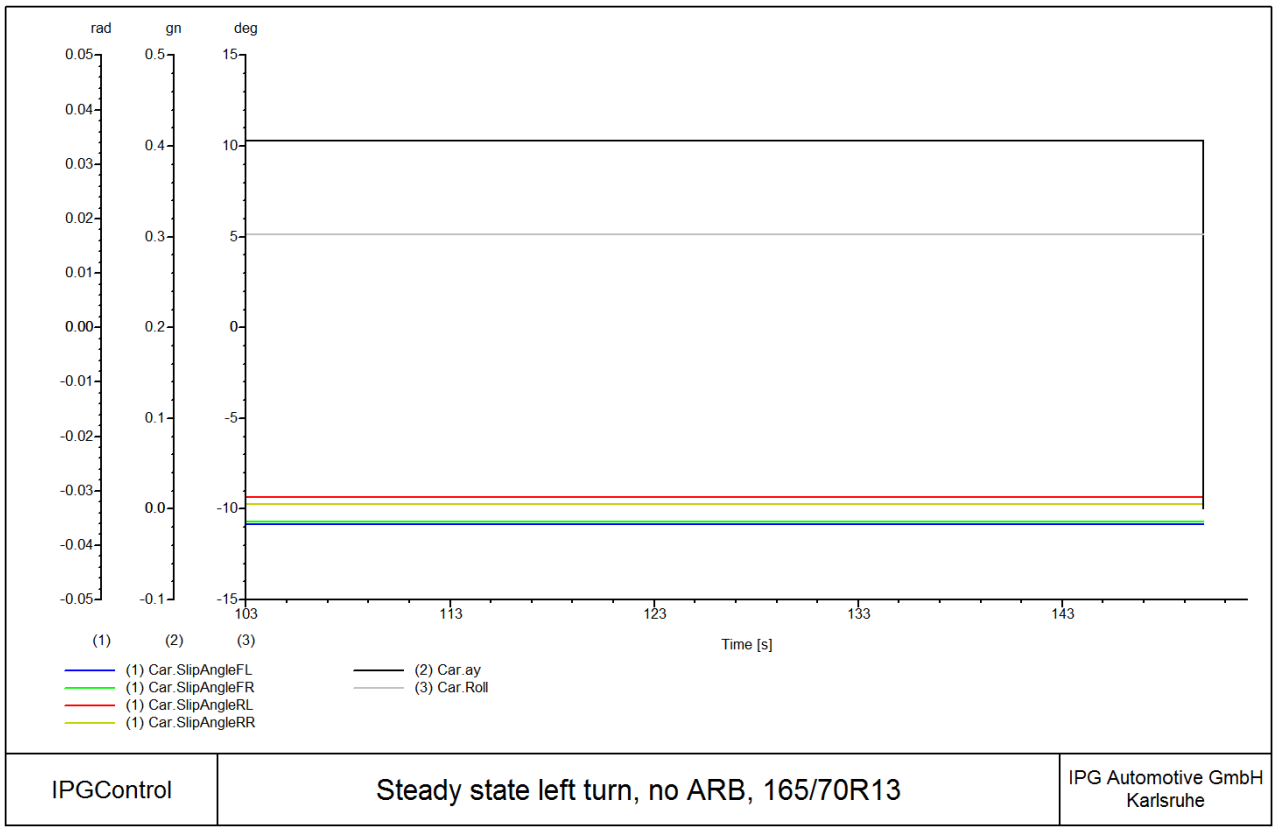

Figure 8.1: *Tyre side slip and vehicle body roll during a steady state curve manoeuvre, R=42 [m], no ARB, 165/70R13 tyre*

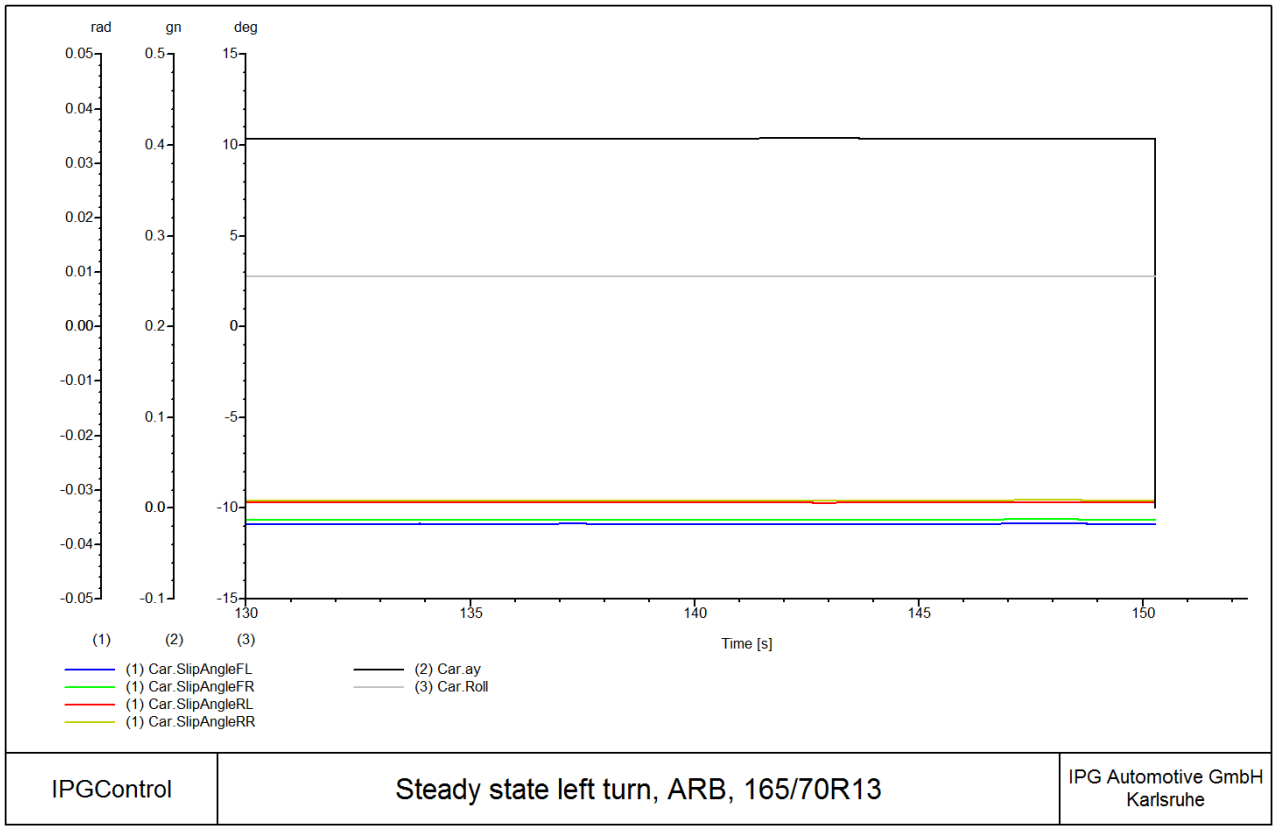

Figure 8.2: *Tyre side slip and vehicle body roll during a steady state curve manoeuvre, R=42 [m], 4400 [N/m] front ARB, 165/70R13 tyre*

8.2.2 Steady state with ARB

The chosen solution is to only add a ARB in the front, for simplicity of not having to add an other component in the rear. By iterative tests in IPG CarMaker it was found that an ARB with the rate of 4400 [N/rad] and an ARB motion ratio of 0,79 is sufficient to solve both problems. The motion ratio is 0,79 for packaging reasons. The result can be seen in Figure 8.2. The roll gradient is approximately 6,2 [deg/g], which is somewhat stiffer than the target if 7 [deg/g] but is the closest to target one can get in order to ensure correct side slip relation between the tyres (more side slip in front than rear). Given now that the ARB rate is known and the vehicle has a general understeering tendency (which is wanted) the next step is to make a set of double lane change (DLC) tests for various speeds and tyres to see if it actually performs well in the Chapter 3 set targets.

8.3 Double lane change test

A set of DLC tests were performed. DLC tests for a speed of 50 [km/h] with and without ARB, DLC for 100 [km/h] with ARB and for different tyre widths and DLC tests for a speed of 50 [km/h] and varying μ to simulate damp and winter conditions. As it was concluded in Section 8.2.2 the final car is to be run with ARB, but that doesn't mean that the tests are irrelevant for the evaluation. It was anticipated that the vehicle would roll too much without the anti-roll bar and that it would also tend to oversteer and be unstable. This was found to be the case in the tests made.

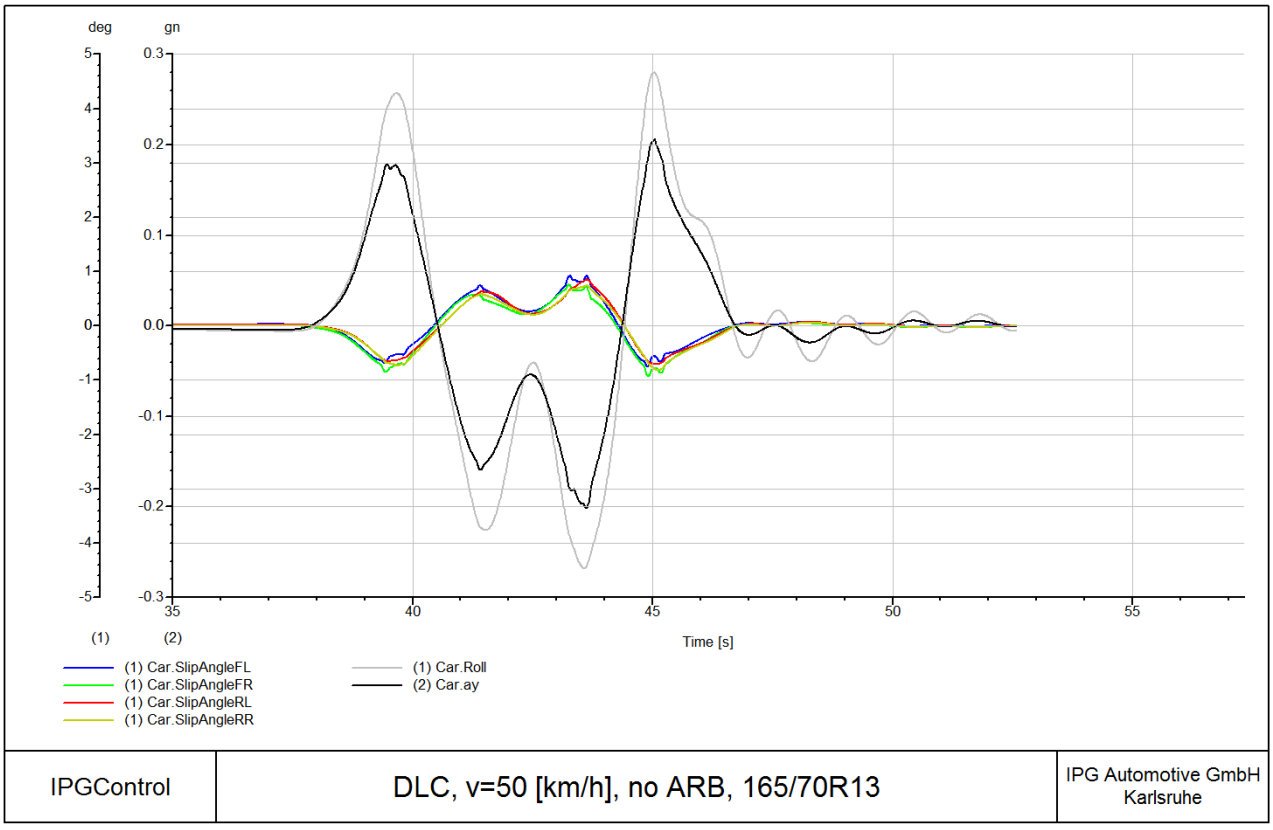

Figure 8.3: *Tyre side slip and vehicle body roll during DLC, v=50[km/h], no ARB, 165/70R13 tyre*

8.3.1 Double lane change, with and without ARB, v=50 [km/h]

The double lane change manoeuvre at 50 [km/h] was set as a design target in Chapter 3. The requirements said that the vehicle should not roll over for the given manoeuvre. The graph in Figure 8.3 shows the suspensions performance for a DLC without an anti-roll bar.

In Figure 8.3 following can be observed:

- The vehicle rolls heavily.
- The side slip of the rear tyres are at multiple points much greater than one of the front tyres. This means that the vehicle can't be regarded as generally understeered.

After the non ARB DLC test, a similar test was performed, but this time with addition of the in Subsection 8.2.2 suggested a front anti-roll bar. That test gave the result seen in Figure 8.4.
In Figure 8.4 it can be seen that:

- The vehicle rolls substantially less than in the non ARB case Figure 8.3.
- The side slip of the rear tyres overall smaller than one of the front tyres. This means that the vehicle is generally understeered, which is regarded as a safe characteristic.

Because of the favourable characteristics the anti-roll bar case gives it is chosen and recommended to use an anti-roll bar for this vehicle.

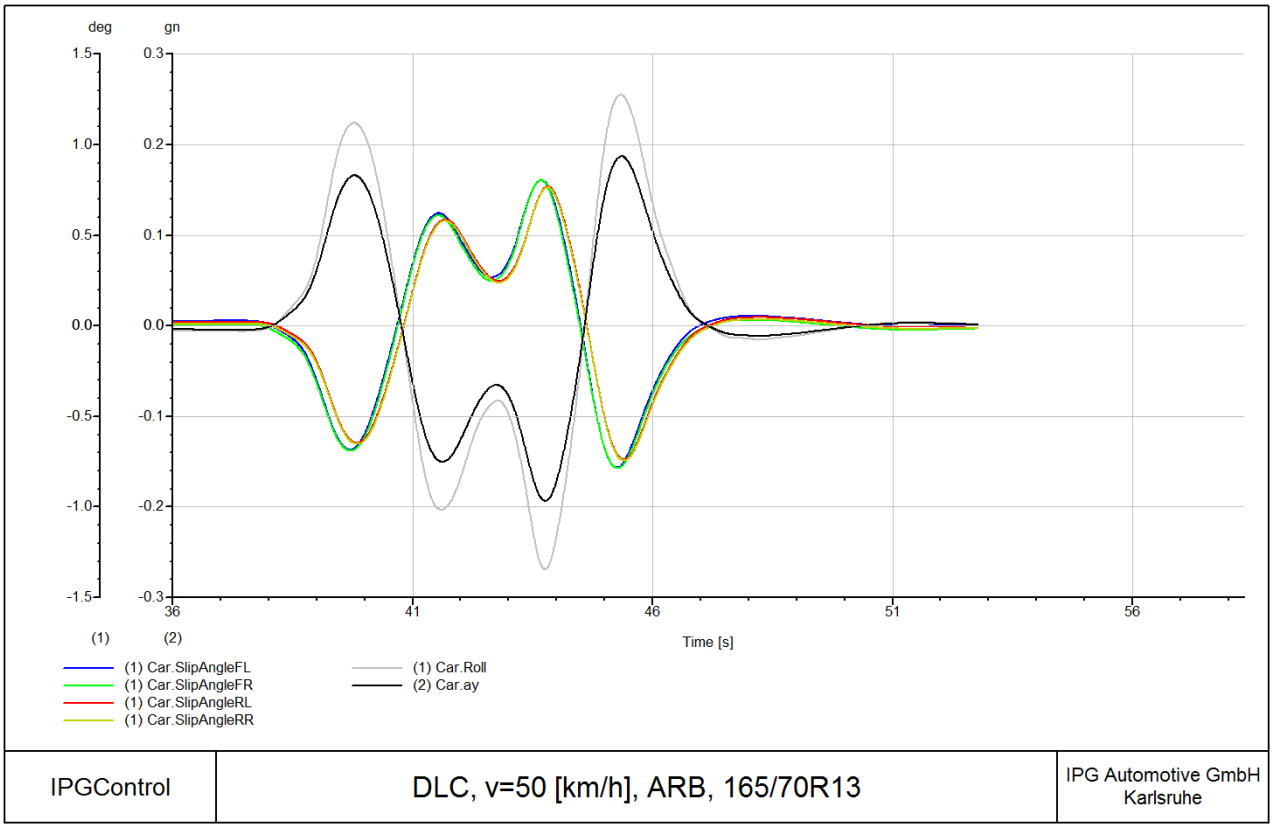

Figure 8.4: *Tyre side slip and vehicle body roll during DLC, v=50[km/h], front ARB, 165/70R13 tyre*

8.3.2 Double lane change, with ARB, v=100 [km/h], various tyre widths

To test what impact the different tyre widths and profile makes on the vehicles handling 3 different tyre sizes were tested (165/70R13, 195/65R15 and 225/60R15). This because there weren't any model of the wanted tyre size (selected in Section 5.1) available in IPG CarMaker so by running tests for various tyre sizes one can predict the handling tendency for a narrower tyre. The graphs for this tests are shown in Figures 8.5, 8.6 and 8.7. It can be seen that the tendency for side slip of the tyres is reduced with increasing width of the tread. The roll angle tends also to increase (somewhat) with increased tyre width. One vital phenomena noticed is the greater tendency of untripped rollover at even higher speeds. This is not relevant for the speeds that the vehicle is designed for, nor even if the design speed were double as big. The vehicle starts to have rollover tendencies (performing DLC) at speeds exceeding 130-140 [km/h] with $\mu_{road} = 1$. It is also to be noted that the side slip angle of the rear tyres tends to be greater than the front ones for all higher speed cases as e.g. in Figure 8.5. This can be interpreted as that the vehicle is at it's stable limit and is on the edge of beginning to oversteer, which is unwanted.

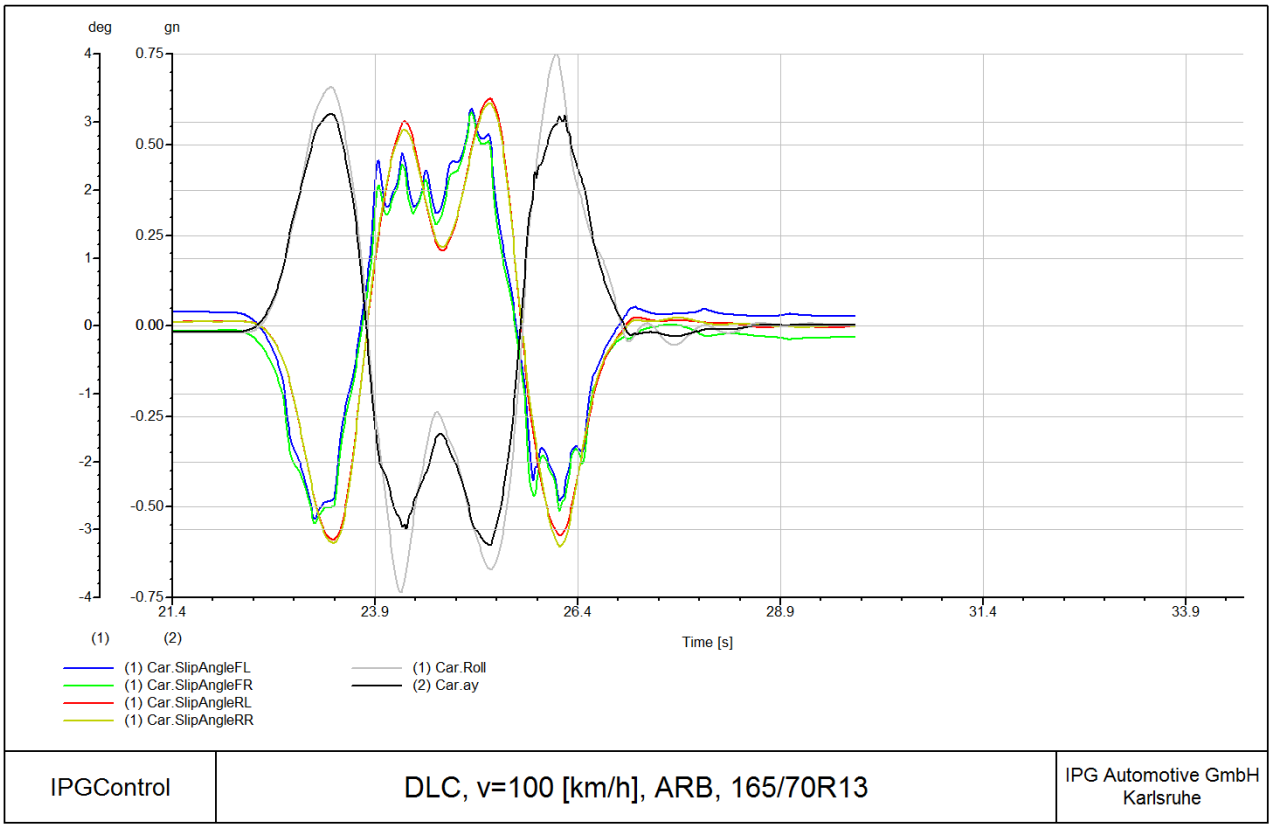

Figure 8.5: *Tyre side slip and vehicle body roll during DLC, v = 100 [km/h], front ARB, 165/70R13 tyre*

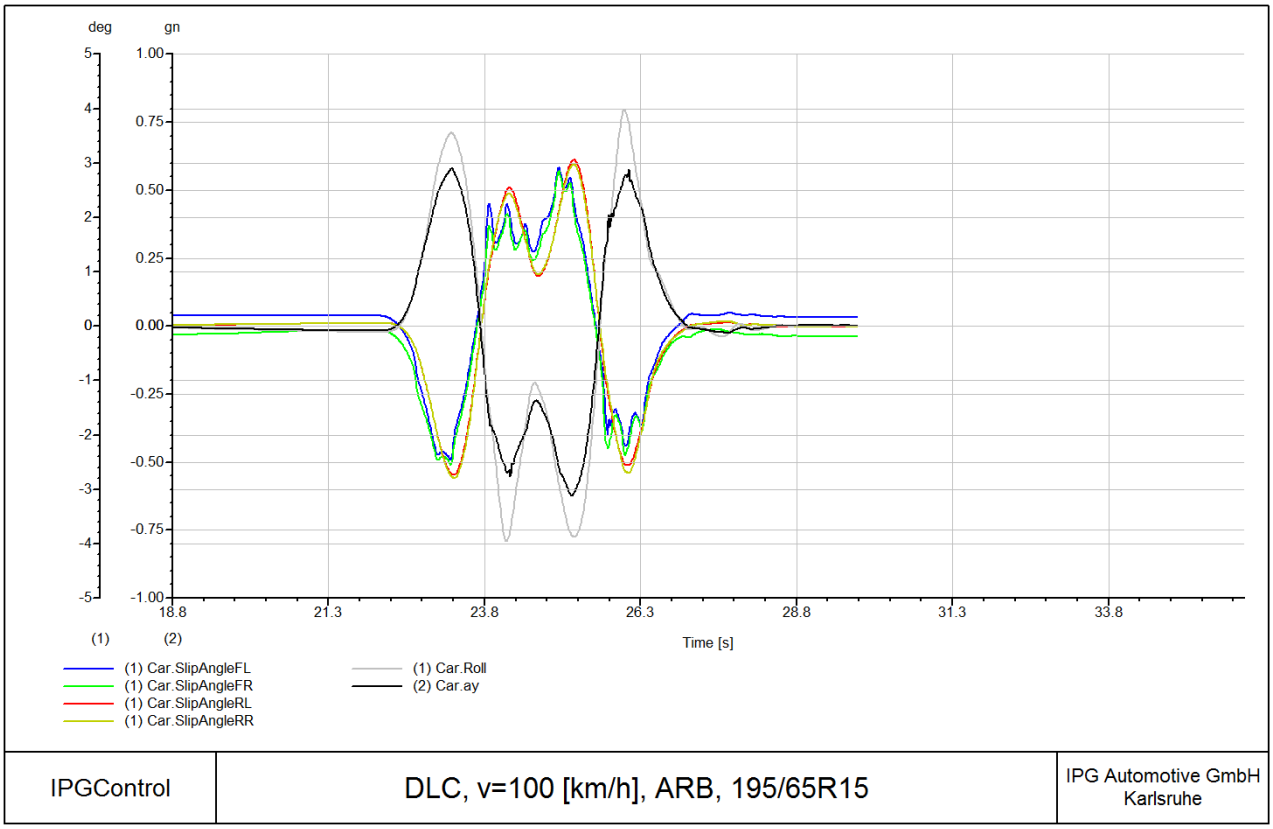

Figure 8.6: *Tyre side slip and vehicle body roll during DLC, v = 100 [km/h], front ARB, 195/65R15 tyre*

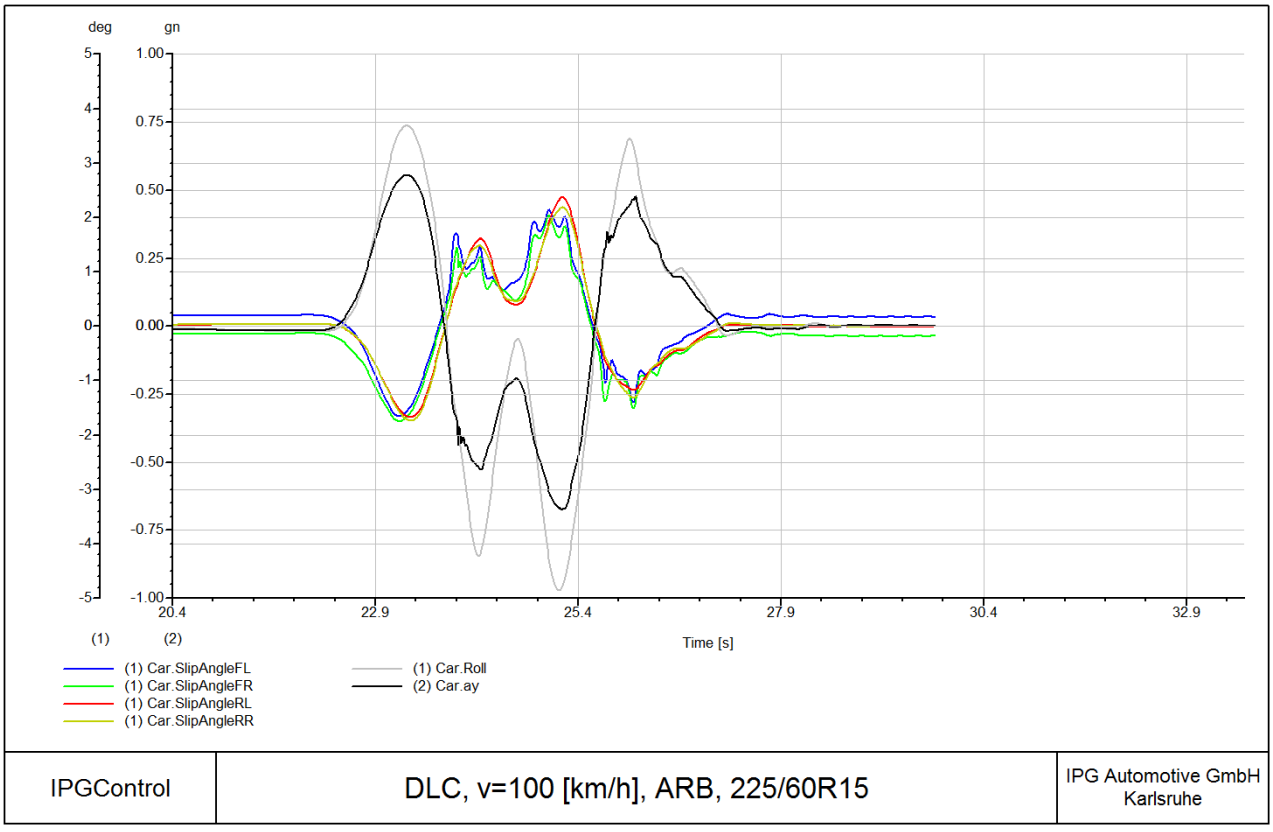

Figure 8.7: *Tyre side slip and vehicle body roll during DLC, v = 100 [km/h], front ARB, 225/60R15 tyre*

8.3.3 Double lane change, with ARB, v=50 [km/h], varying μ_{road}

To test what impact the different road grip/friction coefficient (μ_{road}) makes on the vehicles handling 3 different friction levels were tested ($\mu = 0.7, 0.6, 0.2$, corresponding to slightly damp, wet and icy/snowy conditions [18]) with the narrowest tyre (165/70R13 selected in Section 5.1). In Figures 8.8, 8.9 and 8.10 the results of the tests can be seen. Here it is to be seen that the slip angles rise and the roll angle decreases with decrease in μ_{road}. The increase of slip angles gives the effect that the car isn't as true to it's intended path. For the case of $\mu = 0,2$ the car is on the edge of being oversteered as the rear side slip is larger than the front one. This means that it is either crucial to drive the vehicle on specific winter tyres (which can create higher μ_{road} at bad road conditions) or else this manoeuvre could result in the vehicle spinning out.
Reasonably, as discovered in Subsection 8.3.2 the behaviour (i.e. side slip tendency) will be somewhat bigger for the chosen narrower tyre. However it could also be the contrary as in some conditions the narrower tyre can be better than the wider one as narrower tyres are less prone to aquaplaning (which should however not be a problem at these speeds) and less sensitive to camber angle changes and therefore can preserve a higher grip level.

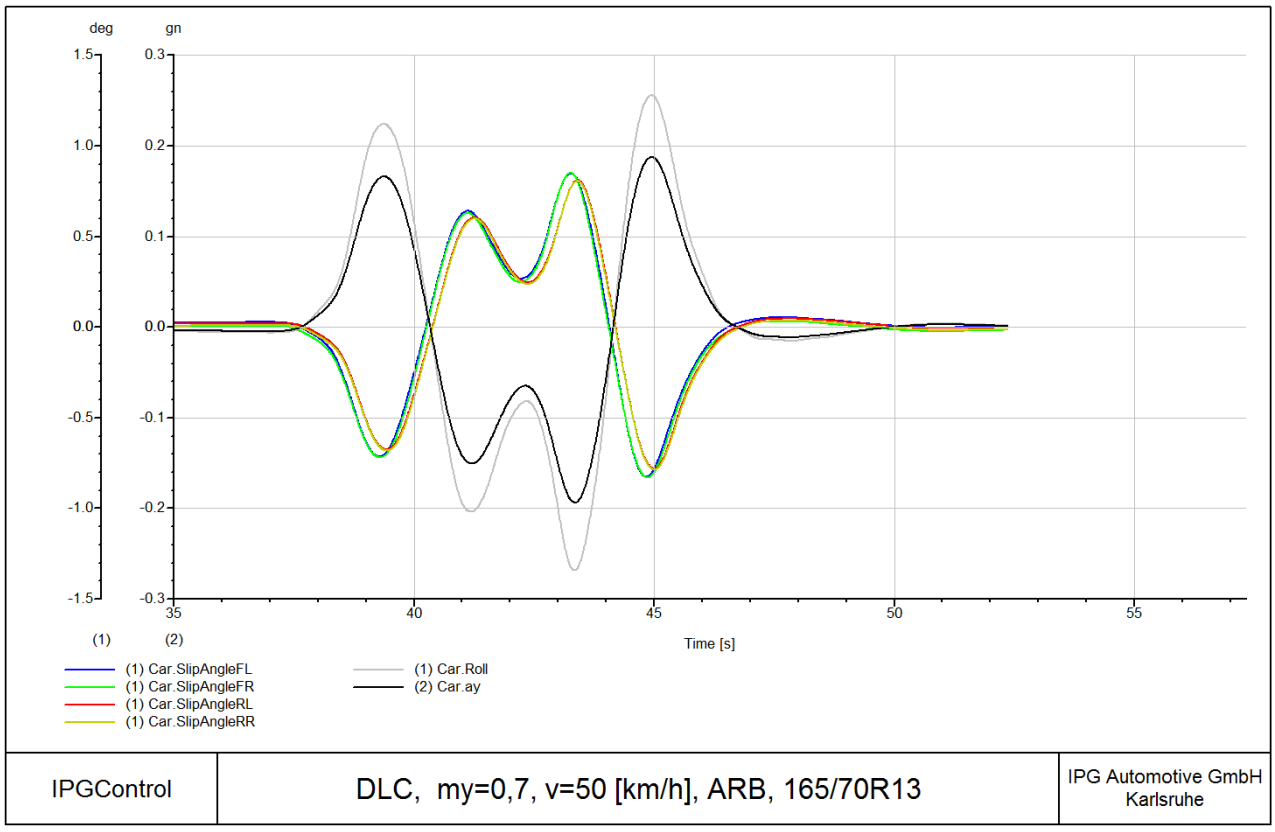

Figure 8.8: *Tyre side slip and vehicle body roll during DLC, $v = 50$ [km/h], $\mu = 0,7$ - slightly damp road, front ARB*

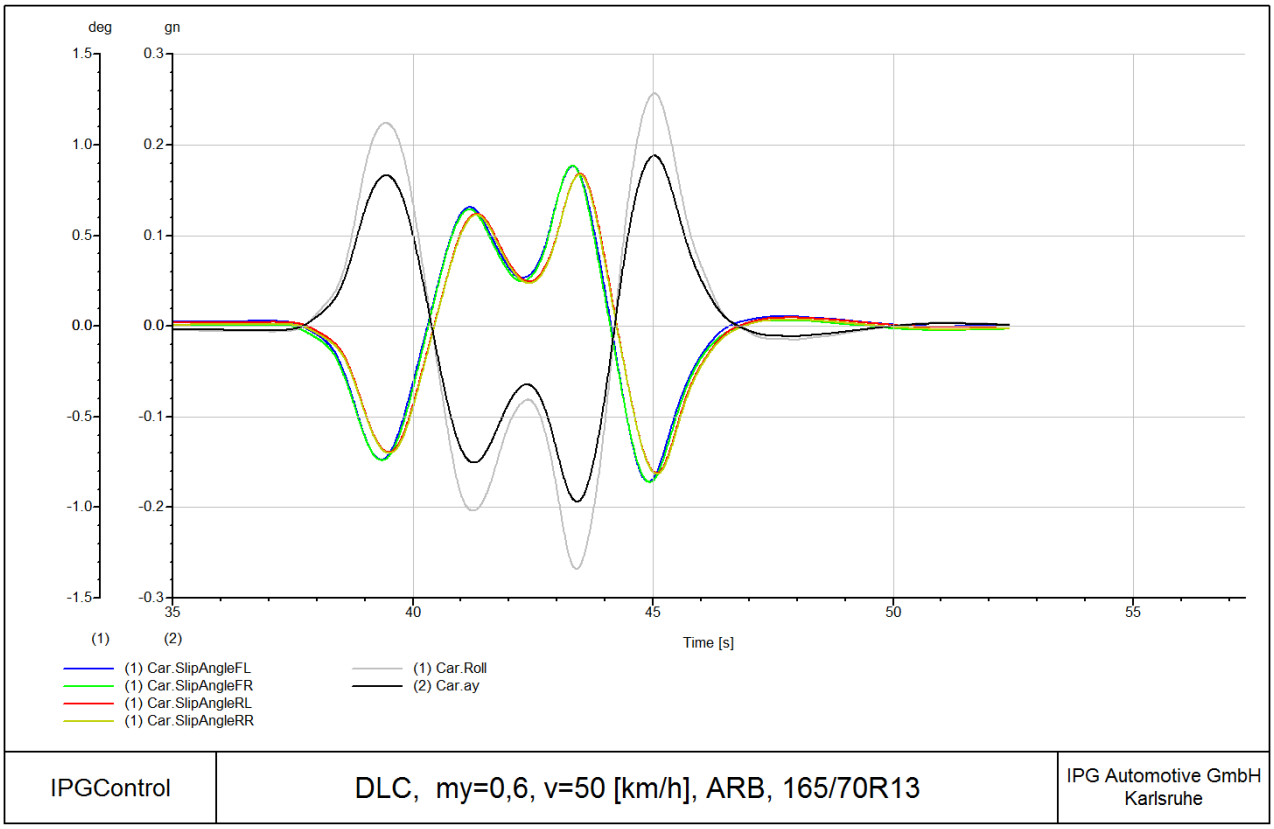

Figure 8.9: *Tyre side slip and vehicle body roll during DLC, $v = 50$ [km/h], $\mu = 0,6$ - wet road, front ARB*

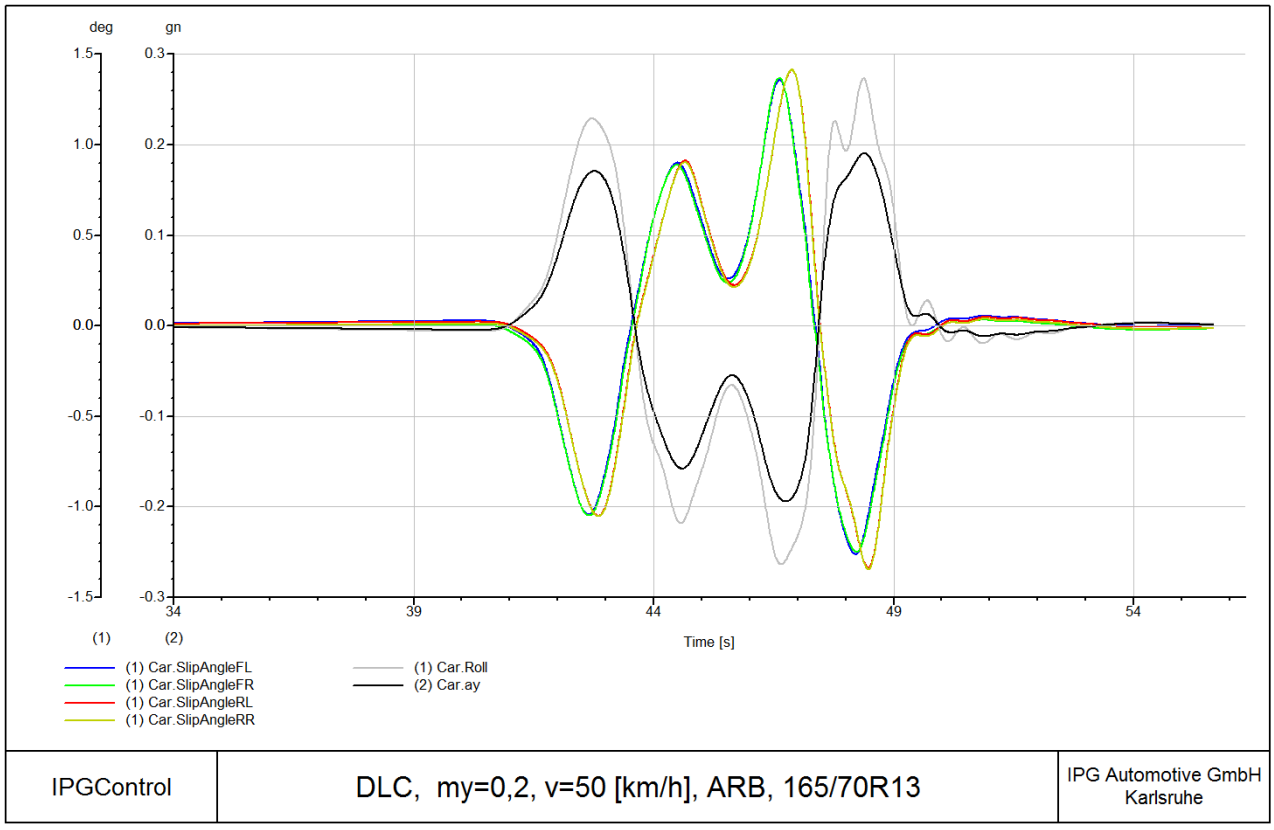

Figure 8.10: *Tyre side slip and vehicle body roll during DLC, $v = 50$ [km/h], $\mu = 0,2$ - snowy/icy road, front ARB*

Chapter 9
CAD - Modelling and testing

This chapter covers the virtual modelling and testing in CATIA V5 and ANSYS 14.

9.1 The rational suspension model

The finished complete design can be seen in Figures 9.1 - 9.3 (but mounts on vehicle/frame). It incorporates an anti-roll bar in the front. The wishbones are shared left to right and front to rear, i.e. only one type lower respectively upper wishbone needs to be manufactured. Same goes for the uprights. The steering arms and rods however are different front to rear, as well as the tie rods. The overall number of individual components is held to just only 25 percent of the number it would have been if no components were identical or interchangeable, which is much more efficient and chap to model, test and fabricate. The corresponding drawings can be found in Appendix E. The full CAD model and corresponding files have been submitted to Sven B. Andersson at Applied Mechanics, Division of Combustion, Chalmers University of Technology.

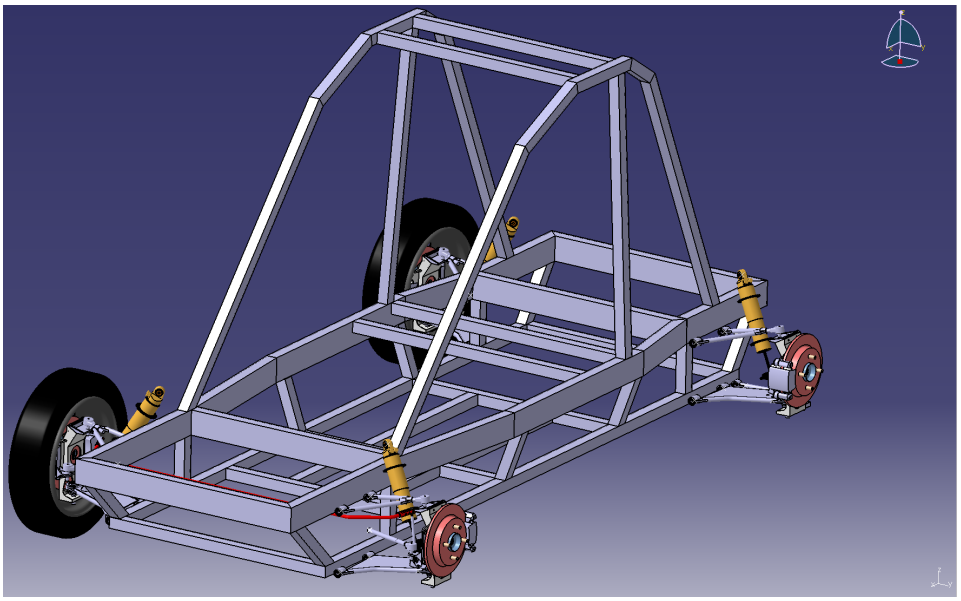

Figure 9.1: *ISO view of the whole vehicle*

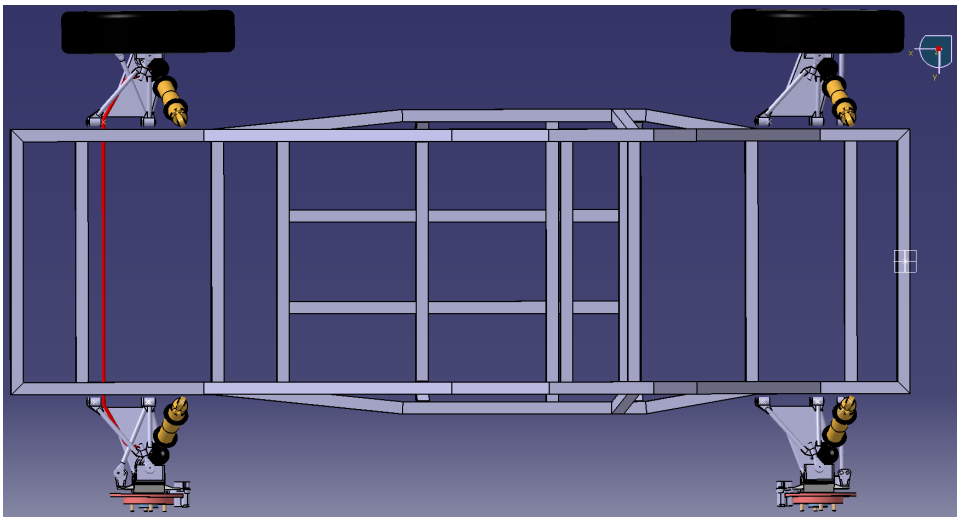

Figure 9.2: *Top view of the whole vehicle*

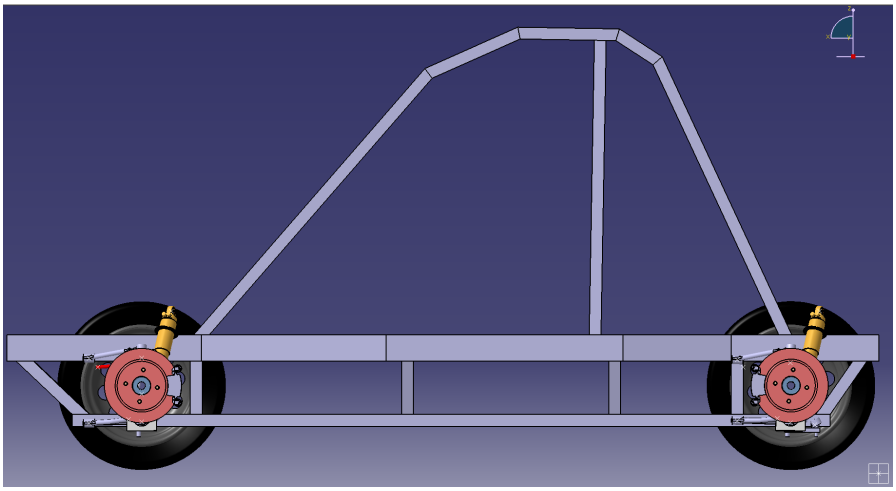

Figure 9.3: *Left side view of the whole vehicle*

9.2 The universal corner

In Figure 9.4 one can see the components mounted to the upright in each corner. The rear steer arm cam be seen in Figure 9.6 as can the upper & lower wishbone and spring and damper assembly. The disc is a Ford Focus Mk1 rear brake disc, and so is the brake calliper carrier. The wheel hub and bearing is from the front axle of the same car. The camber angle can be adjusted by placing shims between the upright and the mount of the upper wishbone (the slightly triangular piece in upper right corner of Figure 9.4). It can also be set by adjusting the upper ball joint (Figure 9.5). If doing so in conjunction with altering the shims one can also adjust the kingpin angle. The caster angle is adjusted by shims (not shown) between the rubber bushings (seen at the end of the wishbones in Figure 9.5 and 9.6). The steer arm and brake calliper carrier alter positions depending on side and if in front or rear of the vehicle. The toe angle can be set by adjusting the steering rods (and connection rods) in front respectively rear. The parts needing manufacturing are made out of mild steel, as it is easy and chap to form and is the material preferred by SFRO (Sveriges Fordonsbyggares Riksorganisation) which is the legislative body that can approve a prototype vehicle of this type for road use.

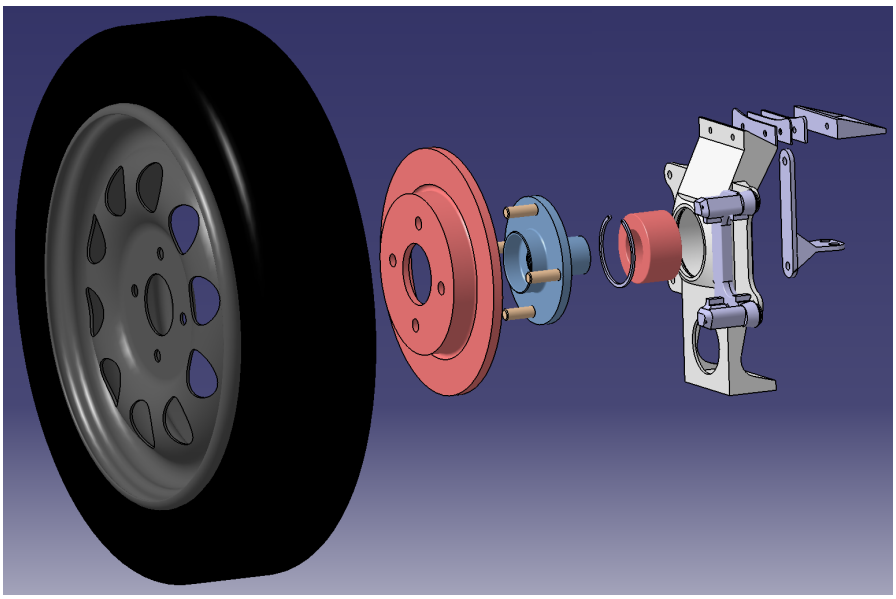

Figure 9.4: *Exploded view of one corner suspension assembly*

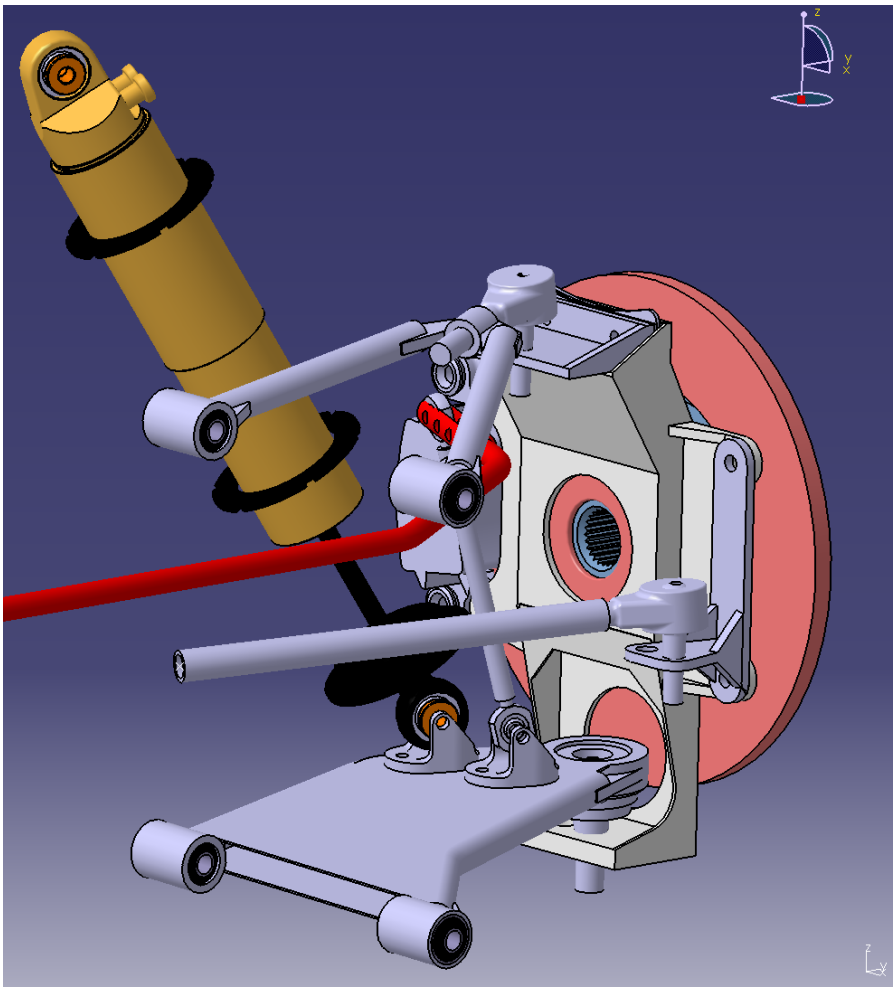

Figure 9.5: *Front left corner suspension assembly*

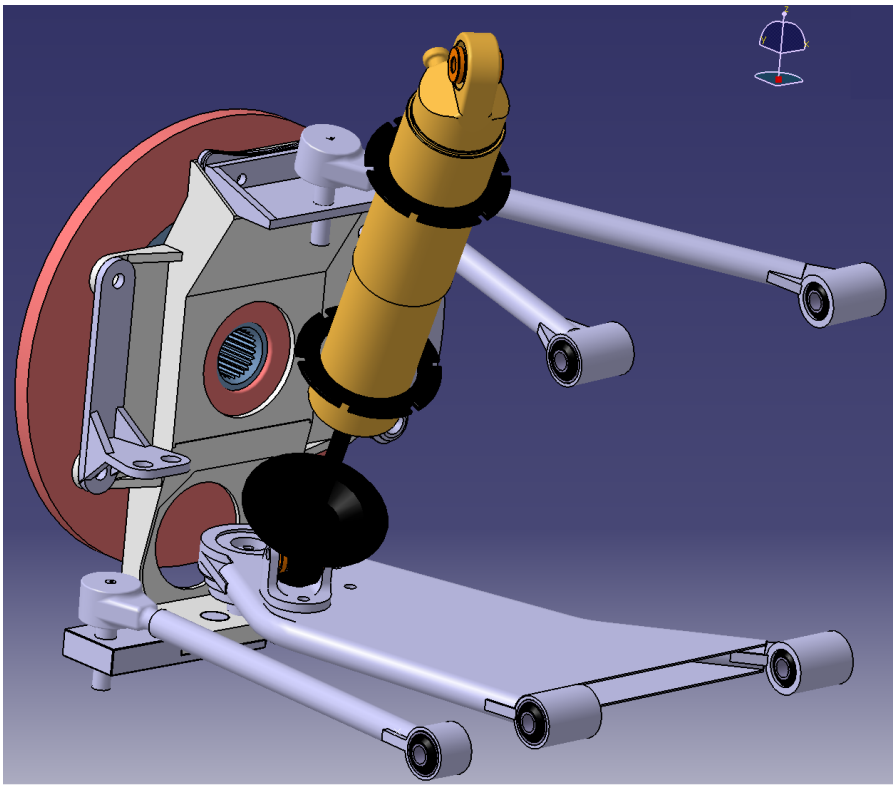

Figure 9.6: *Rear left corner suspension assembly*

9.3 FEA - Finite element analysis

An analysis was performed on the final parts. This analysis was made to ensure that the parts could withstand the 16g vertical load case and not deform due to braking (by applying load cases corresponding to 16g vertical and loads corresponding to a safety factor of at least 2-3 in all other vital directions). There was no analysis performed on side impact of wheel against curb (sliding into curb sideways) as this is regarded as fairly unlikely for this car at this development stage. This FEA was performed in CATIA V5 and then ANSYS 14.0. The parts tested, upright (Figure 9.7), lower and upper wishbone (Figures 9.8 and 9.9) and ARB have all shown a lower (at least 20 % lower) Von Mieses stress than the limiting yield strength of the material (but the damper mount which is let to only handle 10g but can probably be enhanced with a smaller redesign).

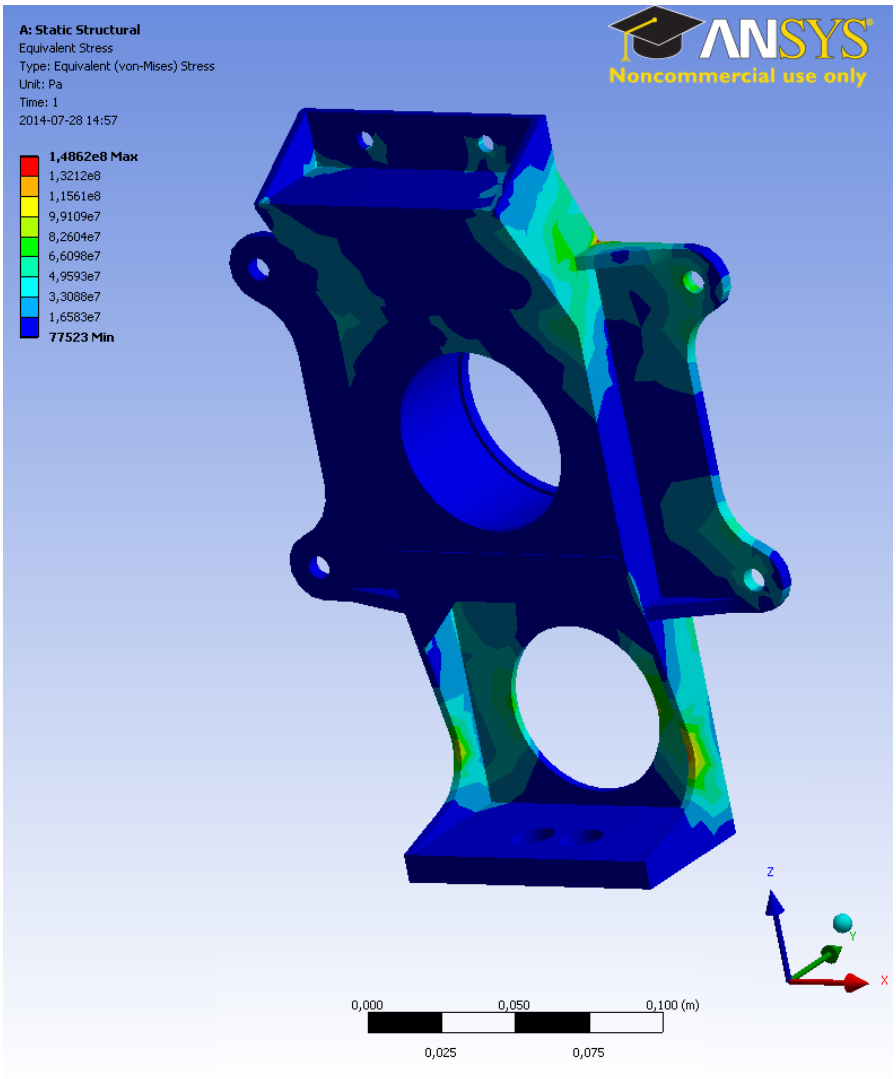

Figure 9.7: *Ansys render of the FEA performed on the upright for 16g z-directional acceleration and fully locked brakes.*

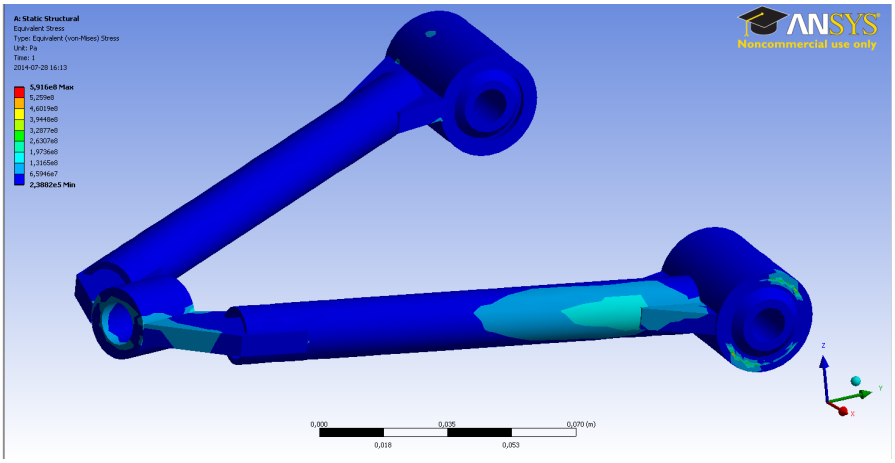

Figure 9.8: *Ansys render of the FEA performed on the upper wishbone for 16g z-directional acceleration and fully locked brakes.*

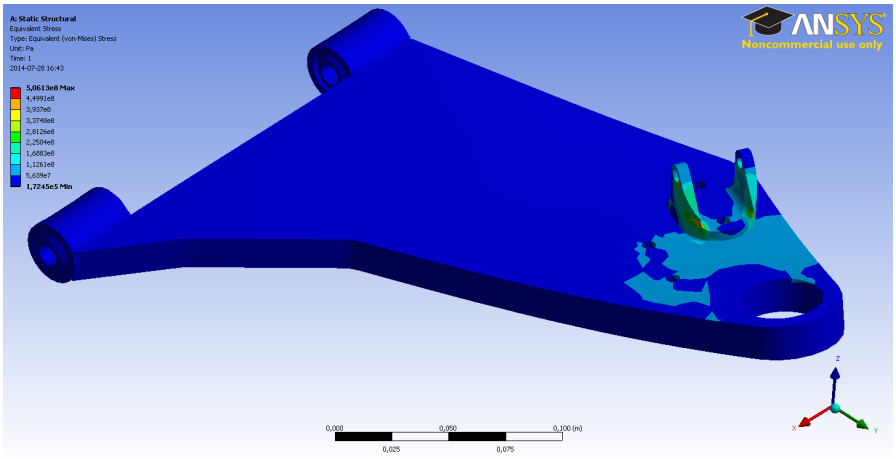

Figure 9.9: *Ansys render of the FEA performed on the lower wishbone for 10g z-directional acceleration and fully locked brakes.*

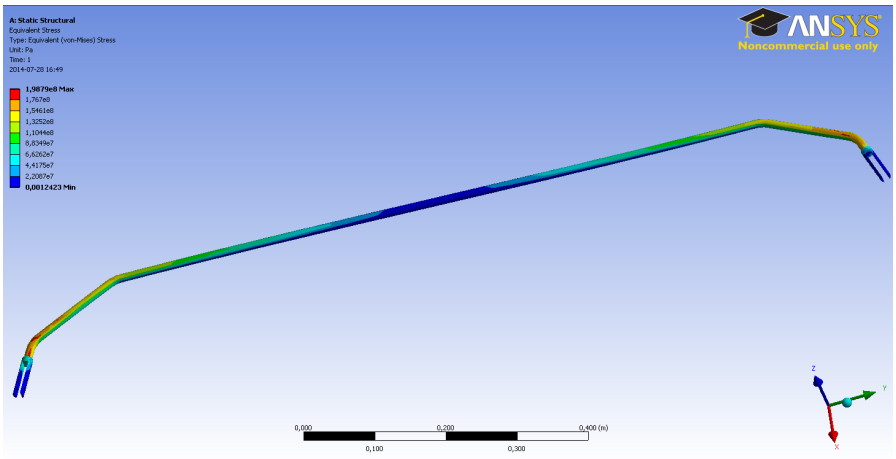

Figure 9.10: *Ansys render of the FEA performed on the anti roll bar for 50 [mm] z-directional displacement.*

Chapter 10
Summary and conclusions

To sum up the work done following can be noted:

- The thesis has provided a much more complete requirement list than the ones availeble at its beginning (Chapter 3).
- A prototype suspension model (hardpoints) and its characteristics has been presented (Chapter 7 and Appendix B).
- A full CAD of the supension has been made (Section 9.1).
- FEA analysis has been undertaken on the CAD-model to analyse structural strength (Section 9.3).
- The suspension, together with an approximative vehicle model has been tested in a full scale virtual car model for dynamical behaviour and response (Chapter 8).

The thesis work has resulted in meeting targets and requirements set in Chapter 3 are as close as possible (mainly everything but the damper mount is complying to the set targets). The damper mount (to lower wishbone) has a stress concentration issue as seen in Figure 9.9. This however can be corrected with a re-design that due to time constraint has to be left for future work. The proposed suspension design should in theory perform well for the set parameters if fabricated.
Two very important factors to design of a small vehicle like this was observed:

- Drivers body makes a big contribution to both the whole systems sprung weight as well as to the systems inertia Section 6.2 & 6.3. This will then influence heavily the vehicles performance depending on load and driver. The vehicle will most probably be less comfortable for a lighter driver and more comfortable for a heavier one, but on the other hand roll less and have lower side slip on the tyres during manoeuvring for lighter driver.
- The ratio unsprung to sprung mass is very high if using conventional car components. Ideally this type of vehicle need tyres, brake system and rims made for the vehicles approximate total weight and not as in this project utilizing same components that are designed for much heavier and powerful vehicles.

Overall the suspension designed performs as good as it can given the situation and limitations to its design. This performance is on pare if not above the target expectations and in most cases also provides safety margins for the case of over speed or overload.

Chapter 11
Future work

The main future continuation of this thesis is the build of the suspension for testing of the UPV prototype (PUNCH). To optimize the design even further some work needs to be done on the damper mount design and maybe some pockets added to the lower wishbone for weight reduction (as the lower wishbone was needed to be strengthened and due to time limits this was done by mainly adding extra material, of which not all is needed for the function). The outer shape (and its volume) of the lower wishbone is however more than enough to accommodate enough material to fulfil the strength criteria.

To analyse stability and safety issues of UPVs it would be desirable to test crash and vehicle dynamics performance in more vehicle type specific tests, as tests that are performed for ordinary cars (that should be able to handle everything from city to highway) might not correspond to the problems or issues of the UPV. E.g. roll over tests might want to be performed for speeds around vehicles top speed (and with a safety margin as in Chapter 8) but with a tighter lane change/curve as city driving often requires a much more transient behaviour than highway driving. One sided bump roll over test should preferably be conducted to ensure that accidental driving onto a curb won't make the vehicle to roll over. Bump during turn (to simulate driving onto a traffic island or edge of a roundabout with the rear, front or both wheels wheel) test could also be beneficial especially as the track width gets narrower as the risk of roll over can then rise. Similar, the crash test with the standard 40 % overlap performed by Euro NCAP might not give the full picture, as the crash forces (and especially acceleration on the human body) when codling with a much heavier vehicle could result in a much worse effect on the occupants than just a crash into a fixed barrier would show. Euro NCAP has a test procedure for a category of "heavy quadricycles" (L7e) into which a UPV most probably would be categorized if needed to be tested (as L7e applies to vehicles with a mass exceeding 350 [kg]). It might also be classified as a "light quadricycle" L6e and then limited to a top speed of 45 [km/h] and a mass sub 350 [kg]. The tests for quadricycles are however performed with 100 % overlap and at a 90 degree angle to the crash structure.

Following recommendations are given for any future suspension work on similar projects:

- Incorporate the suspension into any vehicle design from first stage. That is don't try to retrofit a suspension to an existing frame, but rougher make it a part of the whole structure. This can also enable to use it as a crash structure by dissipating crash force energy by deformation (both permanent and temporary) suspension.

- If a second generation of the vehicle is to be made, it is advisory to maybe try and limit the suspension travel, as the (total with bump stop) 200 [mm] travel of the designed solution probably is way too long for any normal use in city environment. The recommendation would rougher be in the region of 80-150 [mm] suspension travel.

- If possible, try to lower the centre of gravity of the vehicle to limit unnecessary body roll without having to use (or using a less stiff) ARB. That is mainly done by either making the chassis heavier at the bottom (might be impractical for efficiency reasons) or by lowering the seating position. This would impact on the drivers comfort of getting in and out of the vehicle, but maybe a seat that moves in height at entry and exit is a solution.

- If the ride is found to harsh, or the suspension is wanted to be stiffer for less roll, suspending the driver (i.e. the seat) on some spring-damper arrangement could be an answer how to insulate the driver from the harshness of the road. That should be easier than to do so with the whole vehicle as the driver has (generally) lower mass than the whole sprung mass, and therefore less energy (from vertical movement) needs to be dissipated (can be compared with the seat solutions in heavy lorries and buses).

- For a mass produced vehicle, or a vehicle where interior space is highly valued (which is the case with small vehicles more than with bigger one) it is advisory to utilize a suspension type that is as compact as possible. Given the type of driving one is looking at (city driving), the cost and space aspect I'd recommend looking into trailing arm/twist beam solutions. They'd probably give sufficient performance at a much lower cost. A McPherson type suspension is also probably better than the double wishbone in

terms of space, and might even in this case have been a better solution. But this is all mainly given if the frame is made in such way that it's actually made for a certain type of suspension.

- If possible the vehicle should have a track width narrower than today's 1,5 [m], as it could be great in the dense urban areas to be able to utilize one car lane/parking space for 2 or more city vehicles. This however could rise the risk of the vehicle rolling over.
- A great addition to the vehicles performance in manoeuvrability, and also making a narrow track possible (as the front wheels don't need to turn as much for a certain curve radius) is the additional of 4-wheel steering. That could be rougher easily incorporated by utilizing linear motors instead of the rear track rods. To get the drive by wire capability it is recommended to utilize magnetic angle sensors that output an absolute value for the angle so that the system doesn't need to find a zero setting at start-up. For redundancy a minimum of 2 sensors per corner should be implemented.
- Drive by wire capability could also be a great addition and an interesting research area that this vehicle could facilitate. This could be accomplished by incorporating a commercially available pedal and steering wheel setup as i.e. Logitech G27 and a controlling device (computer or SoC device). This could free up now space allocated for steering rack etc. to be used for other purposes. If the vehicle is to be small, space that can be provided to the occupants for comfort or luggage is a valuable asset.
- To reduce the unsprung mass and thereby enhancing road insulation, it could be favourable to either adopt brakes form an existing micro-car or from a moped or motorcycle as the brakes from a production standard car are too big and heavy. It could also be advisable to use inboard brakes and if driven on all four wheels inboard motors and not hub motors (as that would increase the unsprung mass and reduce comfort).

References

[1] M. Kloepper H. Mahmoudi C. Nasif A. R Riazi D. Simkus M. Esmaeli E. Håkansson, "Punch - frame final report", Department of Applied Mechanics, Chalmers University of Technology, Göteborg, Sweden, Tech. Rep., Dec. 2010.

[2] J. Gómez Fernández A Hasselström C. Skaloud D. Atchison N. Coburn, "Punch - 2011", Department of Applied Mechanics, Chalmers University of Technology, Göteborg, Sweden, Tech. Rep., Dec. 2011.

[3] Gunnar Olsson, Leannova AB.

[4] Douglas L. Milliken William F. Milliken, *Race Car Vehicle Dynamics*. SAE International, 1998, ISBN: 978-1-56091-526-3.

[5] Bengt Jacobson et al, *Vehicle Dynamics, Compendium for Course MMF062*. Chalmers University of Technology, 2012.

[6] J. Y. Wong, *Theory of Ground Vehicles*, 4th. John Wiley & Sons, 2008, ISBN: 978-0-470-17038-0.

[7] J. Reimpell, H. Stoll, and J. W. Betzler, *The Automotive Chassis – Engineering Principles*, 2nd. Butterworth Heinemann, 2001, ISBN: 0-7506-5054-0.

[8] European Tyre and Rim Technical Organization, *Standards manual*, 2010.

[9] Michalel Costin and David Phipps, *Racing and Sports Car Chassis Design*, reprint. Albion Scott Ltd., 1991, ISBN: 0-86255-035-1.

[10] *Theory of Ground Vehicles*, 8th. Bentley Publishers, 2011, ISBN: 978-0-8376-1686-5.

[11] Wikipedia, *Understeer and oversteer*, 20140611. [Online]. Available: `http://en.wikipedia.org/wiki/Understeer_and_oversteer`.

[12] Professor Dr.-Ing. Jörg Feldhusen Professor Dr.-Ing. Karl-Heinrich Grote, *Dubbel - Taschenbuch für den Maschinenbau*, 23rd ed. Springer Verlag.

[13] Matt Giarffa, *Springs dampers part 1-6*. [Online]. Available: `http://www.optimumg.com/technical/technical-papers/`.

[14] TRAK SPAX, *Spax da*, 20140225. [Online]. Available: `http://www.spax.co.uk/racing_products-trakspaxda.php`.

[15] *Anthropometric specifications for large sized male dummy (side view)*, Transportation Reasearch Institute, University of Michgan, Nov. 1963.

[16] C. Omoto W. R. Santschi J. DuBois, *Moments of inertia and centers of gravity of the living human body*, North American Aviation Inc Los Angeles CA, Accession Number: AD0410451, May 1963.

[17] THE EUROPEAN PARLIAMENT and THE COUNCIL OF THE EUROPEAN UNION, *Directive 2002/44/ec of the european parliament and of the council*, 2002.

[18] Michelin, *The tyre grip*. [Online]. Available: `automotive.ing.unibs.it/~gadola/Michelin/GRIP.PDF`.

Appendix A

Computation of centre of gravity and moment of inertia - frame

This appendix covers the computation & measurement of the centre of gravity (COG) of the frame. It is to be noted that coordinate system used is according to the DIN-70000, i.e. x-axis positive in the direction of vehicle (forwards), y-axis positive right to left (top view) and z-axis positive upwards. Origin is situated at the rear most point of vehicle at ground level, along the centreline.

A.1 MATLAB code for COG computation

```
clc
clear all
close all
%% Cumputation COG of frame

m=47;                          % frame mass [kg]
L=2570.5/1000;                 % frame lower x-dir members length [m]
W=870/1000;                    % frame lower y-dir members width [m]
gc=.160;                       % Ground clearance of frame [m]

h_lift=linspace(0,1.2,13);      % lift height of frame lower beam at foremost point [mm]

w1=[26.39 26.64 26.91 27.06 27.14 27.3 27.62 27.81 28.1 28.29 28.49 28.57 28.5];    % lift1 of
    frame along x-dir, [kg]

w2=[26.6 26.77 26.9 26.97 27.07 27.29 27.65 27.71 27.77 28.27 28.34 28.4 28.97];    % lift2 of
    frame along x-dir, [kg]

l_f=((w1(1))*(L)/m)             % Distance CoG to front of the lower beam [m]
l_r=(((m-w1(1))*(L))/m)         % Distance CoG to rear in meters

% assuming that left to right side is symmetical
i=1;    % initiating a value
while i<14

    alfa(i)=asin(h_lift(i)/L);      % Computing the lift angle

    delta_l_r_1(i)=(w1(i)*L/m)-l_f; % Computing the change in l_r for case 1
    delta_l_r_2(i)=(w2(i)*L/m)-l_f; % Computing the change in l_r for case 2

    h1(i)=delta_l_r_1(i)/tan(alfa(i));
    h2(i)=delta_l_r_2(i)/tan(alfa(i));

    i=i+1;
end
h=[h1+h2]./2;                  % Adding the 2 h-vecotrs for the 2 test cases together and deviding by
    2
h(1)=[];                       % Removing the 1st element in h_v as it is NaN

h=mean(h);                     % Taking the average value of h

h_v_m=.480;                    % Height of CoG [m] (assumed from initial computation, but turned out
    to be erroneous.

error=(1-((h+gc)/h_v_m))*100% Computing the error betweent he original computed h, and the
    correctly computed h (here with gc, as original h also had gc included) [%].

CoG_x=l_r+.165                 % Distance CoG to rear [m] (165mm from lower beam end to end of frame),
     ie the x-coord of CoG
CoG_y=0                        % y-coord of CoG [m]
CoG_z=h+gc                     % z-coord of CoG [m], CoG_z of frame (h) plus ground clearance (gc)
```

Appendix B
Hardpoint locations iteration

This appendix declares the hardpoints and motion ratios that were concluded from the suspension simulation (performed in IPG Kinematics see Chapter 7).

Point	x [mm]	y [mm]	z [mm]
Wheel Center	2500	750	297.5
Center of Tire Contact	2500	750	0
Force Application Tire Forces	2500	755.8	0
Body - Chassis Subframe Front	2680	460	170
Body - Chassis Subframe Rear	2500	460	175
Wheel Carrier - Lower Wishbone	2510	726	176
Wheel Carrier - Upper Wishbone	2500	679	424
Wheel Carrier - Steering Rod	2600	694	284
Subframe - Bushing Front Lower Wishbone	2680	460	170
Subframe - Bushing Rear Lower Wishbone	2500	460	175
Vehicle - Bushing Front Upper Wishbone	2680	460	390
Vehicle - Bushing Rear Upper Wishbone	2500	460	391
Chassis Subframe - Stabilizer Bar	2650	460	360
Stabilizer Bar - Stabilizer Link	2500	626,6	372,3
Stabilizer Link - Wheel Suspension	2521,7	659,9	216,3
Steering Rod - Steering Rack	2500	460	270
Chassis Subframe - Steering Gearbox	2580	400	270
Spring - Body	2400	460	550
Spring - Wheel Suspension	2477	647	217
Damper - Body	2400	460	550
Damper - Lower Wishbone	2477	647	217
Axle Drive Shaft - Differential	2500	460	297.5
Axle Drive Shaft - Wheel	2500	750	297.5

Figure B.1: *Hardpoint coordinates front*

Point	x [mm]	y [mm]	z [mm]
Wheel Center	299	748,6	297,5
Center of Tire Contact	299	748,6	0
Force Application Tire Forces	299	754,6	0
Body - Chassis Subframe Front	480	460	179
Body - Chassis Subframe Rear	300	460	172
Wheel Carrier - Lower Wishbone	310	724,5	176
Wheel Carrier - Upper Wishbone	297	678	424
Wheel Carrier - Steering Rod	218	725	173
Subframe - Bushing Front Lower Wishbone	480	460	179
Subframe - Bushing Rear Lower Wishbone	300	460	172
Vehicle - Bushing Front Upper Wishbone	480	460	385
Vehicle - Bushing Rear Upper Wishbone	300	460	375
Chassis Subframe - Stabilizer Bar	540	460	500
Stabilizer Bar - Stabilizer Link	340	600	450
Stabilizer Link - Wheel Suspension	299	640	215
Steering Rod - Steering Rack	218	460	170
Chassis Subframe - Steering Gearbox	218	440	170
Spring - Body	200	460	550
Spring - Wheel Suspension	274,5	647	214
Damper - Body	200	460	550
Damper - Lower Wishbone	274,5	647	214
Axle Drive Shaft - Differential	299	460	297,5
Axle Drive Shaft - Wheel	299	750	297,5

Figure B.2: *Hardpoint coordinates rear*

Position wheel contact point, z [mm]	Damper length [mm]	Damper angle to xy-plane (deg)	Change damper length [mm]	MR
100	319,057	56,329	14,723	0,73615
80	333,78	56,535	14,482	0,7241
60	348,262	56,891	14,164	0,7082
40	362,426	57,37	13,855	0,69275
20	376,281	57,967	3,426	0,6852
15	379,707	58,13	3,41	0,682
10	383,117	58,8	3,394	0,6788
5	386,511	58,475	3,377	0,6754
0	389,888	58,653	3,363	0,6724
-5	393,251	58,843	3,347	0,6694
-10	396,598	59,035	3,333	0,6666
-15	399,931	59,232	3,318	0,6636
-20	403,249	59,434	13,14	0,657
-40	416,389	60,297	12,942	0,6471
-60	429,331	61,24	12,772	0,6386
-80	442,103	62,265	12,538	0,6269
-100	454,641	63,375	12,661	0,63305

Figure B.3: *Motion ratio front damper travel*

Position wheel contact point, z [mm]	Damper length [mm]	Damper angle to xy-plane (deg)	Change damper length [mm]	MR
100	319,243	57,247	15,169	0,75845
80	334,412	57,319	14,806	0,7403
60	349,218	57,561	14,47	0,7235
40	363,688	57,942	14,162	0,7081
20	377,85	58,444	3,463	0,6926
15	381,313	58,587	3,452	0,6904
10	384,765	58,736	3,465	0,693
5	388,23	58,891	3,449	0,6898
0	391,679	59,052	3,433	0,6865
-5	395,112	59,22	3,416	0,6832
-10	398,528	59,393	3,402	0,6804
-15	401,93	59,572	3,386	0,6772
-20	405,316	59,756	13,406	0,6703
-40	418,722	60,548	13,164	0,6582
-60	431,886	61,423	12,903	0,64515
-80	444,789	62,38	12,821	0,64105
-100	457,61	63,419	12,712	0,6356

Figure B.4: *Motion ratio rear damper travel*

Appendix C

Spring and damper dimensioning

This appendix covers the calculations of the suspension characteristics, as spring rate, damper rate, roll rate. Springs let the suspension move versus the body (in contrary to rigidly mounted wheels) whereby insulating the vehicle body and the driver from the road unevenness. The dampers in an automotive suspension refrains the spring from oscillate freely and makes the ride less shaky for the driver, as they usually are tuned to dampen out the oscillation induced by a bump within one to two periods of spring movement (assuming the movement of the spring to be described by e.g. a sinusoidal function). To ensure that the vehicle keeps the right ride height at curb level and that driver isn't exposed to road harshness correct spring rates and damping coefficient is crucial. The calculations performed in this chapter can also be seen in C.1 (MATLAB calculations).

C.1 Matlab code for suspension values

```
clc
clear all
close all

g=9.81;         % Gravitational acceleration [m/s^2]
%% Spring rate calculation. All values per wheel if not other is stated

m_u=40;                             % Unsprung mass [kg]/corner

F_sf=619.1739-m_u*g;                % Force in spring front [N]
F_sr=769.1793-m_u*g;                % Force in spring rear [N]

m_sf=F_sf/g;                        % Unsprung mass front
m_sr=F_sr/g;                        % Unsprung mass rear

c_t=200000;                         % Spring rate tyre [N/m] (assumed)

alpha_f=28.74*pi/180;               % Angle damper to z-axis front
alpha_r=28.54*pi/180;               % Angle damper to z-axis rear

d_dtrf=64.753;                      % Damper travel full rebound to curb front[mm]
d_dtrr=65.931;                      % Damper travel full rebound to curb rear[mm]

f_rf=1;                             % Ride frequency front [Hz]
f_rr=1.1;                           % Ride frequency rear [Hz]

MR_f0=.6724;                        % Motion ration front
MR_r0=.6865;                        % Motion ration rear

c_w_f=(2*pi*f_rf)^2*m_sf;           % Wheel rate front [N/m]
c_w_r=(2*pi*f_rr)^2*m_sr;           % Wheel rate rear [N/m]

C_sf=c_w_f*(1/MR_f0^2)/1000;        % Spring rate front [N/mm]
C_sr=c_w_r*(1/MR_r0^2)/1000;        % Spring rate rear [N/mm]

d_tr_f_n=F_sf/(C_sf*cos(alpha_f)); % Needed travel of spring from free length to curb achieve
    enough vertical force
d_f_preload=d_tr_f_n-d_dtrf;        % Preload compression distance (at full rebound) front
F_f_preload=d_f_preload*C_sf;       % Preload force in spring front

d_tr_r_n=F_sr/(C_sr*cos(alpha_r)); % Needed travel of spring from free length to curb achieve
    enough vertical force
d_r_preload=d_tr_r_n-d_dtrr;        % Preload compression distance (at full rebound) rear
F_r_preload=d_r_preload*C_sr;       % Preload force in spring front

%% Damper calculations
D_crf=2*sqrt(c_w_f*m_sf)/MR_f0;     % Critical damping front [N*s/m]
D_crr=2*sqrt(c_w_r*m_sf)/MR_r0;     % Critical damping rear [N*s/m]
```

```
zeta=0.5;                           % Damping ratio
D_f=D_crf*zeta;                     % Damping front
D_r=D_crr*zeta;                     % Damping front


%% ARB rate calculation. All values per wheel if not other is stated
phi_A=7;                            % Desired roll gradient value of 7 degrees per g lateral
    acceleration
w=1.5;                              % Track width
MR_FA=.7913;                        % Assumed motion ratio ARB front
MR_RA=.7913;                        % Assumed motion ratio ARB rear
h=.480;                             % COG height [m]

C_f_tot=1/((1/c_w_f)+(1/c_t));      % Total vertical spring rate front
C_r_tot=1/((1/c_w_r)+(1/c_t));      % Total vertical spring rate rear
C_s_tot=(C_f_tot+C_r_tot);          % Total vertical spring rate for whole vehicle (spring+tyre
    rate with account to MR)/side

a_y=g;                        % Small lateral acceleration. Should correspond to phi_A*a_y degrees

F_yw=a_y*(m_sr+m_sf);               % Lateral force due to lateral acceleration on the sprung mass
    a_y*m_s

p_x=a_y*(m_sr+m_sf)*h*2*C_s_tot/(C_s_tot^2*w^2)*180/pi/(a_y/g); % Vehicle inclination for a_y
    lateral acceleration [deg/g]

p_x1=a_y*(m_sr+m_sf)*h*2*C_s_tot/(C_s_tot^2*w^2-(m_sr+m_sf)*g*h*2*C_s_tot)*180/pi/(a_y/g);  %
    Vehicle inclination for a_y lateral acceleration with compensation for movement of COG [deg/g]
```

Appendix D
Ride quality

This appendix covers the calculations of the suspension ride quality. The computation is made and based on files (provided by the department) from 3rd assignment in the vehicle dynamics course MMF062 at Chalmers University of Technology.

D.1 Initial values

In order to be able to make the computation initial values are plugged into the initial values file. As the computation in the original assignment is made for vertical motion only, and doesn't take motion ratios and angled dampers / springs into consideration the values are altered accordingly. The wheel rate is used for the spring value and the damping constant (of the in Subsection 6.1.2 computed values) is divided by the motion ratio (front and rear respectively). This is to be seen in Appendix D.2. Here also the assumed top speed on respective type of road is specified, the distance that is to be travelled and the time total time of travel for a day.

D.2 Matlab code, suspension initial values

```
%%%%%%%%%%%%%%%%%%%%%%%%%%%%%%%%%%%%%%%%%%%%%%%%%%%%%%%%
% Vehicle Dynamics, MMF062
% Vertical assignment, initialize parameters
%
% Add your own code where "%ADD YOUR CODE HERE" are stated
%
clear all;
close all;
clc;

set(0,'DefaultAxesFontSize',12)
set(0,'DefaultAxesLineWidth',2)
set(0,'defaultlinelinewidth',2)

%%%%%%%%%%%%%%%%%%%%%%%%%%%%%%%%%%%%%%%%%%%%%%%%%%%%%%%%
% Vehicle parameters [SI units]
%
totalSprungMass = 180;
totalUnsprungMass = 160;
wheelBase = 2.2;
distanceCogToFrontAxle = 0.58 * wheelBase;
momentOfInertia = 39.868;    % Moment of interia of whole vehicle accoring to IPG CarMaker
frontAxleSuspStiff = 912;   % Front wheel rate (rouded up)
rearAxleSuspStiff = 1835;    % Rear wheel rate (rouded up)
frontAxleSuspDamp = 140;     % Front damping constant divided times motion ratio (rouded up)
rearAxleSuspDamp = 195;      % Rear damping constant divided times motion ratio (rouded up)
tireStiff = 200000;          % Assumed tyre stifness
tireDamp = 0;                % Assuming no damping in tyre

% Other parameters Task 1
frequencyVector = [0.1 : 0.01 : 50]';
angularFrequencyVector = 2 * pi * frequencyVector;
deltaAngularFrequency = 2 * pi * 0.01;

% Other parameters Task 2
roadDisplacementAmplitude = 1;
roadSeverity = 10E-6;
vehicleVelocity = 80/3.6;
roadWaviness = 2.5;
frontAxleSuspDampVector = [1000 : 100 : 9000];
frontAxleSuspStiffVector = [0.5 0.75 1 1.25 1.5 2]*frontAxleSuspStiff;

% Other parameters Task 3
% road distribution
roadSeveritySmooth = 1E-6;
roadSeverityRough = 10E-6;
roadSeverityVeryRough = 100E-6;
```

```
roadWavinessSmooth = 3;
roadWavinessRough = 2.5;
roadWavinessVeryRough = 2;

totalDrivingTime = 8*60*60;                 % 8h driving period
totalDistance = 50E3;                       % Total distance of route (there and back)[s]
distanceSmoothRoad = .7*totalDistance;      % Assuming 80% good road
distanceRoughRoad = 0.3*totalDistance;      % Assuming 20% bad road
distanceVeryRoughRoad = 0.0*totalDistance; % Assuming 0% very rough road as this is a city vehicle

vehicleVelocitySmooth = 50/3.6;    % Assuming max allowed vehicle velocity on good road type 50km/h
vehicleVelocityRough = 30/3.6;
vehicleVelocityVeryRough = 8/3.6;
```

D.3 Matlab code, ride quality calculation

```
%%%%%%%%%%%%%%%%%%%%%%%%%%%%%
% Vehicle Dynamics, MMF062
% Vertical assignment, Task 3

clear all;
close all;
clc;
%%%%%%%%%%%%%%%%%%%%%%%%%%%%%%%%%%%%%%%%%%%%%%%%%%%%
%% Load parameters from file "InitParameters.m"

InitParameters

%%%%%%%%%%%%%%%%%%%%%%%%%%%%%%%%%%%%%%%%%%%%%%%%%%%%
%% Task 3.1

numberOfTripsPerDay = totalDrivingTime/...
    (distanceSmoothRoad/vehicleVelocitySmooth+distanceRoughRoad/vehicleVelocityRough+
        distanceVeryRoughRoad/vehicleVelocityVeryRough);

% i)
% Calculate road spectrum
roadSpectrumSmooth = zeros(length(angularFrequencyVector),1);
roadSpectrumRough = zeros(length(angularFrequencyVector),1);
roadSpectrumVeryRough = zeros(length(angularFrequencyVector),1);

for j = 1 : length(angularFrequencyVector)
    roadSpectrumSmooth(j,:) = vehicleVelocitySmooth^(roadWavinessSmooth-1)*roadSeveritySmooth*
        angularFrequencyVector(j)^(-roadWavinessSmooth);
    roadSpectrumRough(j,:) = vehicleVelocityRough^(roadWavinessRough-1)*roadSeverityRough*
        angularFrequencyVector(j)^(-roadWavinessRough);
    roadSpectrumVeryRough(j,:) = vehicleVelocityVeryRough^(roadWavinessVeryRough-1)*
        roadSeverityVeryRough*angularFrequencyVector(j)^(-roadWavinessVeryRough);
end

% Calculate transfer functions for front wheel Zr to Ride
% You can use result from Task 1

% Consider one single front wheel
sprungMassFront = (1-distanceCogToFrontAxle / wheelBase) * totalSprungMass/2;
unsprungMassFront = totalUnsprungMass/4;

% Identify indiviual matricies Mf, Cf, Df, DDf and DCf
massMatrixFront = [sprungMassFront 0;0 unsprungMassFront]; % Mf

dampMatrixFront = [frontAxleSuspDamp -frontAxleSuspDamp;
    -frontAxleSuspDamp tireDamp+frontAxleSuspDamp]; % Df

stiffMatrixFront = [frontAxleSuspStiff -frontAxleSuspStiff;
    -frontAxleSuspStiff tireStiff+frontAxleSuspStiff]; % Cf

loadDampMatrixFront = [0;tireDamp]; % DDf

loadStiffMatrixFront = [0;tireStiff]; % DCf

% Calculate transfer function matrix front wheel, Hf
```

```
transferFunctionFrontZrToZ = zeros(length(massMatrixFront),length(angularFrequencyVector)); % Hf

for j = 1 : length(angularFrequencyVector)
    transferFunctionFrontZrToZ(:,j) = (-angularFrequencyVector(j)^2 * massMatrixFront + ...
        i * angularFrequencyVector(j) * dampMatrixFront + stiffMatrixFront) \ ...
        (i * angularFrequencyVector(j) * loadDampMatrixFront + loadStiffMatrixFront);
end

transferFunctionFrontZrToRide = zeros(length(angularFrequencyVector),1);

for j = 1 : length(angularFrequencyVector)
    transferFunctionFrontZrToRide(j,:) = -angularFrequencyVector(j)^2 * transferFunctionFrontZrToZ
        (1,j);
end

% Calculate acceleration response spectrum for all roads

psdAccelerationSmooth = zeros(length(angularFrequencyVector),1);
psdAccelerationRough = zeros(length(angularFrequencyVector),1);
psdAccelerationVeryRough = zeros(length(angularFrequencyVector),1);

for j = 1 : length(angularFrequencyVector)
    psdAccelerationSmooth(j,:) = abs(transferFunctionFrontZrToRide(j,:)).^2*roadSpectrumSmooth(j,:)
        ;
    psdAccelerationRough(j,:) = abs(transferFunctionFrontZrToRide(j,:)).^2*roadSpectrumRough(j,:);
    psdAccelerationVeryRough(j,:) = abs(transferFunctionFrontZrToRide(j,:)).^2*
        roadSpectrumVeryRough(j,:);
end

%%%%%%%%%%%%%%%%%%%%%%%%%%%%%%%%%%%%%%%%%%%%%%%%%%%%
% ii)
% Calculate rms values weighted according to ISO2631
[weightedRmsAccelerationSmooth] = CalculateIsoWeightedRms(frequencyVector,psdAccelerationSmooth);
[weightedRmsAccelerationRough] = CalculateIsoWeightedRms(frequencyVector,psdAccelerationRough);
[weightedRmsAccelerationVeryRough] = CalculateIsoWeightedRms(frequencyVector,
    psdAccelerationVeryRough);

%%%%%%%%%%%%%%%%%%%%%%%%%%%%%%%%%%%%%%%%%%%%%%%%%%%%
% iii)
% Calculate time averaged vibration exposure value for 8h period
timeOnSmoothRoad = (distanceSmoothRoad / vehicleVelocitySmooth)*numberOfTripsPerDay;
timeOnRoughRoad = (distanceRoughRoad / vehicleVelocityRough)*numberOfTripsPerDay;
timeOnVeryRoughRoad = (distanceVeryRoughRoad / vehicleVelocityVeryRough)*numberOfTripsPerDay;

timeWeightedMsAcceleration = (weightedRmsAccelerationSmooth^2*timeOnSmoothRoad + ...
    weightedRmsAccelerationRough^2*timeOnRoughRoad +...
    weightedRmsAccelerationVeryRough^2*timeOnVeryRoughRoad)/(timeOnSmoothRoad+timeOnRoughRoad+
        timeOnVeryRoughRoad);

timeWeightedRmsAcceleration = sqrt(timeWeightedMsAcceleration);

disp(['timeWeightedRmsAcceleration =' num2str(timeWeightedRmsAcceleration),' m/s2 (1.15)',...
    ', numberOfTripsPerDay = ' num2str(numberOfTripsPerDay)]);
disp(['vehicleVelocitySmooth = ' num2str(vehicleVelocitySmooth*3.6),' km/h',...
    ', vehicleVelocityRough = ' num2str(vehicleVelocityRough*3.6),' km/h',...
    ', vehicleVelocityVeryRough = ' num2str(vehicleVelocityVeryRough*3.6),' km/h'])
```

D.4 Matlab code, road insulation

```
%%%%%%%%%%%%%%%%%%%%%%%%%%%%%%%%%%%%%%%%%%%%%%%%%%%%
% Vehicle Dynamics, MMF062
% Vertical assignment, Task 1
%
%
clear all;
close all;
clc;
%%%%%%%%%%%%%%%%%%%%%%%%%%%%%%%%%%%%%%%%%%%%%%%%%%%%
%% Load parameters from file "InitParameters.m"

InitParameters
```

```
%%%%%%%%%%%%%%%%%%%%%%%%%%%%%%%%%%%%%%%%%%%%%%%%%%%%
%% Task 1.2
%
% Consider one single front wheel, identify sprung mass and unsprung mass

sprungMassFront = (1-distanceCogToFrontAxle / wheelBase) * totalSprungMass/2;
unsprungMassFront = totalUnsprungMass/4;

% Identify indiviual matricies Mf, Cf, Df, DDf and DCf

massMatrixFront = [sprungMassFront 0;0 unsprungMassFront]; % Mf

dampMatrixFront = [frontAxleSuspDamp -frontAxleSuspDamp;
    -frontAxleSuspDamp tireDamp+frontAxleSuspDamp]; % Df

stiffMatrixFront = [frontAxleSuspStiff -frontAxleSuspStiff;
    -frontAxleSuspStiff tireStiff+frontAxleSuspStiff]; % Cf

loadDampMatrixFront = [0;tireDamp]; % DDf

loadStiffMatrixFront = [0;tireStiff]; % DCf

% Calculate transfer function Zr to Z front wheel, Hf

% Pre-allocate matrix
transferFunctionFrontZrToZ = zeros(length(massMatrixFront),length(angularFrequencyVector)); % Hf

for j = 1 : length(angularFrequencyVector)
    transferFunctionFrontZrToZ(:,j) = (-angularFrequencyVector(j)^2 * massMatrixFront + ...
        1i * angularFrequencyVector(j) * dampMatrixFront + stiffMatrixFront) \ ...
        (1i * angularFrequencyVector(j) * loadDampMatrixFront + loadStiffMatrixFront);
end

%%%%%%%%%%%%%%%%%%%%%%%%%%%%
% Consider one single rear wheel, identify sprung mass and unsprung mass

sprungMassRear = (distanceCogToFrontAxle / wheelBase) * totalSprungMass/2;
unsprungMassRear = totalUnsprungMass/4;

% Derive indiviual matricies Mr, Cr, Dr, DDr and DCr
massMatrixRear = [sprungMassRear 0;0 unsprungMassRear]; % Mr

dampMatrixRear = [rearAxleSuspDamp -rearAxleSuspDamp;
    -rearAxleSuspDamp tireDamp+rearAxleSuspDamp]; % Dr

stiffMatrixRear = [rearAxleSuspStiff -rearAxleSuspStiff;
    -rearAxleSuspStiff tireStiff+rearAxleSuspStiff]; % Cr

loadDampMatrixRear = [0;tireDamp]; % DDr

loadStiffMatrixRear = [0;tireStiff]; % DDr

% Calculate transfer function Zr to Z rear wheel, Hr

% Pre-allocate matrix
transferFunctionRearZrToZ = zeros(length(massMatrixRear),length(angularFrequencyVector)); % Hr

for j = 1 : length(angularFrequencyVector)
    transferFunctionRearZrToZ(:,j) = (-angularFrequencyVector(j)^2 * massMatrixRear + ...
        1i * angularFrequencyVector(j) * dampMatrixRear + stiffMatrixRear) \ ...
        (1i * angularFrequencyVector(j) * loadDampMatrixRear + loadStiffMatrixRear);
end

%%%%%%%%%%%%%%%%%%%%%%%%%%%%%%%%%%%%%%%%%%%%%%%%%%%%
%% Task 1.3
%
% Front wheel
% Calculate transfer functions for front wheel Zr to Ride, Suspension travel and Tyre force
transferFunctionFrontZrToRide = zeros(length(angularFrequencyVector),1);
transferFunctionFrontZrToTravel = zeros(length(angularFrequencyVector),1);
```

```
transferFunctionFrontZrToForce = zeros(length(angularFrequencyVector),1);

for j = 1 : length(angularFrequencyVector)
    transferFunctionFrontZrToRide(j,:) = -angularFrequencyVector(j)^2 * transferFunctionFrontZrToZ
        (1,j);
    transferFunctionFrontZrToTravel(j,:) = transferFunctionFrontZrToZ(2,j)-
        transferFunctionFrontZrToZ(1,j);
    transferFunctionFrontZrToForce(j,:) = tireStiff * (1-transferFunctionFrontZrToZ(2,j));
end

% Rear wheel
% Calculate transfer functions for rear wheel Zr to Ride, Suspension travel and Tyre force
transferFunctionRearZrToRide = zeros(length(angularFrequencyVector),1);
transferFunctionRearZrToTravel = zeros(length(angularFrequencyVector),1);
transferFunctionRearZrToForce = zeros(length(angularFrequencyVector),1);

for j = 1 : length(angularFrequencyVector)
    transferFunctionRearZrToRide(j,:) = -angularFrequencyVector(j)^2 * transferFunctionRearZrToZ(1,
        j);
    transferFunctionRearZrToTravel(j,:) = transferFunctionRearZrToZ(2,j)-transferFunctionRearZrToZ
        (1,j);
    transferFunctionRearZrToForce(j,:) = tireStiff * (1-transferFunctionRearZrToZ(2,j));
end

% Plot the transfer functions
figure;
semilogx(frequencyVector,db(abs(transferFunctionFrontZrToRide)),'-b',...
    frequencyVector,db(abs(transferFunctionRearZrToRide)),'--r');
axis([0 50 -10 100]);grid
legend('Front','Rear',-1);
xlabel('Frequency [Hz]');
ylabel('abs(H)');
title('Magnitude of transfer function Ride Comfort');

figure;
semilogx(frequencyVector,db(abs(transferFunctionFrontZrToTravel)),'-b',...
    frequencyVector,db(abs(transferFunctionRearZrToTravel)),'--r');
axis([0 50 -60 10]);grid
legend('Front','Rear',-1);
xlabel('Frequency [Hz]');
ylabel('abs(H)');
title('Magnitude of transfer function Suspension Travel');

figure;
semilogx(frequencyVector,db(abs(transferFunctionFrontZrToForce)),'-b',...
    frequencyVector,db(abs(transferFunctionRearZrToForce)),'--r');
axis([0 50 30 130]);grid
legend('Front','Rear',-1);
xlabel('Frequency [Hz]');
ylabel('abs(H)');
title('Magnitude of transfer function Road Grip');

%%%%%%%%%%%%%%%%%%%%%%%%%%%%%%%%%%%%%%%%%%%%%%%%%%%%
%% Task 1.4
%
% Front wheel
resonanceFreqFrontBounce=sqrt((1/(1/frontAxleSuspStiff+1/tireStiff))/sprungMassFront)
resonanceFreqFrontHop=sqrt((frontAxleSuspStiff+tireStiff)/unsprungMassFront)

% Rear wheel

resonanceFreqRearBounce=sqrt((1/(1/rearAxleSuspStiff+1/tireStiff))/sprungMassRear)
resonanceFreqRearHop=sqrt((rearAxleSuspStiff+tireStiff)/unsprungMassRear)
```

Appendix E

Drawings - Catia V5

This appendix showcases the drawings of the various parts that need to be manufactured. They were created with Catia V5. The full CAD model and corresponding files have been submitted to Sven B. Andersson at Applied Mechanics, Division of Combustion, Chalmers University of Technology. Note that the drawings shown are created in A4 format, so the given scale in the drawing is not correct in this paper.

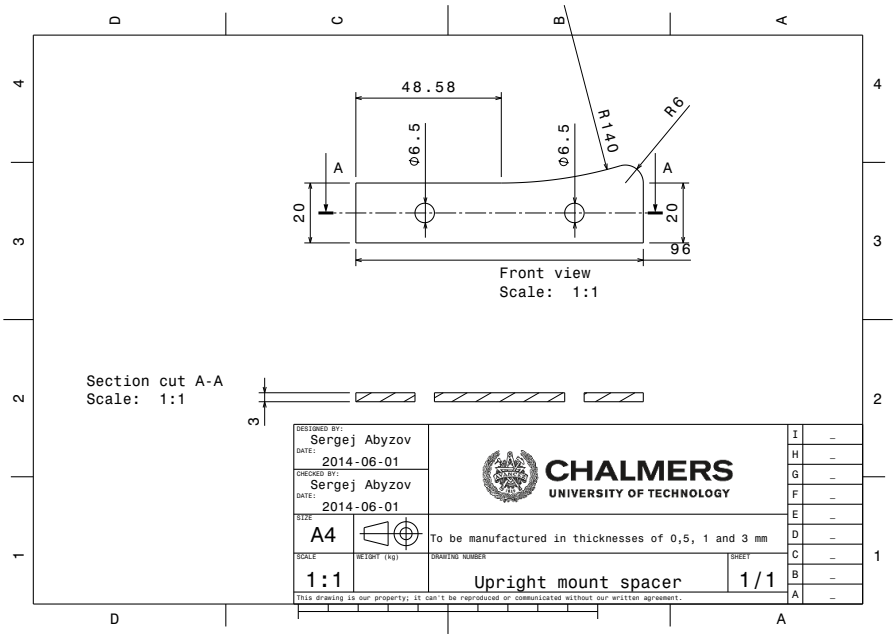

Figure E.1: *Uprigt spacer, manufactured in various thickness of 0,5 to 3 [mm]*

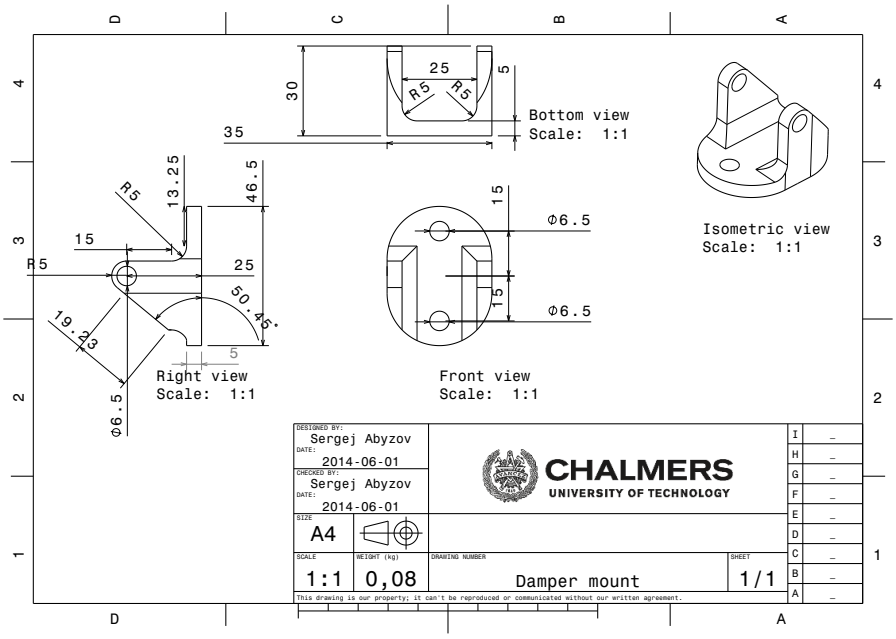

Figure E.2: *Damper mount*

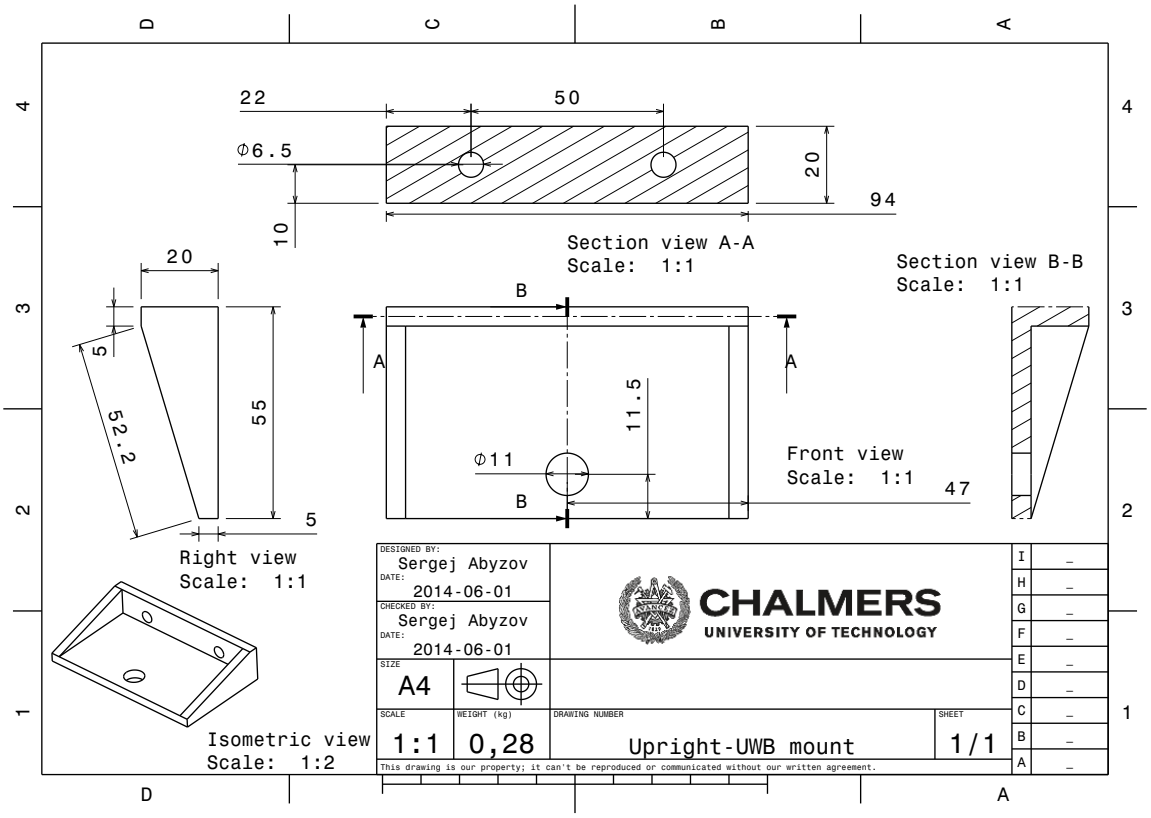

Figure E.3: *Uprigt fixture (upper ball joint mount)*

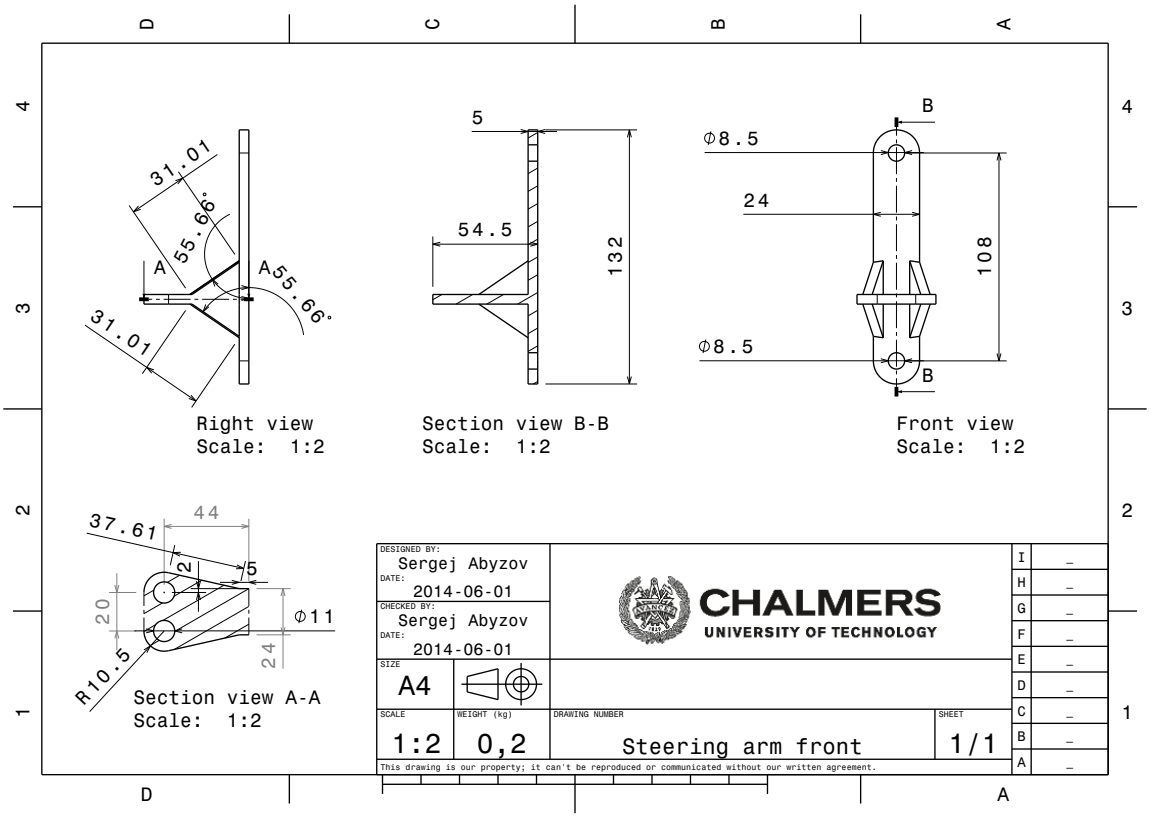

Figure E.4: *Front steer arm*

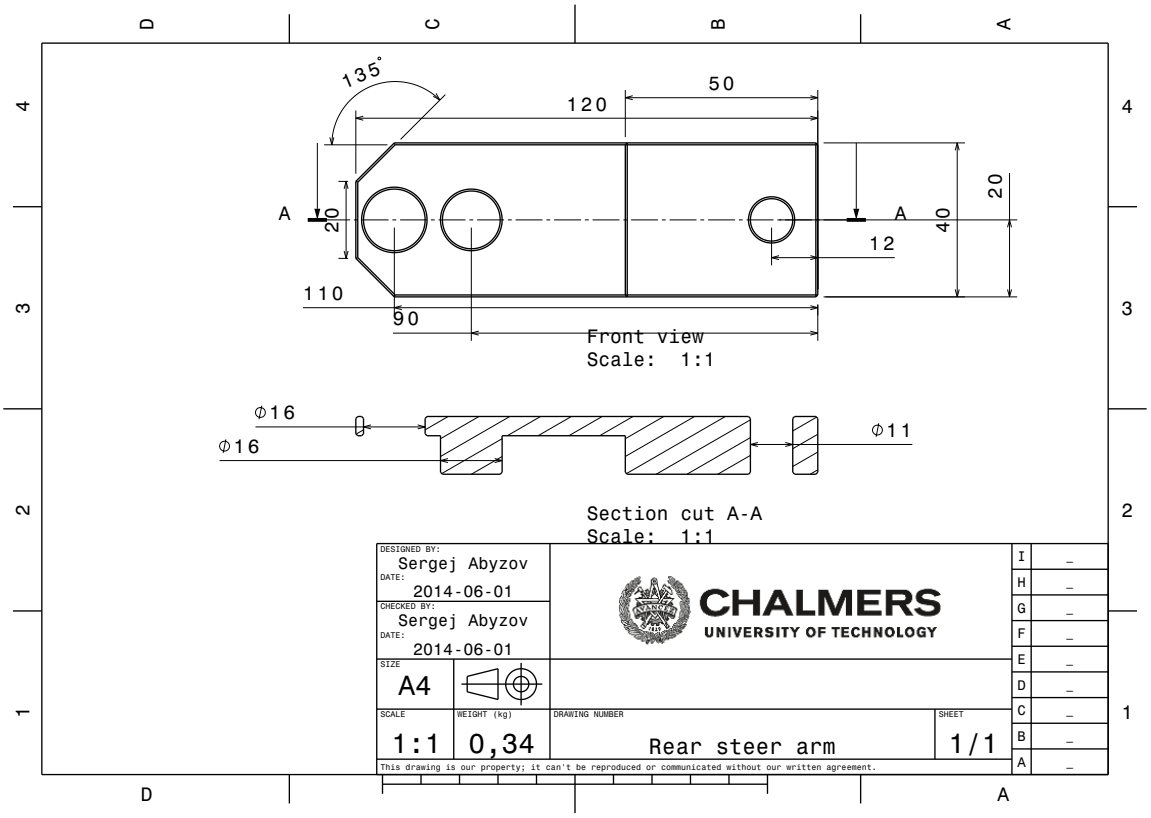

Figure E.5: *Rear steer arm)*

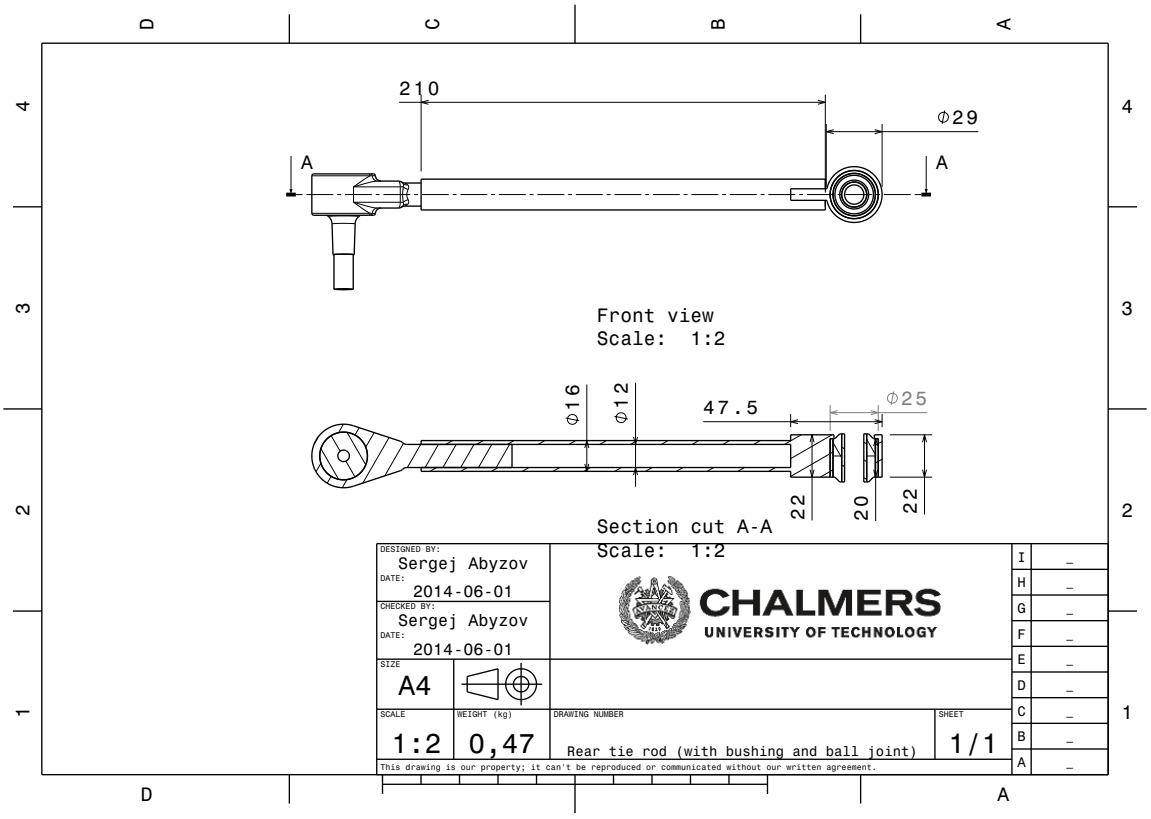

Figure E.6: *Rear tie rod*

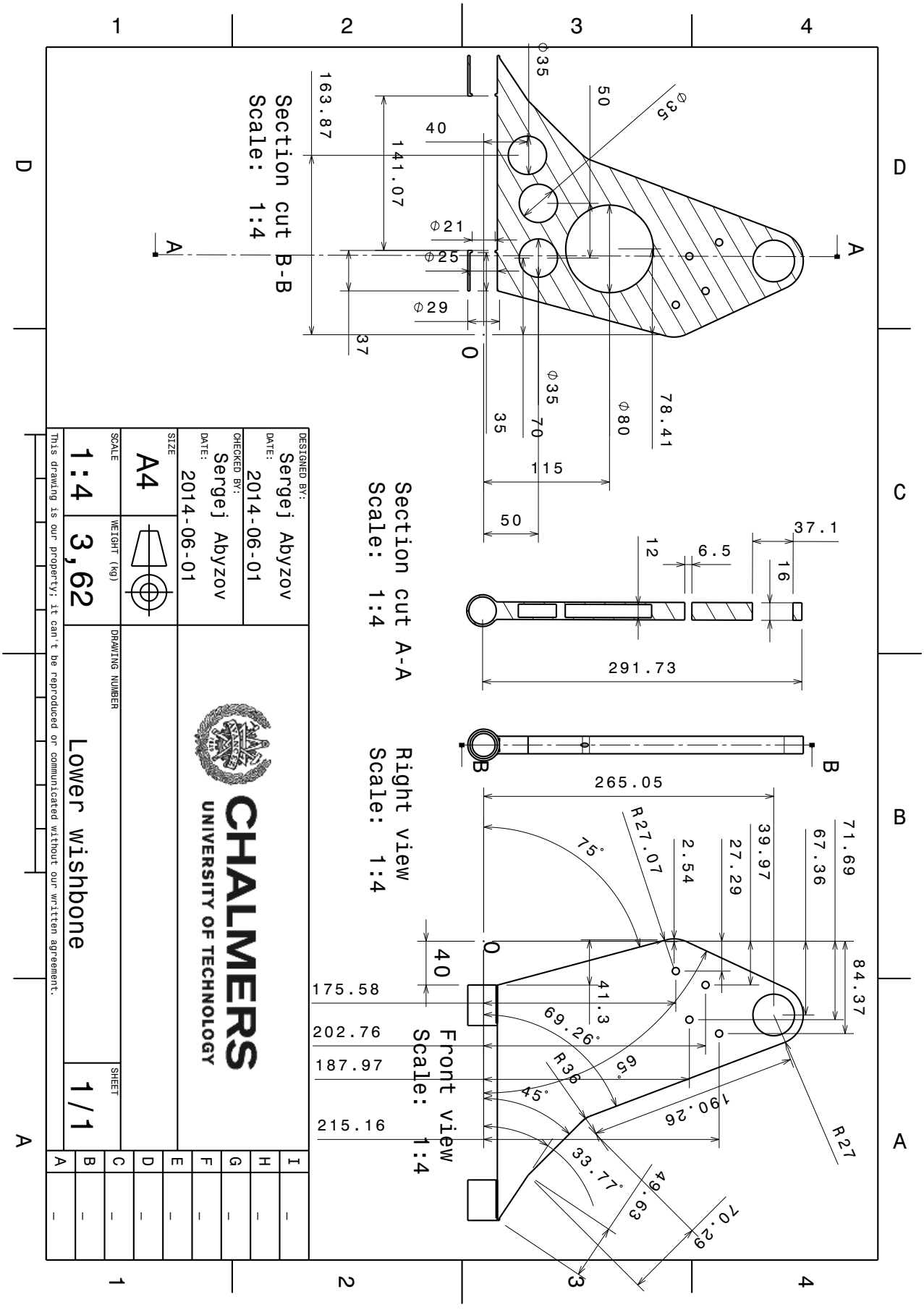

Figure E.7: *Lower wishbone)*

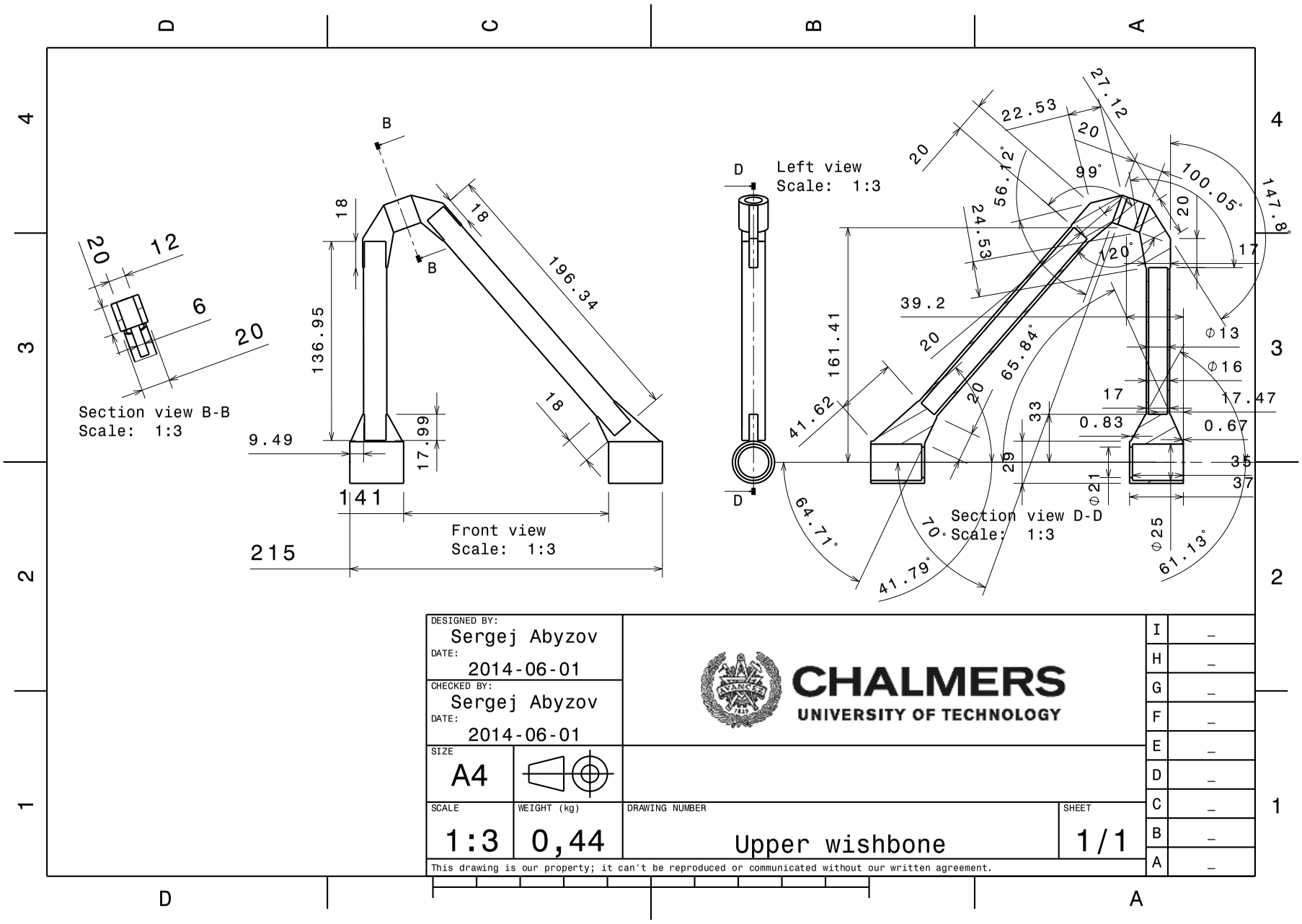

Figure E.8: *Upper wishbone*

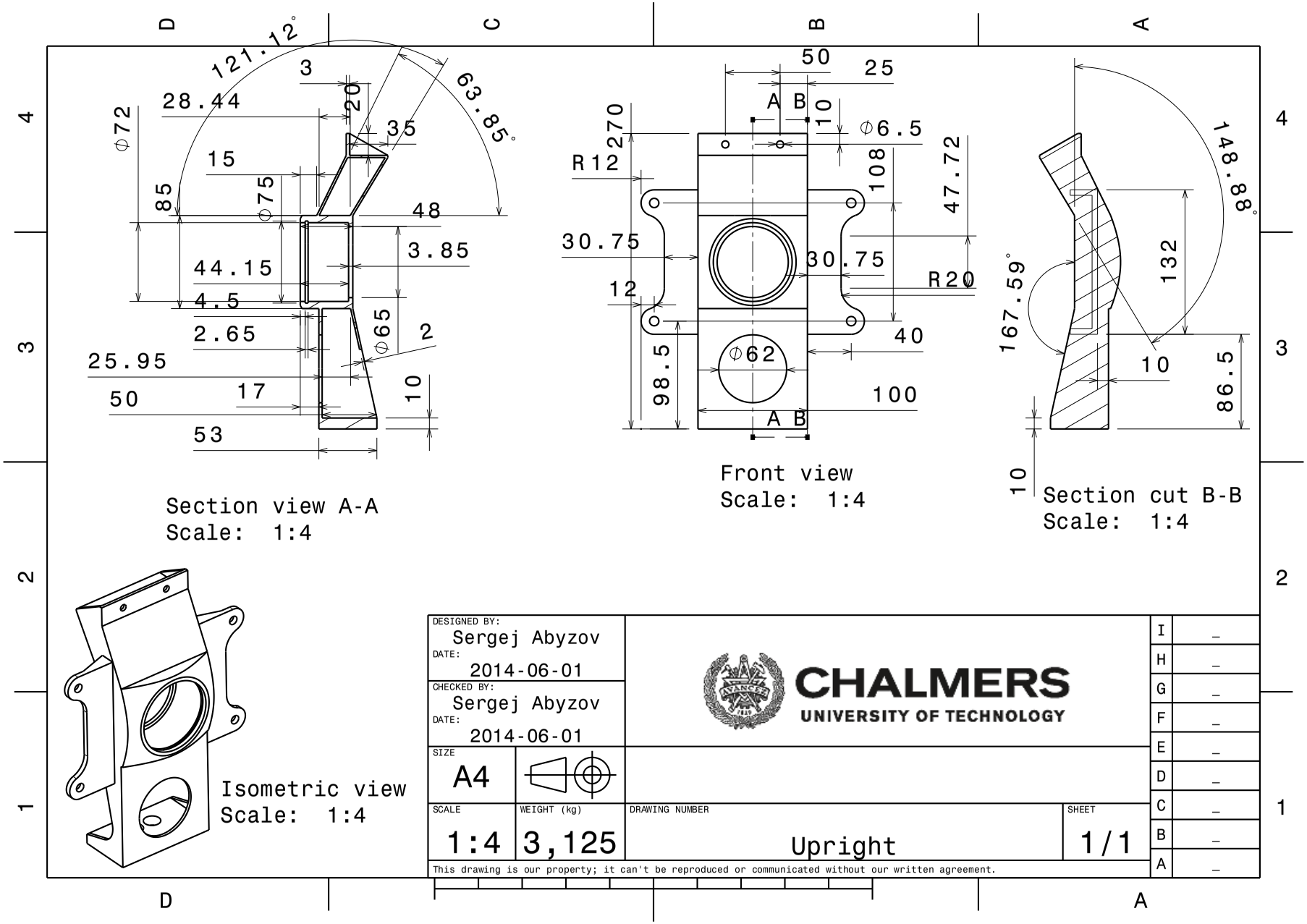

Figure E.9: *Drawing of uprigt*

Appendix F
Software evaluation

This appendix covers the evaluation of simulation software needed for the project. The main reason why this is written is because the issue of learning new software and finding the proper field of use of them took quite a significant time of the project.

F.1 IPGKinematics

The IPGKinematics is a stand alone program within the IPG CarMaker F.2 suite. It is used for generating/creating dynamic models of the suspension. Each axle has to be set up in separate models (ie files). To evaluate the characteristics over the wheel movement of the suspension one has to run the simulation and open up the wanted plot describing the characteristic that is to be analysed. If one wants to alter the curve, ie the behaviour of the suspension the point(-s) that need to be modified are altered by changing their value in coordinate table and then the simulation is run again. This is the main weak point of the program, as one can't see the real time change of the characteristics, especially as one point might affect more than just one criteria, e.g. some point might affect both the camber change and the toe angle change, but this is not too easy to see directly. For this project this software ended up as being used mainly to create suspension models from data computed in LSA SHARK (Appendix F.3)ll as the files generated here are compatible with IPG CarMaker and therefore makes usage of CarMaker and the parametrization of vehicle in it easier.

F.1.1 IPGKinematics plotting tool

To rationalize the plotting of graphs of main interest a MATLAB-script was made. This script is to be put into the following directory: \project folder\Data\Chassis\ - folder and run after alterations have been made and saved (as saving generates the output files) in IPGKinematics. This script imports the result files, rearranges some data and plots wanted values against each other. This enables the user to quickly asses the results and alter a points position. The script below is the one used for this project. By using the plotting tool (script) the user achieves a environment closer to an WYSIWYG-UI over the standard black box iterative one, which in it's turn makes the result analysis easier and faster to perform.

```
clc                             % Cleares the Command Window
clear all                       % Cleares all saved variables in Workspace
close all                       % Closes all open windows, as plot figures etc

%% Font parallel bump

P_f = importdata('front_1500_parallel.txt') % imports wanted textfile
u_Pf=P_f.colheaders;            % saves the units
pf=P_f.data;                    % saves just the data,
h_pf=char('WheelTravel','Toe angle','Camber angle','TrackChange','LongTrackChange','RCLat','RCVert'
    ,'RCHeig','Anti-Squat','Anti-Dive','KPOffset','KPInclination','Caster trail','CastAngle');   %
    creates a matrix with the characters of headers
h_pf=cellstr(h_pf);             % h_p = cellstr(h_p) places each row of the character array h_p
    into separate cells of h_p


pf=sortrows(pf,1);              % Sorts the rows in P according to ascending order of column 1
pf(:,2)=pf(:,2)./60;            % Converts degree minutes to degrees
u_Pf(2)=cellstr('[deg]');       % Converts unit of [min] to [deg]

wtf=pf(:,1);                    % Saves the wheel travel into own vector
toef=pf(:,2);                   % Saves the toe angle into own vector
camf=pf(:,3);                   % Saves the camber angle into own vector
trackchf=pf(:,4);               % Saves the track change (lat) into own vector
trackchlf=pf(:,5);              % Saves the track change (long) into own vector
RCLatf=pf(:,6);                 % Saves the roll centre lat position into own vector
RCVertf=pf(:,7);                % Saves the roll centre vert position into own vector
RCHeigf=pf(:,8);                % Saves the roll centre height position into own vector
```

```
AntiSquat=pf(:,9);              % Saves the roll centre height position into own vector
AntiDive=pf(:,10);              % Saves the roll centre height position into own vector
KPOffset=pf(:,11);              % Saves the roll centre height position into own vector
KPInclination=pf(:,12);         % Saves the roll centre height position into own vector
Castertrail=pf(:,13);           % Saves the roll centre height position into own vector
CasteAngle=pf(:,14);            % Saves the roll centre height position into own vector

dtoef=diff(toef);
dcamberf=diff(camf);
dtrackff=diff(trackchf);
dtracklff=diff(trackchlf);

dff=[dtoef dcamberf dtrackff dtracklff];

h_df=char('Toe angle change','Camber angle change','Track width change','Wheel base change');   %
    creates a matrix with the characters of headers
h_df=cellstr(h_df);             % h_p = cellstr(h_p) places each row of the character array h_p
    into separate cells of h_p
u_df=char('deg/mm','deg/mm','mm/mm','mm/mm');   % creates a matrix with the characters of headers
u_df=cellstr(u_df);             % h_p = cellstr(h_p) places each row of the character array h_p
    into separate cells of h_p

figure()                        % Creates an emptu figure if i'th numbering (vs the first figure
    created)
for i=1:length(h_pf)           % Checking length of unique variables

    subplot(4,5,i);
    plot(pf(:,1),pf(:,(i)))         % Plotting wheel travel (bump) vs various variables
    xlabel([h_pf(1) u_Pf(1)])       % Writing xlabel and unit
    ylabel([h_pf(i) u_Pf(i)])       % Writing ylabel and unit
    grid on                         % Turning grid on
    hold on
end
for j=1:4
    subplot(4,5,(length(h_pf)+j));
    plot([-130:1:130]',dff(:,(j)))         % Plotting wheel travel (bump) vs various variables
    xlabel([h_pf(1) u_Pf(1)])       % Writing xlabel and unit
    ylabel([h_df(j) u_df(j)])       % Writing ylabel and unit
    grid on                         % Turning grid on
end
suptitle('Front axle parallel bump')    % Adding title to the figure

% Front axle fitted derivative values

dtoeff=fit([-130:1:130]',dtoef,'poly3','Exclude', [131]);
dcamberff=fit([-130:1:130]',dcamberf,'poly3','Exclude', [131]);
dtrackfff=fit([-130:1:130]',dtrackff,'poly3','Exclude', [131]);
dtracklfff=fit([-130:1:130]',dtracklff,'poly3','Exclude', [131]);

figure()
plot(dtoeff,'b')                     %
title('Fitted dtoe/bump front axle')% Adding title to the figure
xlabel('Bump [mm]')                 % Writing xlabel and unit
ylabel('Toe angle change [deg/mm bump]') % Writing ylabel and unit
legend off
grid on

figure()
plot(dcamberff,'b')
title('Fitted dcamber/bump front axle') % Adding title to the figure
xlabel('Bump [mm]')                 % Writing xlabel and unit
ylabel('Camber angle change [deg/mm bump]') % Writing ylabel and unit
legend off
grid on

figure()
plot(dtrackfff,'b')
title('Fitted track width change/bump front axle') % Adding title to the figure
xlabel('Bump [mm]')                 % Writing xlabel and unit
ylabel('Track width change [mm/mm bump]') % Writing ylabel and unit
legend off
```

```
grid on

figure()
plot(dtracklfff,'b')
title('Fitted wheel base change/bump front axle') % Adding title to the figure
xlabel('Bump [mm]')                 % Writing xlabel and unit
ylabel('Wheel base change [mm/mm bump]') % Writing ylabel and unit
legend off
grid on


%% Rear parallel bump

P_r = importdata('rear_1500_parallel.txt') % imports wanted textfile P=importdata('name of
    textfile.fileextension')
u_Pr=P_r.colheaders;            % saves the units
pr=P_r.data;                    % saves just the data,
h_pr=char('WheelTravel','Toe angle','Camber angle','TrackChange','LongTrackChange','RCLat','RCVert'
    ,'RCHeig','Anti-Squat','Anti-Dive','KPOffset','KPInclination','Caster trail','CastAngle');   %
    creates a matrix with the characters of headers
h_pr=cellstr(h_pr);             % h_p = cellstr(h_p) places each row of the character array h_p
    into separate cells of h_p


pr=sortrows(pr,1);              % Sorts the rows in P according to ascending order of column 1
pr(:,2)=pr(:,2)./60;            % Converts degree minutes to degrees
u_Pr(2)=cellstr('[deg]');       % Converts unit of [min] to [deg]

h_dr=char('Toe angle change','Camber angle change','Track width change','Wheel base change');   %
    creates a matrix with the characters of headers
h_dr=cellstr(h_dr);             % h_p = cellstr(h_p) places each row of the character array h_p
    into separate cells of h_p
u_dr=char('deg/mm','deg/mm','mm/mm','mm/mm');   % creates a matrix with the characters of headers
u_dr=cellstr(u_dr);             % h_p = cellstr(h_p) places each row of the character array h_p
    into separate cells of h_p


dtoer=diff(pr(:,2));
dcamberr=diff(pr(:,3));
dtrackr=diff(pr(:,4));
dtracklr=diff(pr(:,5));

dfr=[dtoer dcamberr dtrackr dtracklr];

figure()                        % Creates an emptu figure if i'th numbering (vs the first figure
    created)
for i=1:length(h_pr)            % Checking length of unique variables

subplot(4,5,i);
plot(pr(:,1),pr(:,(i)),'r')         % Plotting wheel travel (bump) vs various variables
xlabel([h_pr(1) u_Pr(1)])       % Writing xlabel and unit
ylabel([h_pr(i) u_Pr(i)])       % Writing ylabel and unit
grid on                         % Turning grid on
end
for j=1:4
    subplot(4,5,(length(h_pr)+j));
    plot([-130:1:130]',dfr(:,(j)),'r')         % Plotting wheel travel (bump) vs various variables
    xlabel([h_pr(1) u_Pr(1)])       % Writing xlabel and unit
    ylabel([h_dr(j) u_dr(j)])       % Writing ylabel and unit
    grid on                         % Turning grid on
end
suptitle('Rear axle parallel bump')    % Adding title to the figure

% Front axle fitted derivative values

dtoerf=fit([-130:1:130]',dtoer,'poly4','Exclude', [131]);
dcamberrf=fit([-130:1:130]',dcamberr,'poly4','Exclude', [131]);
dtrackrf=fit([-130:1:130]',dtrackr,'poly4','Exclude', [131]);
dtracklrf=fit([-130:1:130]',dtracklr,'poly4','Exclude', [131]);

figure()
```

```
plot(dtoerf,'r')                        %
title('Fitted dtoe/bump rear axle')% Adding title to the figure
xlabel('Bump [mm]')                     % Writing xlabel and unit
ylabel('Toe angle change [deg/mm bump]') % Writing ylabel and unit
legend off
grid on

figure()
plot(dcamberrf,'r')
title('Fitted dcamber/bump rear axle') % Adding title to the figure
xlabel('Bump [mm]')                     % Writing xlabel and unit
ylabel('Camber angle change [deg/mm bump]') % Writing ylabel and unit
legend off
grid on

figure()
plot(dtrackrf,'r')
title('Fitted track width change/bump rear axle') % Adding title to the figure
xlabel('Bump [mm]')                     % Writing xlabel and unit
ylabel('Track width change [mm/mm bump]') % Writing ylabel and unit
legend off
grid on

figure()
plot(dtracklrf,'r')
title('Fitted wheel base change/bump rear axle') % Adding title to the figure
xlabel('Bump [mm]')                     % Writing xlabel and unit
ylabel('Wheel base change [mm/mm bump]') % Writing ylabel and unit
legend off
grid on



%% Both axles in same graphs
figure()                            % Creates an emptu figure if i'th numbering (vs the first figure
    created)
for i=1:length(h_pr)                % Checking length of unique variables

subplot(4,4,i);
plot(pf(:,1),pf(:,(i)))             % Plotting wheel travel (bump) vs various variables
hold on
plot(pr(:,1),pr(:,(i)),'r')         % Plotting wheel travel (bump) vs various variables

xlabel([h_pr(1) u_Pr(1)])           % Writing xlabel and unit
ylabel([h_pr(i) u_Pr(i)])           % Writing ylabel and unit
grid on                             % Turning grid on
end
% legend('Front','Rear')
suptitle('Font and rear axles parallel bump')    % Adding title to the figure


%% Front axle steering only

S = importdata('front_1500_steering_ko.txt') % imports wanted textfile
u_S=S.colheaders;                   % saves the units
s=S.data;                           % saves just the data,
h_s=char('TraRack','WhlAngL','WhlAngR','CamberL','KPOffset','TrackCh','Ackerman','TrackDif','
    SteerDif','AckError','AckPCent','StRodAng','TrackDia','TurnDia'); % creates a matrix with the
    characters of headers
h_s=cellstr(h_s);                   % h_s = cellstr(h_s) places each row of the character array h_s
    into separate cells of h_s

u_s=char('[mm]','[deg]','[deg]','[deg]','[mm]','[mm]','[deg]','[deg]','[deg]','[deg]','[%]','[deg]'
    ,'[m]','[m]');    % creates a matrix with the characters of units
u_s=cellstr(u_s);                   % u_s = cellstr(u_s) places each row of the character array u_s
    into separate cells of u_s

s=sortrows(s,1);                    % Sorts the rows in P according to ascending order of column 1
figure()
for i=1:length(h_s)
```

```
    subplot(4,4,i);             % creates the i'th element in a 4x4 subplot
    plot(s(:,1),s(:,(i)))       % plots the i'th element
    xlabel([h_s(1) u_s(1)])     % picks the set value in the header vector
    ylabel([h_s(i) u_s(i)])     % picks the i'th+1 value in the headers and units vectors
    grid on
end
suptitle('Front axle steering') % Adding title to the figure
```

F.2 IPG CarMaker

The IPG CarMaker is a software suite that enables among others full vehicle driving simulation. This was set as verification method for the whole project. The target goal was to perform a double lane change manoeuvre at vehicles top speed of 50km/h without roll over. The input model for the suspenion utilized was created with IPGKinematics Appendix F.1 with the aid of the plotting script Appendix F.1.1 to analyse the results.

F.3 Lotus Suspension Analysis SHARK

The Lotus Suspension Analysis SHARK, LSA SHARK or in this thesis short SHARK is a suspension analysis software developed and marketed by Lotus Cars UK. It is a very comprehensive software where both front and rear suspension can be modelled simultaneously. It also performs instant (real time) updates of the result/characteristics graphs at movement/manipulation of a point (SHARK works on WYSIWYG-UI principle). This real time update enables efficient work with a good overview of what happens to the overall system at the manipulation of one specific hard point. The first iteration of the suspension geometry was developed using SHARK and then the coordinates of the hard points were imported into IPGKinematics Appendix F.1 where they were further modified.